NTNU
Norwegian University of
Science and Technology

University of Padua
Department of Industrial Engineering

Master Thesis in Electrical Engineering

Modeling, control and performance assessment of a Wave Energy Converter equipped with an All-Electric Power Take-Off

Supervisor: Prof. Nicola Bianchi (UNIPD)

Co-Supervisor: Prof. Elisabetta Tedeschi (NTNU)

Majoring: Alessandro Bozzetto

ACADEMIC YEAR 2012-2013

Problem description

Modeling, control and performance assessment of a Wave Energy Converter equipped with an All-Electric Power Take-Off.

The first goal of the thesis will be the complete wave-to-wire modeling of a point absorber Wave Energy Converter (WEC), by using suitable software tool (Matlab-Simulink). Then an appropriate operating point for the system will be selected and the preliminary design of the electrical machine for the targeted (constant torque) application will be performed. This will be the basis for refined Power Take-Off (PTO) modeling aimed at the evaluation of expected power performance in different sea states, which is strongly intermittent due to the nature of the waves, in accordance to a specific sea scatter diagram. The corresponding yearly energy production will be then calculated. As a final part of the project, the impact of different operating conditions of the system on the overall power performance will be investigated and discussed.

The thesis is developed within a research collaboration between NTNU and Ocean Harvesting Technology AB.

Assignment given: 08 March 2013
Supervisor: Nicola Bianchi, UNIPD
Co-Supervisor: Elisabetta Tedeschi, NTNU

Abstract

This thesis project is focused on the study of a device for the production of electric energy starting from sea waves. As starting point the following paper is considered: “Luigi Alberti, Elisabetta Tedeschi, Nicola Bianchi, Maider Santos, Alessandro Fasolo, (2013) "Effect of the generator sizing on a wave energy converter considering different control strategies", COMPEL: The International Journal for Computation and Mathematics in Electrical and Electronic Engineering, Vol. 32 Iss: 1, pp.233 – 247”; in the thesis new control strategies to improve the power extracted by the wave energy converter (WEC) from the waves are considered and developed.

The proposed WEC is based on a point absorber which has the same hydrodynamic characteristics of that described in the above mentioned paper.
Based on the current trend in the wave energy devices closest to the market, two different types of devices are considered and systematically compared. They are here called bidirectional and unidirectional. What distinguish the bidirectional case from the unidirectional one is that in the bidirectional case the Power Take-Off (PTO) is always connected to the buoy and the entire ascending and descending motion is used for energy production, while in the unidirectional the PTO is connected to the buoy only when the motion is ascending, and, as a consequence, only one direction of the motion is used for the energy production. Furthermore, the control applied to the PTO is different compared to the most common control techniques generally used for this kind of devices, like passive loading and reactive control. In fact, the considered cases have as main characteristic the use of constant values of torque applied to the vertical motion of the buoy in one or in both directions. The traditional passive loading is considered only in the beginning of the thesis to have an immediately comparison of the results obtained by the new controls, instead the reactive control is not considered.

Subsequently two constraints are introduced into the model, which are the power limit and the buoy position control. These constraints allow having a more realistic behavior of the WEC; several different values for the power limit are considered and consequent considerations are made; instead for the buoy position control the limit is fixed and serves to prevent that the device goes out of the water also when operating in high energy sea states.

As a first step the behavior is checked for three reference sea states. Subsequently the analysis is extended considering the occurrence of each sea state in four locations (Wave Hub, AUK, Haltenbanken and EMEC) which are European places with a favorable wave climate and equipped for the performance evaluation of WECs. The aim of these analyses is to determine the yearly energy that could be extracted for each location. These evaluations could be used as a basis for preliminary economic considerations, which, however, are beyond the scope of this thesis project.

In the following part of the thesis a permanent magnet synchronous generator (PMSG) is implemented and also the electric drive to control the behavior of the generator; the torque control is used to control the PMSG, and field weakening of the generator is applied in order to allow over-speed operation. To calculate the losses of the generator and consequently the efficiency a real-time model to calculate the power losses is made. This allows a more precise evaluation of the electrical power

that can be extracted by the considered WEC when the non-ideal efficiency associated to the electric PTO is taken into account.

Matlab-Simulink is the software used to implement the models, a lot of comments and considerations about the different kinds of inputs values and structure of the models are made in order to optimize the solutions time.

Sommario

Questo lavoro di tesi si concentra sullo studio di un dispositivo di produzione dell'energia elettrica a partire dal moto ondoso. Come punto di partenza si è considerato il paper seguente: "Luigi Alberti, Elisabetta Tedeschi, Nicola Bianchi, Maider Santos, Alessandro Fasolo, (2013) "Effect of the generator sizing on a wave energy converter considering different control strategies", COMPEL: The International Journal for Computation and Mathematics in Electrical and Electronic Engineering, Vol. 32 Iss: 1, pp.233 – 247"; in questa tesi vengono considerate e studiate delle nuove strategie di controllo per aumentare la potenza estratta dal wave energy converter (WEC) dalle onde.

Il WEC proposto è basato su un point absorber che ha le stesse caratteristiche idrodinamiche di quello descritto nel paper menzionato precedentemente.
In base ai dispositivi attualmente in commercio, vengono considerati e sistematicamente comparati due differenti tipi di dispositivi. Vengono chiamati rispettivamente bidirezionale ed unidirezionale. Quello che distingue il caso bidirezionale da quello unidirezionale è che nel bidirezionale la Power Take-Off (PTO) è sempre connessa alla boa e quindi tutto il moto ascendente e discendente viene usato per la produzione di energia, mentre nell'unidirezionale la PTO è connessa alla boa solo quando il moto è ascendente, e, di conseguenza, solo una direzione del moto è usata per la produzione di energia. Inoltre, il controllo applicato alla PTO è diverso rispetto alle più comuni tecniche di controllo generalmente usate per questo tipo di dispositivi, come il passive loading e il reactive control. Infatti, i casi considerati hanno come caratteristica principale l'uso di valori costanti di coppia applicata al moto verticale della boa in una o entrambe le direzioni. Il tradizionale passive loading è considerato solo all'inizio della tesi per aver un immediata comparazione dei risultati ottenuti dai nuovi controlli, invece il reactive control non viene considerato.

Successivamente due vincoli sono introdotti nel modello, i quali sono il limite di potenza e il controllo di posizione della boa. Questi vincoli permettono di avere un comportamento più realistico del WEC; sono testati diversi valori per il limite di potenza; invece per il controllo di posizione della boa è fissato e serve per prevenire l'uscita del dispositivo dall'acqua anche quando funziona in stati di mare molto energetici.

Come primo step il modello è testato per tre stati di mare di riferimento. Successivamente l'analisi è estesa considerando l'occorrenza di ciascun stato di mare in quattro locations (Wave Hub, AUK, Haltenbanken and EMEC) Europee con un clima favorevole alle onde ed equipaggiate per la valutazione delle performance dei WECs. L'obiettivo della tesi è di determinare l'energia annuale estraibile da ciascuna locations. Queste valutazioni possono essere usate come basi per una preliminare considerazione economica, la quale, comunque, è al di là dello scopo di questa tesi.

Nella parte seguente della tesi è implementato un generatore sincrono a magneti permanenti (PMSG) con anche l'azionamento per il controllo del suo comportamento durante il funzionamento; il controllo di coppia è usato per controllare il PMSG, e il field weakening del generatore è utilizzato per consentire il funzionamento a velocità superiori della nominale. Per calcolare le perdite del generatore e conseguentemente l'efficienza, viene implementato un modello in

tempo reale per calcolare le perdite. Questo consente una più precisa valutazione della potenza elettrica estraibile dal WEC considerato, quando non viene associata un efficienza ideale al PTO elettrico.

Il programma utilizzato per le simulazioni e l'implementazione dei modelli è Matlab-Simulink, molti commenti e considerazioni sono sui differenti valori e strutture dei modelli creati con l'idea di ottimizzare il tempo di simulazione per avere le soluzioni.

Preface

This project is my master thesis and represents the final work in the Master course *Electrical Engineering* at the University of Padua. I made this thesis during my Erasmus time in Trondheim (Norway) at Norwegian University of Technology and Science (NTNU).
I want to thank all the people that helped and supported me during my thesis works, in particular my Supervisor Nicola Bianchi; a special thanks also to my Co-Supervisor Elisabetta Tedeschi for all the time that she spent for me and for always having her door open for me giving support and advice.
At my family I want to say a special thanks to support me during all of my years at university and also for the precious advices that they always give to me, this Master is also about yours.
And finally but not less important, a thanks to all of my friends which are always ready to help me in whatever situations.

Alessandro

Contents

List of Figures

LIST OF FIGURES

List of Tables

Nomenclature

ρ	[kg/m^3]	Water density
τ	[s]	Time shift
S_ζ^B	[-]	Bretschneider spectrum
ω	[rad]	Angular frequency
ω_m	[rad/s]	Mechanical speed
ω_e	[rad/s]	Electromechanical speed
μ_0	[Vs/Am]	Magnetic constant
η	[-]	Efficiency
Ψ_{pm}	[Vs]	Permanent magnet flux
Ψ_n	[Vs]	Nominal magnetic flux
β	[-]	Steinmetz constant
$cos\varphi$	[-]	Load factor
$2p$	[-]	Poles number
A	[kVA]	Apparent power
A, B	[-]	Definition parameters
a, b, c	[-]	Field weakening coefficient
a_∞	[kg]	Added mass at infinite frequency
B	[T]	Magnetic flux density
B_L	[kg/s]	Added damping
c_1	[-]	Mechanical constant
D_i	[m]	Air gap diameter
F_E	[N]	Excitation force
F_L	[N]	Load force
f	[Hz]	Frequency
G_{OL}	[-]	Open loop gain
G_{CL}	[-]	Close loop gain
g_{tot}	[m]	Total air gap
g	[m/s^2]	Gravity constant
h, Hs	[m]	Wave amplitude
I, i	[A]	Current
K_{rad}	[-]	Radiation impulse response function
K	[N/m]	Hydrostatic stiffness
KP	[N/m]	Stiffness coefficient
K_s	[A/m]	Electric load
K_p	[-]	PI regulator gain
k_h	[-]	Hysteresis constants
k_e	[-]	Eddy current constants

L_S	[mH]	Stator leakage inductance
L_{stk}	[m]	Air gap length
M	[kg]	Mass
M_L	[kg]	Reactive component
N	[-]	Turns number
n	[rpm]	Generator speed
P, p	[kW]	Power
p	[-]	Pole pairs number
R_S	[Ω]	Stator resistance
s	[m]	Buoy position
$\dot{s}$	[m/s]	Buoy speed
$\ddot{s}$	[m/s^2]	Buoy acceleration
T	[Nm]	Torque
T_i	[s]	PI regulator time constant
Te	[s]	Energy period
Tz	[s]	Zero crossing period
t	[s]	Time
U, u	[V]	Voltage
V, v	[V]	Voltage
$Volume$	[m^3]	Iron machine volume

1. Introduction

In the last years the energy problem required more and more attention. That happens because the natural reserves of oil, gas and coke are finishing.
In addition fossil fuels are very polluting and that particular opens the way for new researches and studies about the so-called renewable energy. One of the most recent subjects of study, among these renewable energies is the wave-energy.
Approximately in 2050 the 15% of world electric energy production [1] can be obtained with this new technology, at present in this time the studies of wave energy show a strong increase. In this way, the combination of renewable energies and fossil fuels partially resolves the problems of environment pollution and electric energy production.
The power in a wave is proportional to the square of the wave amplitude and to the period. Therefore, long period (~7–10 s), large amplitude (~5 m) waves have average energy fluxes between 85 and 120 kW per meter width of incoming wave.

$$\boldsymbol{P = \frac{1}{4}\frac{\rho g^2 a^2 T}{2\pi} = \frac{\rho g^2 h^2 T}{64\pi}} \qquad [\boldsymbol{W/m}] \tag{1.1}$$

In the previous formula ρ is the water density in kg/m^3, g is the gravity constant, h is the wave amplitude in meter and T is the energy period in second [2].
Nearer the coastline the average energy of a wave decreases due to interaction with the seabed. Energy dissipation in near shore areas can be compensated by natural phenomena such as refraction or reflection, leading to energy concentration (’hot spots’) [3].

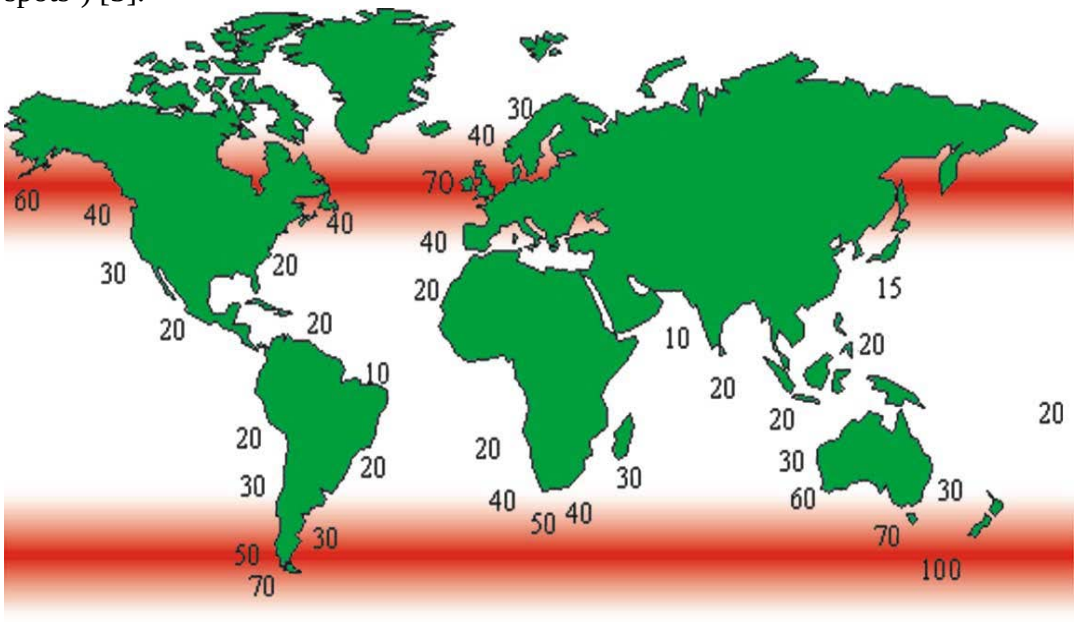

Figure 1.1 - Global wave power distribution in kW/m of crest length

Situated at the end of the long, stormy fetch of the Atlantic, the wave climate along the western coast of Europe is characterized by particularly high energy. Only the southern parts of South America and the Antipodes have a more energetic wave climate, due to circumpolar storms near the Atlantic. Recent studies [3] assign for the area of the north-eastern Atlantic (including the North Sea) available wave power

resources of about 290 GW. The long-term annual wave power level increases from about 25 kW/m off the southernmost part of Europe's Atlantic coastline (Canary islands) up to 75 kW/m off Ireland and Scotland. When moving further north it decreases to 30 kW/m off the northern part of the Norwegian coast. In the North Sea, the resource changes significantly, varying from 21 kW/m in the most exposed (northern) area to about half of that value in the more sheltered (southern) area. In the Mediterranean basin, the annual power level off the coasts of the European countries varies between 4 and 11 kW/m, the highest values occurring in the area of the south-western Aegean Sea. This area is characterized by a relatively long fetch and high wind energy potential. The entire annual deep-water resource along the European coasts in the Mediterranean is of the order of 30 GW, the total wave energy resource for Europe resulting thus to 320 GW [1].
Furthermore, wave energy is more predictable than for instance wind energy since the waves are built up by the wind during a long period of time and then continues to swell after the wind subsides. This leads to a relatively slower variation in the average energy.
It's important to appreciate the difficulties that wave power development is facing. The most important of them are:

- Strong irregularity of amplitude, frequency and phase of the waves; It's difficult to obtain a device that can be used in entire range of excitation frequency.
- The structural loading in event of extreme weather conditions, such as hurricanes, may be 100 times as high as the normal average loading.
- The coupling of slow motion (~0.1 Hz) and irregular frequency of a wave to electrical generators required ~500 times greater frequency.

It becomes apparent, that the design of a wave energy converter has to be highly sophisticated to be operationally efficient and reliable on one hand, and economically feasible on the other. As with all renewable energy sources, the available resource and variability at the installation site has to be determined first. Present trends support devices of moderate power generation levels up to 1.5–2 MW, or small, modular devices of 100–200 kW rated power, which may meet multi-Megawatt demands when installed in arrays [3].
The common power grid required a relatively steady power level and, consequently, the power generation should be generated on an even level, to avoid the need of leveling the power, before it is delivered to the power grid. If done in the latter way, transformers and cables must be heavily over-dimensioned in relation to the mean power, and there is a need for costly energy storage means to smoothen the power before it reaches the grid connection [4].

2. Various converters technologies applied in the wave energy

There is a wide variety of wave energy technologies, resulting from different ways in which energy can be absorbed from the waves, and also depending on the water depth and on the location (shoreline, near-shore, offshore). These technologies is relatively new and a lot of project replacing the older just before that will finish, or sometimes before they start.
Several methods have been proposed to classify wave energy systems, according to location, to working principle and to size ("point absorbers" versus "large" absorbers). In the following figure there is a general classification of wave energy technologies.

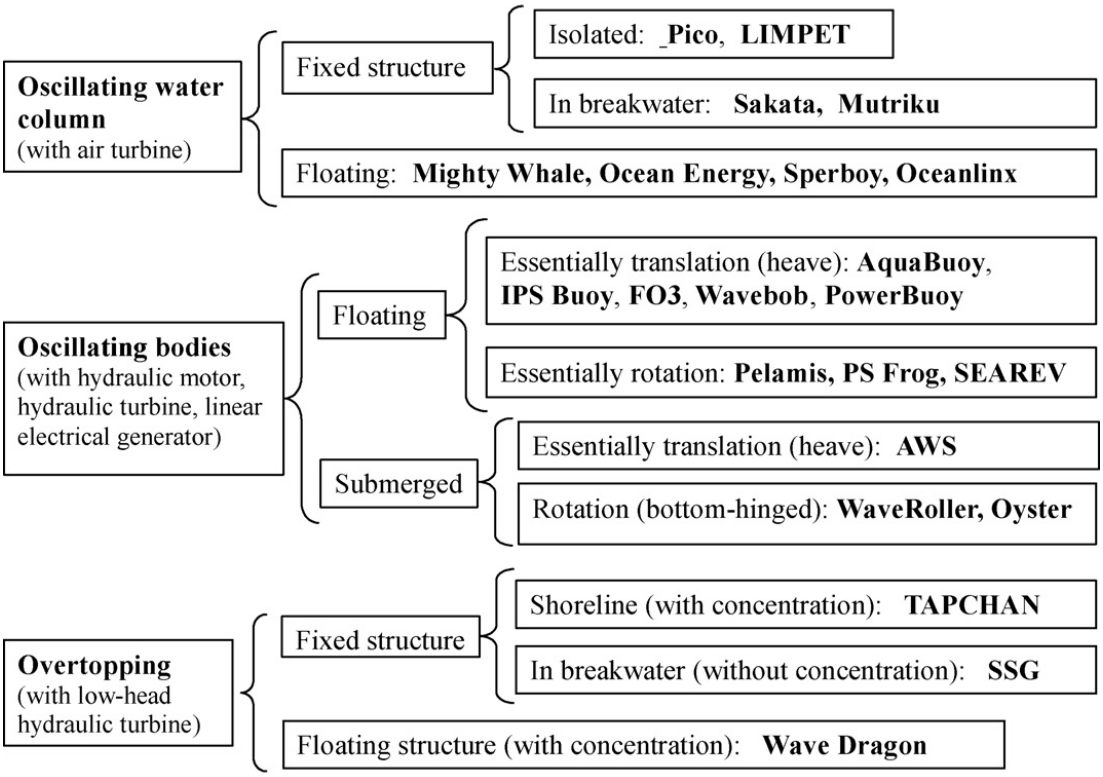

Figure 2 - The various wave energy technologies

All of the comments and figures in this chapter are from [5].

2.1 The oscillating water column (OWC)

Fixed-structure OWC
Based on various energy-extracting methods, a wide variety of systems has been proposed but only a few full-sized prototypes have been built and deployed in open coastal waters. Most of these are or were located on the shoreline or near shore, and are sometimes named first generation devices. In general these devices are fixed to a rocky cliff or stand on the sea bottom. The main advantages of the shoreline devices are easier installation and maintenance, and the fact that they do not require deep-water moorings and long underwater electrical cables.

The oscillating water column device comprises a partly submerged concrete or steel structure, open below the water surface, inside which air is trapped above the water free surface.

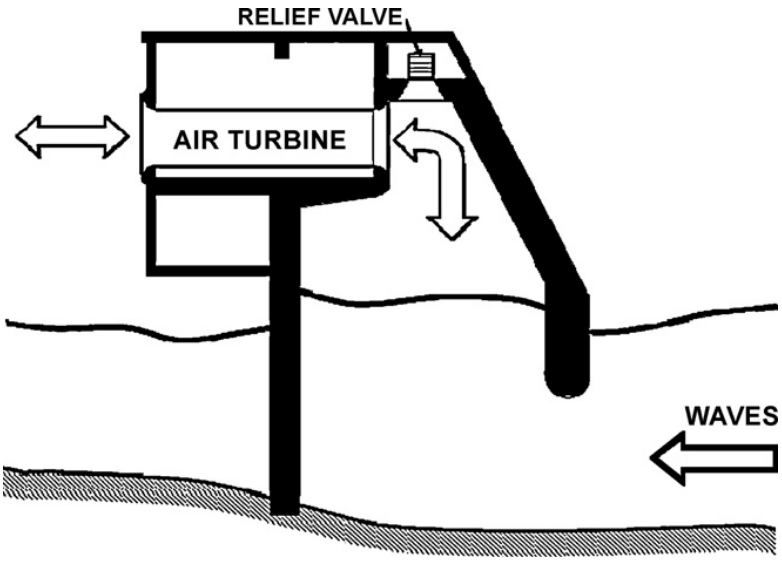

Figure 3 - Cross-sectional view of a bottom-standing OWC (Pico plant)

The oscillating motion of the internal free surface produced by incident waves makes the air flow through a turbine that drives an electrical generators.
Full sized OWC prototypes were built in Norway (1985), Japan (1990), India (1990), Portugal (1999), UK (2000). Another devices was installed in Scotland (OSPREY) and in 1995 was completely destroyed by the sea. In all of these cases the structure is fixed and excepted for OSPREY was made of concrete.
Usually the cross-sectional area of these OWCs (at mid water-free-surface level) lies in the range 80-250 m^2. The common installed power capacity is (or was) in the range 60-500 kW, expected for OSPREY which was 2 MW.
Another technology under test was made in Australia (2005) by the Australian company Energetech which is using a large parabolic-shape collector.
The design and construction of the structure (excluding the air turbine) are the most critical issues in OWC technology, and the most influential on the economics of energy produced from the waves. The costs of operation and maintenance (O&M) are low and the civil construction dominates the cost of the OWC plant.
A lot of different geometries of structure are being tested in the last years, in particular in the straits of Messina (Italy), Spain and Portugal.

Floating-structure OWC

The first OWC deployed in the sea were floating devices developed in Japan between 1960s and 1970s under the leadership of Yoshio Masuda which invented a new geometry for a floating OWC: the Backward Bent Duct Buoy (BBDB). In the BBDB, the OWC is bent backward from the incident wave direction, compared to the frontward facing duct is more advantageous.

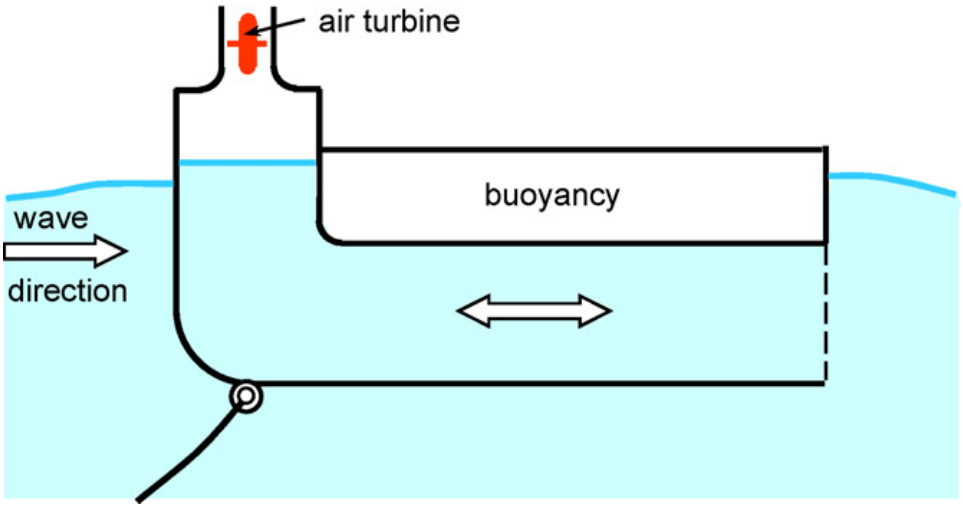

Figure 4 - Schematic representation of the Backward Bent Duck Buoy (BBDB)

In this device the length of the water column could be sufficiently large to achieve the resonance, while the oscillation of the floating structure must be within acceptable limits.
A lot of BBDB converters were studied and tested in China and Japan, in 2006 a big BBDB converter has been tested in the Galway Bay (western Ireland).
Another type of converter is called Mighty Whale and it was developed by the Japan Marine Science and Technology Center. A device of this type was installed near the Gokasho Bay, Japan in 1998, the total power rated is 110 kW, displacement 4400 t.
The Spar Buoy is the simplest concept for a floating OWC, it's an axisymmetric device which has a submerged vertical tail tube open at both ends, fixed to a floater that moves essentially in heave. The length of the tube determines the resonance frequency of the inner water column. An air turbine is moved by the air flow displaced by the motion of the OWC. Several types of wave-powered navigation buoy have been based on this concept, which has also been considered for large scale energy concept. The Sloped Buoy is another kind of device which is very similar with the Spar Buoy. The British Department of Trade and Industry (DTI) prepared a report where compared three types of floating OWCs for electricity generation in an Atlantic environment: BBDB, Sloped Buoy and Spar Buoy. No one of these is absolute the best, every system have strengths and weaknesses.
One of the last devices developed with this technology is Orecon and it was installed in UK. Orecon is a multi-resonance converter with several vertical OWCs of different lengths, each chamber being connected to an air turbine.

2.2 Oscillating body systems

Offshore devices are basically oscillating bodies, either floating or fully submerged; they exploit the more powerful wave regimes available in deep water (over 40 m water depth). Compared to the first generation of converters offshore devices are more complex and required more maintenance and long underwater electrical cables. Only recently this kind of converters has been developed.

Single-body heaving buoys

It's the simplest oscillating-body device, in most cases such systems are conceived as point absorbers (i.e. their horizontal dimensions are much smaller than the wavelength).

The first device developed with this technology was the G-1T in Tokio Bay (1980), the Norwegian Buoy which was tested in Trondheim Fjord in 1983 and an evolution of the Norwegian Buoy which was tested in Denmark (1990). All the used PTO was an early example of the hydraulic ram in a circuit and G-1T included a gas accumulator.

Two recent devices were tested in Sweden and Oregon (September 2008), the Swedish device was developed by Uppsala University and uses a linear electrical generator placed on the ocean floor. A line from the top of the generator is connected to a buoy located at the ocean surface, acting as power takeoff. Springs attached to the translator of the generator store energy during half a wave cycle and simultaneously act as a restoring force in the wave troughs.

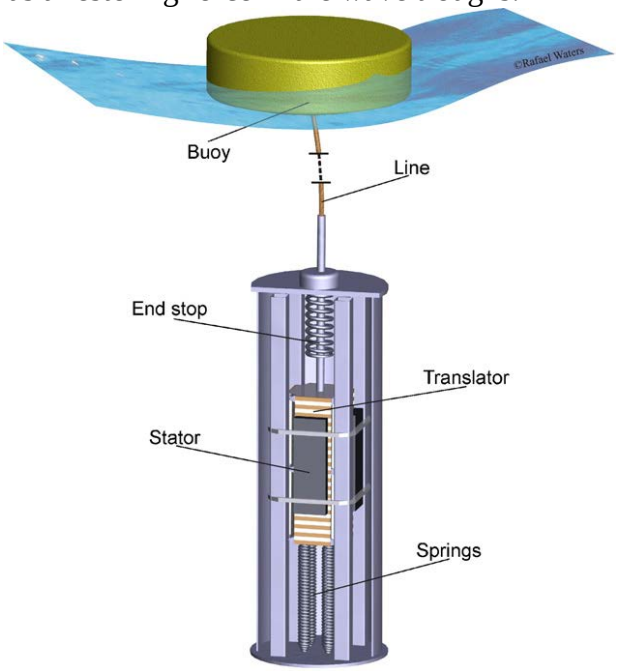

Figure 5 - Swedish heaving buoy with linear electrical generator (courtesy of Uppsala University)

The device tested in Oregon consists of a deep-draught spar and an annular saucer-shaped buoy. The forces imposed on the spar by the relative velocity of the body are converted into electricity by a permanent magnet linear generator.

Two-body heaving systems

The single floating body has a problem due to the distance between the free surface and the bottom and/or tidal oscillations in sea level, instead in the multi-body systems the energy is converted from the relative motion between two bodies oscillating differently. An early example of a two-point body heaving system is the Bipartite Point Absorber concept, it is based on two floaters where the outer one is a structure that acts as the reference and the inner one acts as the resonating absorber. The Wavebob was an evolution of the Bipartite Point Absorber in which the mass of

the inner body is increased by rigidly connecting it to a fully submerged body located sufficiently far underneath; it's been developed in Ireland.
One of the most important two-body point absorbers is the IPS buoy, initially developed in Sweden by the company Interproject Service. In this devices there is a buoy rigidly connected to a fully submerged vertical tube open at both ends. The tube contains a piston whose motion relative to the floater-tube system drives a PTO mechanism. Later a lot of improvements about this model were developed. The first prototype of the IPS buoy was tested in 1980 in Sweden.

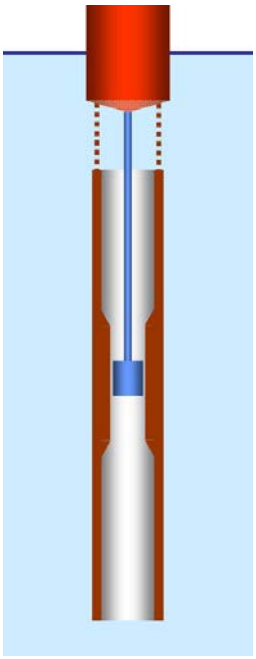

Figure 6 - Schematic representation of the IPS buoy

The AquaBuOY is a wave energy converter, developed in the 2000s and tested in 2007 in the Pacific Ocean off the coast of Oregon. It's a modern device based on the concept of the IPS buoy.
The most recent device based to the concept of the two-body point absorber was developed by Ocean Power Technology and it is called PowerBuoy. A disc-shaped floated reacts against a submerged cylindrical body, terminated as its bottom and by a large horizontal damper plat whose function is to increase the inertia through the added mass of the surrounding water. The relative heaving motion between the two bodies is converted into electrical energy by means of a hydraulic PTO. This device was installed in Spain (September 2008) and subsequently in Scotland (2009).

Figure 7 - The PowerBuoy prototype deployed off Santoña, Spain, in 2008 (courtesy of Ocean Power Technologies)

Fully submerged heaving systems

The Archimedes Wave Swing (AWS), a multi-cell array of flexible membrane absorbers which covert wave power to pneumatic power through compression of air within each cell. The cells are inter-connected, thus allowing interchange of air between cells in anti-phase. Turbine-generator sets are provided to convert the pneumatic power to electricity. A prototype was developed with 2 MW of power rated and tested with success in 2004, the AWS was the first converter using a linear electrical generator.

.

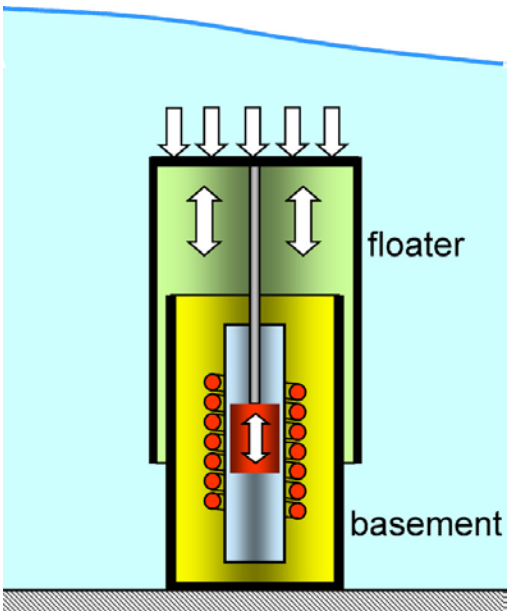

Figure 8 - Schematic representation of the Archimedes Wave Swing

Pitching devices

In the oscillating-bodies previously described the energy conversion is associated with a relative translational motion. There are other oscillating-body systems in which the energy conversion is based on relative rotation rather than translation. The first important device which used this technology is the nodding Duck (Stephen

Salter, University of Edinburg). Basically it is a cam-like floater oscillating in pitch. The first versions consisted of a string of Ducks mounted on a long spine aligned with the wave crest direction, with a hydraulic-electric PTO system. A lot of new versions based on the original Duck were developed in the following years.

Figure 9 - The Duck version of 1979 equipped with gyroscopes (courtesy of University of Edinburgh)

Another important convertor was the Cockerell Raft, which is the predecessor of a more successful device, the Pelamis and also the McCabe Wave Pump.
The Pelamis (UK) is a snake-line slack-moored articulated structure composed of four cylindrical sections linked by hinged joints, and aligned with the wave direction. In this device there is a gas accumulator that provide some energy storage. The Pelamis was for a lot of years the most tested and modeled device, a set of Pelamis was installed in Scotland (2004) and in Portugal (2008). The McCabe Wave Pump consists of three rectangular steel pontoons hinged together, with the heaving motion of the central pontoon damped by a submerged horizontal plate. Two sets of hydraulic rams and a hydraulic PTO convert the relative rotational motions of the pontoons into useful energy. A 40 m long prototype was deployed in 1996 off the coast of Kilbaha, County Clare, Ireland.

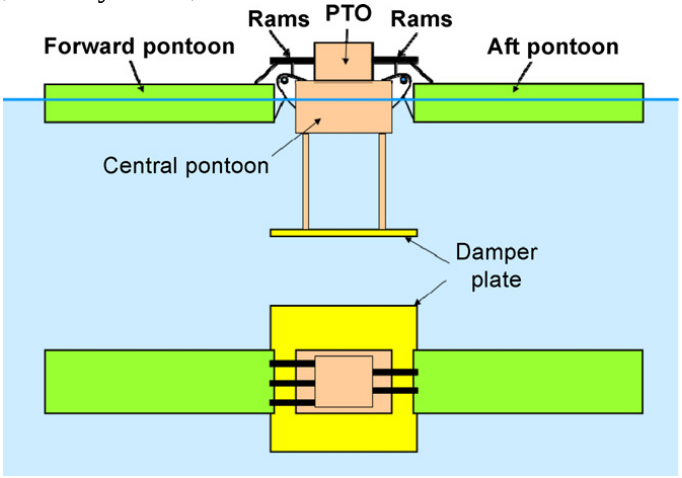

Figure 10 - Side and plan views of the McCabe Wave Pump

Two-body systems have been conceived in which only one body is in contact with the water: the other body is located above the water or is totally enclosed inside the wetted one.
A typical device based on the totally enclosed hull concept is the Frog, of which several offshore point-absorber versions have been developed at Lancaster University, UK.

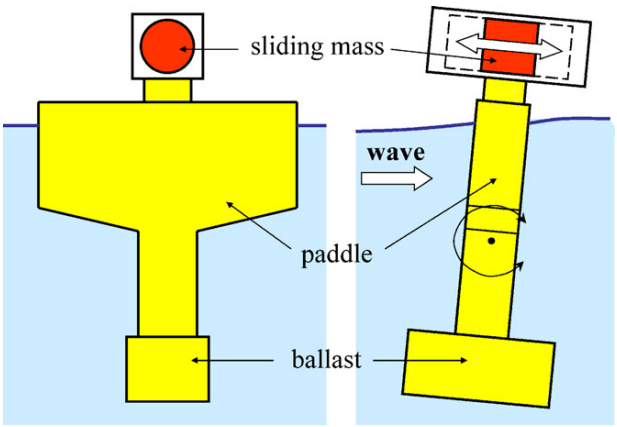

Figure 11 - Front and side views of the PS Frog MK 5

The Searev wave energy converter, developed at Ecole Centrale de Nantes (France), is a floating device enclosing a heavy horizontal-axis wheel serving as an internal gravity reference. The system is based on an oscillating pendulum in which neither end-stops or any security systems are needed to limit the stroke.

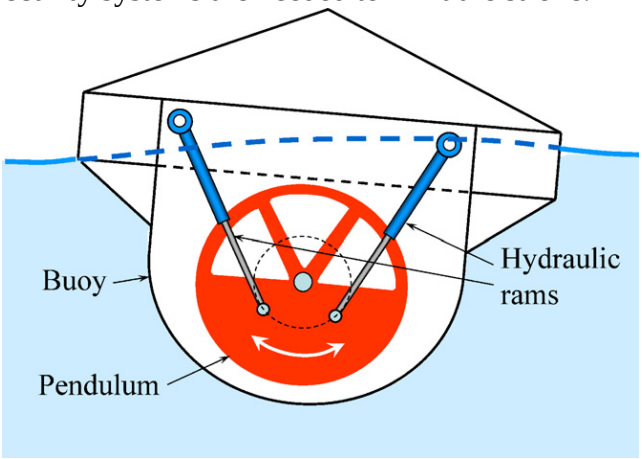

Figure 12 - Schematic representation of the Searev

The Spanish company Oceantec is developing another offshore floating energy converter that extracts energy basically from the pitching motion. The energy conversion process is based on the relative inertial motion that the waves cause in a gyroscopic system. This motion is used to feed an electrical generator through a series of transformation stages. A prototype was developed in September 2008 in Spain.

Bottom-hinged systems

These devices are based to the invention of Stephen Salter, which consists of a buoy spar, with symmetry about the vertical axis, that can swing about a universal joint at the sea bottom. The power take-off reaction to the sea bed is via a set of cables

wound several times round a winch-drum leading both fore and aft in the prevailing wave direction. The wave-activated reciprocating rotation of the drum is converted into useful energy by means of a hydraulic system.

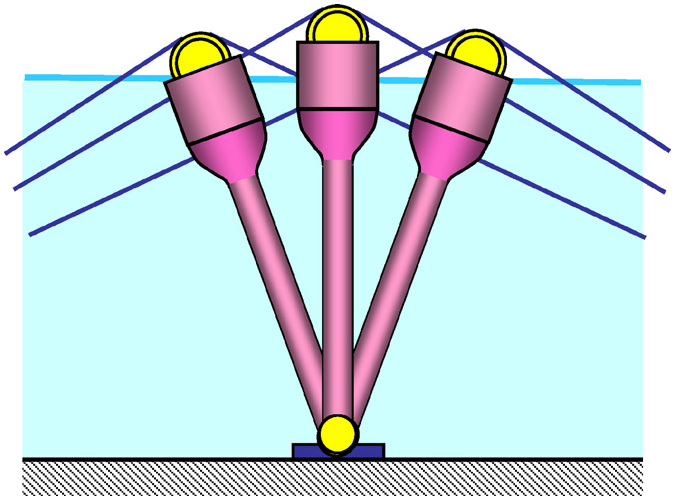

Figure 13 - The swinging mace in three angular positions

Two devices were tested, the first in called WaveRoller in Portugal (2008) and the other called Oyster, bigger than the first, in Scotland (2009).

Many-body systems

In some cases, the device consists of a large set of floating point absorber reacting against a common frame and sharing a common PTO. This is the case of FO3 (Norwegian project), a nearshore or offshore system consisting of an array of 21 axisymmetric buoys oscillating in heave with respect to a large floating structure of square platform with very low resonance frequency and housing a hydraulic PTO. Two of these kinds of devices were developed in Denmark (Wave Star project) and another one in Brazil, which is an hyperbaric device.

2.3 Overtopping converters

In this kind of converters the water is capture and introduce into a reservoir, where it is stored at a level higher than the average free-surface level of the surrounding sea. The potential energy of the stored water is converted into useful energy through more or less conventional low-head hydraulic turbines. The two more famous devices which use a fixed structure is the Tapchan (tapered Channel Wave Power Device), developed in Norway in the 1980s and the SSG (Seawave Slot-Cone Generator) which is a European project.

The Wave Dragon is a device developed in Denmark, whose slack-moored floating structure consists of two wave reflectors focusing the incoming waves towards a doubly curved ramp, a reservoir and a set of low-head hydraulic turbines. It is based on a floating structure and a prototype of the Wave dragon has been deployed in Nissum Bredning, Denmark, was grid connected in May 2003 and has been tested for several years.

2.4 Final considerations

In this thesis the point absorber (buoy) is deepened and a different kinds of control for the PTO will be considered. Basically two devices are used which have the same structure but different type of operation, in the first (called bidirectional) the energy is converted during both the directions of the buoy motion, in the second only one direction is considered for power production (ascending motion).

3. Starting model

The starting model is very similar to the model described in [3]. It is composed of a cylindrical point absorber in heave with a hemispherical bottom (buoy), which is directly coupled to a rotating electrical machine via gearbox. The radius and the draught of the point absorber are both equal to 5 m. Its mass is M = 670140 kg. The gear ratio is equal to 20 and the pinion radius is 0.1 m.
In the first part of the work, which is presented in the following paragraphs, in the model the electrical machine is not considered and all the parts associated at this (thus neglecting corresponding losses), because with these first simulations the goal is to understand better which values of the PTO torque (and corresponding PTO force) should be applied to obtain the maximum average mechanical power. Therefore these values will be applied as inputs into next models.

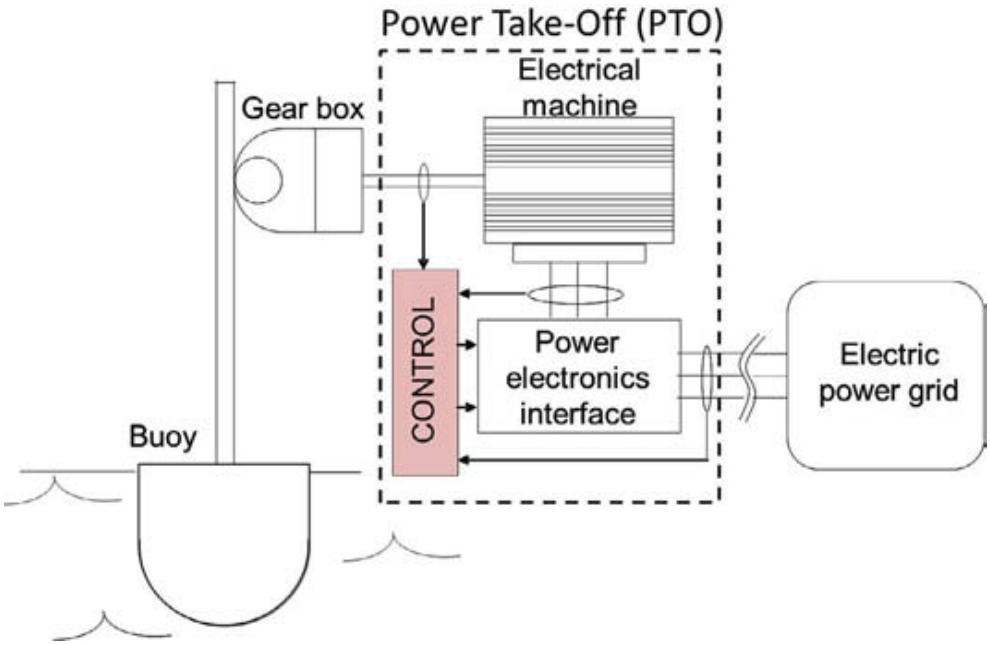

Figure 14 - Simplified model of the WEC (reproduces from [3])

3.1 Hydrodynamic model

In order to properly represent the interaction between the sea waves and the point absorber, which is a single degree of freedom device, the Cummins equation can be used (Cummins, 1962) [6]:

$$\boldsymbol{F_E(t) + F_L(t) = (M + a_\infty)\ddot{s}(t) + \int_\infty^t K_{rad}(t-\tau)\dot{s}(\tau)d\tau + Ks(t)} \qquad \textbf{(3.1)}$$

Where $\dot{s}$ is the speed of the buoy, $\ddot{s}$ its acceleration and s is its position. F_E is the excitation force applied by the waves to the point absorber and F_L is the force applied by the PTO. The radiation force that represents the effect of radiated waves produces by the buoy oscillation needs also be to taken into account. In equation (3.1) it is expressed by the convolution integral, K_{rad} being the radiation impulse response

function. Moreover, M is the mass of the device including the contribution due to the PTO inertia, K is the hydrostatic stiffness and a_∞ represents the value of added mass at infinite frequency (Falnes, 2002) [7].

3.2 Control of the point absorber

In order to extract energy from sea waves it is necessary to create a destructive interference between the incident waves and the waves generated by the vertical motion of the point absorber itself, which, in turn, depends on the action exerted on it by the electrical machine. By controlling the force applied by the electric machine it is thus possible to tune the device according to the sea state, with the goal of maximizing the power extraction [8].
As a first case it is considered that the PTO force applied has constant module and sign concordant to the speed of the buoy, thank to this the mechanical power is always positive. This is referred in the following as "bidirectional case" or "case1". For implementing this case in the simulation model the sign of the buoy velocity is considered with the block called "Sign", this block returns +1 if the buoy velocity is higher than zero, zero if the buoy velocity is equal to zero and -1 if the buoy velocity is lower than zero. The constant torque is multiplied by the result of the block "Sign" and this is the real torque applied by the electric machine. Then the real torque is multiplied by the ratio between gear and pinion radius for obtaining the PTO force, which is one of the input of the hydrodynamic model.
As a second case only one direction of speed (positive for simplicity) it is considered for power production and PTO force is applied with constant module and sign concordant to the speed. When the speed is equal or less than zero it's considered void as a result the PTO force is zero in this case. This is referred in the following as "unidirectional case" or "case2".
In the unidirectional case the only aspect that changes is that only the positive velocity of the buoy is exploited, therefore the applied torque is positive or zero.
The last control strategies that is used is called passive loading (case3), when passive loading is applied the force exerted by the PTO is proportional to the actual velocity of the point absorber in both the directions, according to a constant control coefficient B_L:

$$\boldsymbol{F_L(t) = B_L \dot{s}(t)} \qquad \textbf{(1.2)}$$

In this case the instantaneous power extracted from the point absorber is always positive [9]. There is another type of control strategy, which is called complex-conjugate (reactive) control, but in this thesis it isn't considered.
For all the simulations the value of M_L isn't defined, because it's used only in the complex-conjugate control.
As a result in all the three cases the mechanical power is always positive.

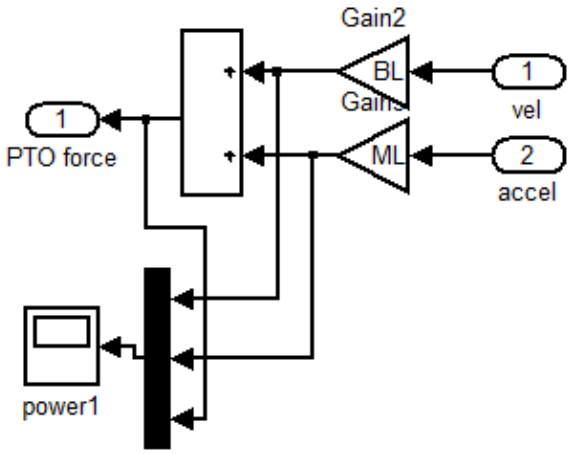

Figure 15 - Passive Loading control block in Simulink (PTO)

As you can see for a passive loading control it is sufficient to set at zero the value of M_L. This is referred in the following as "case3".

3.3 Wave profile generator in Matlab

The simulation time of the Simulink model is 900 seconds (s), for having more realistic results a wave profile of 900 s is necessary, which is considered representative of a sea state. The energy of a sea state is often represented as a function of the frequency of the incident waves by an energy spectrum, which can be analytically modeled starting form one or more parameters. In the following it is assumed that the sea state can be represented by a Bretschneider spectrum [6] (Cummins).

$$S_{\zeta}^{B}(\omega) = \frac{A}{\omega^5} e^{-\frac{B}{\omega^4}} \tag{3.3}$$

In equation (3.3) is expressed the Bretschneider spectrum in which *A* and *B* are definitions parameters, functions of the wave system features and ω is the angular frequency.
From the energy spectrum and by knowing the physical and geometric properties of the considered point absorber, the excitation forces exerted by the waves on the WEC can be calculated, as explained in [10].
In the following figure is plotted an example of wave profile over time, considering a time simulation of 540 s.

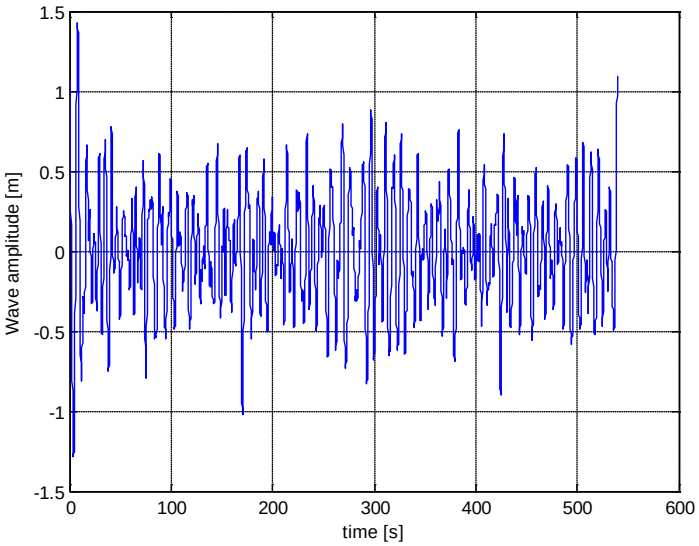

Figure 16 - Incident wave profile *Hs* = 1.414 m, *Te* = 7.713 s.

3.4 Simulink model

A program in Matlab is written and a Simulink model is implemented which is composed by a hydrodynamic model, a block for the passive loading control and the bidirectional/unidirectional case and visualization part with a lot of scope blocks. This hydrodynamic model implements the equation (3.1), and the most important components of this model are the PTO block for the WEC (control) and the block of the State-Space Radiation Force. With an appropriate setting of the switches the different cases can be implemented: this model is very flexible and the mechanic power is calculated as product of PTO force and velocity of the buoy.

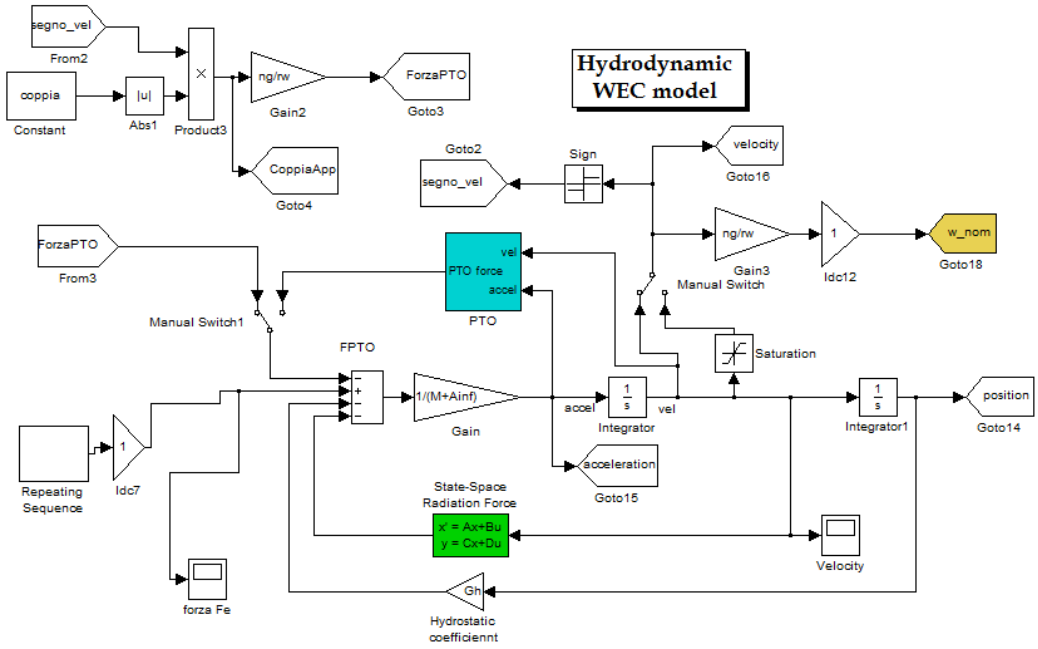

Figure 17 - Hydrodynamic model in Simulink

4. Results of simulations with no constraints

In this chapter all the simulations are made without constraints, so there are no limits of power, torque, PTO force, buoy velocity and position. It's an ideal situations used as starting point to understand the basic operation of the system.
Three different sea states are used: the first is called "low energy (sea state)", the second "medium energy (sea state)" and the last one "high energy (sea state)".
In these figures the incident wave profile is shown for every case, in which *Te* is the energy period and *Hs* is the significant wave height.

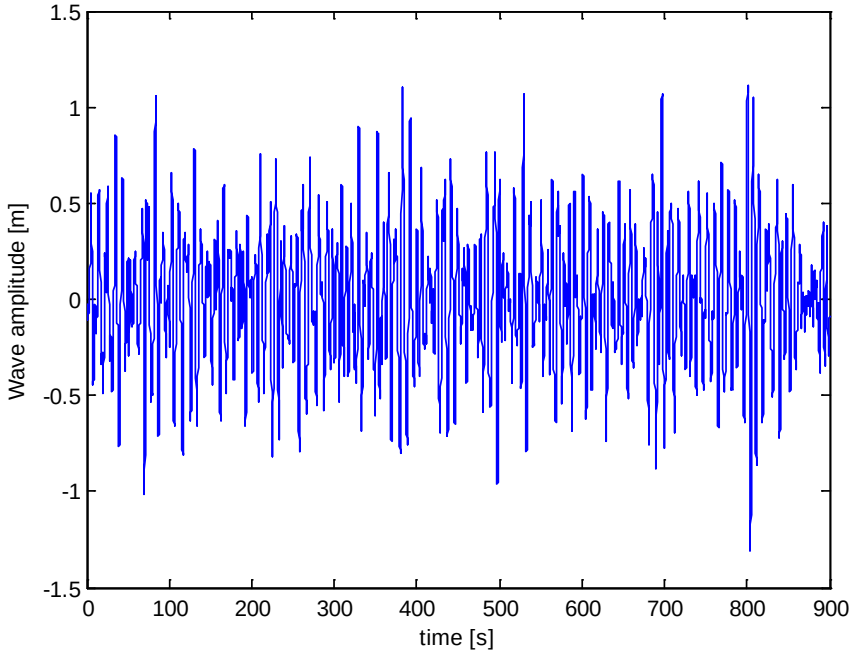

Figure 18 - Incident wave profile "low energy", *Hs* = 1.414 m, *Te* = 7.713 s.

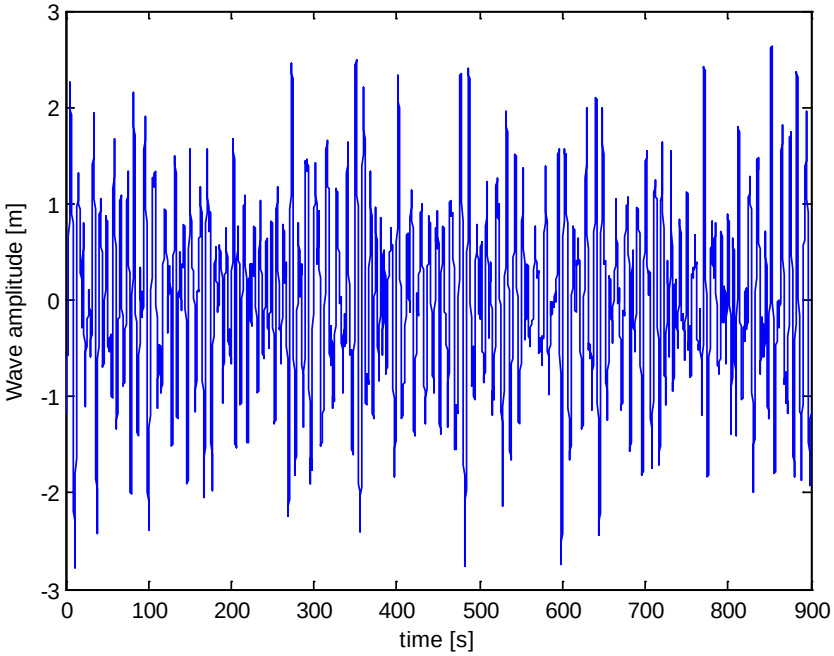

Figure 19 - Incident wave profile "medium energy", *Hs* = 3.75 m, *Te* = 9.5 s.

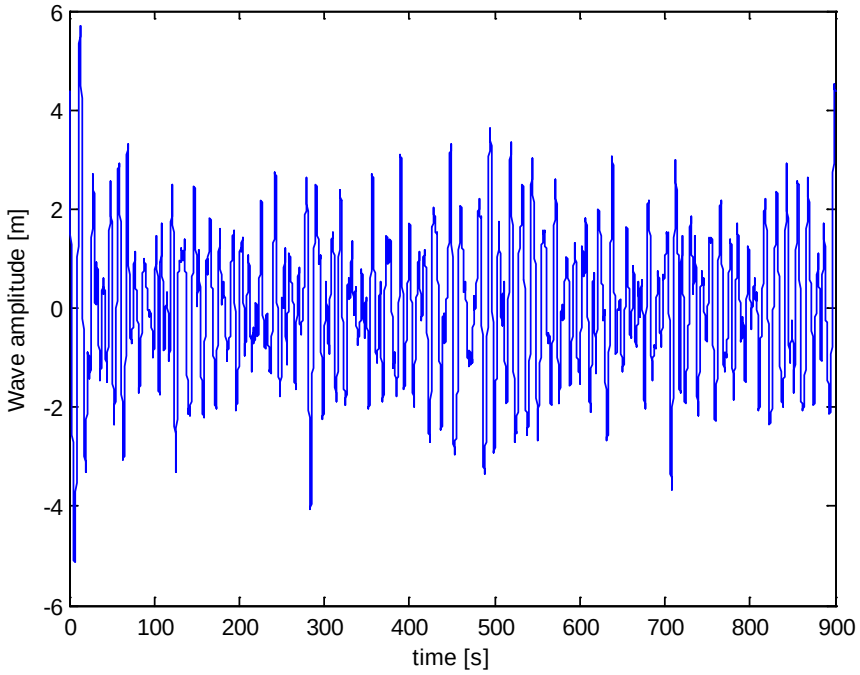

Figure 20 - Incident wave profile "high energy", *Hs* = 5.75 m, *Te* = 12.5 s.

These sea states are always the same for all the simulations. The Bretschneider spectrum generator would give different incident waves for the same *Hs* and *Te* used, because some parameters, like the phase used in the program, are generated randomly every time the wave generation is run [10]. This is why is important to use every time the same incident wave profiles.

4.1 Average mechanical power extracted

All of the three cases for every sea states are considered and there are general considerations in common which can be made:

- For all the diagrams there is a peak of the average power corresponding to a value of PTO force or the damping coefficient applied, for values of applied PTO force/damping coefficient lower or higher than this the mechanical power decreases.
- The higher the sea state energy is, the higher the PTO force/damping coefficient applied to obtain the peak of the average power.
- The maximum average mechanical power which can be extracted is the same for every control technique used in corresponding sea states.

In the following figure the results of the bidirectional case are plotted.

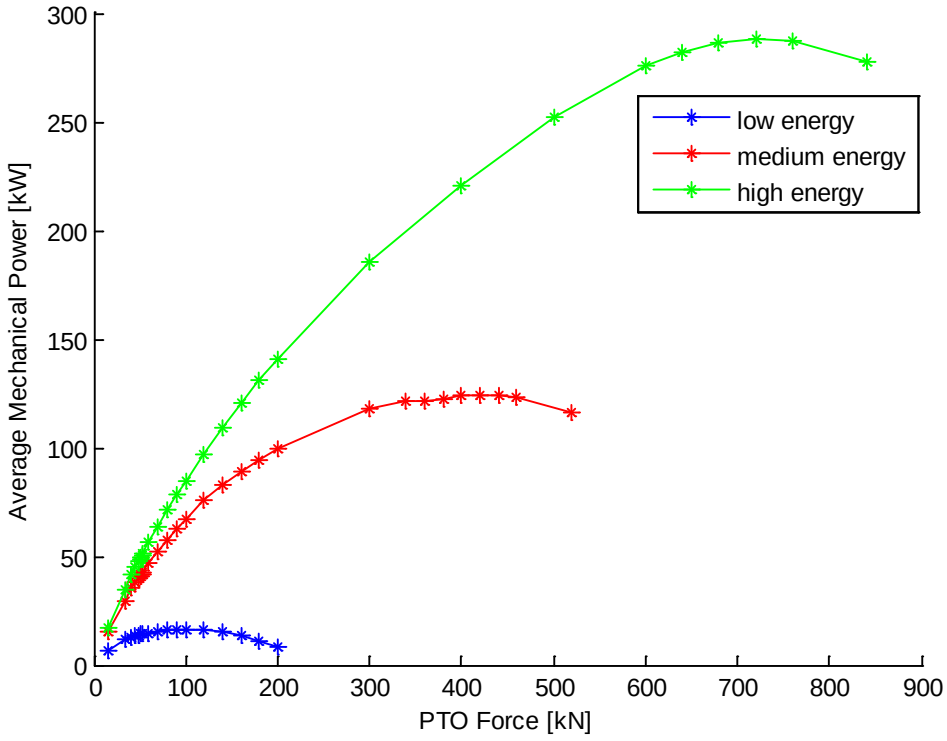

Figure 21 - Diagram Mechanical Power -PTO Force Bidirectional case

On this figure there are a lot of considerations to make. In the low energy sea state the maximum average mechanical power is very low, it's around 20 kW and is obtained with a PTO force close to 100 kN. Therefore the torque of the electric machine to obtain the maximum average mechanical power in this case must be 500 Nm, which is a little-medium value of torque for the standard machine installed in these typical applications.
For the medium energy sea state the situation changes and the peak power is about 125 kW with a PTO force applied of 400 kN, which corresponds to 2 kNm of applied torque. The same considerations can be made for the high energy sea state, in which

the peak power is 290 kW with a PTO force applied of 750 kN. Therefore the torque in this case is equal to 3.75 kNm.
As can be seen in the following figure the unidirectional case is plotted.

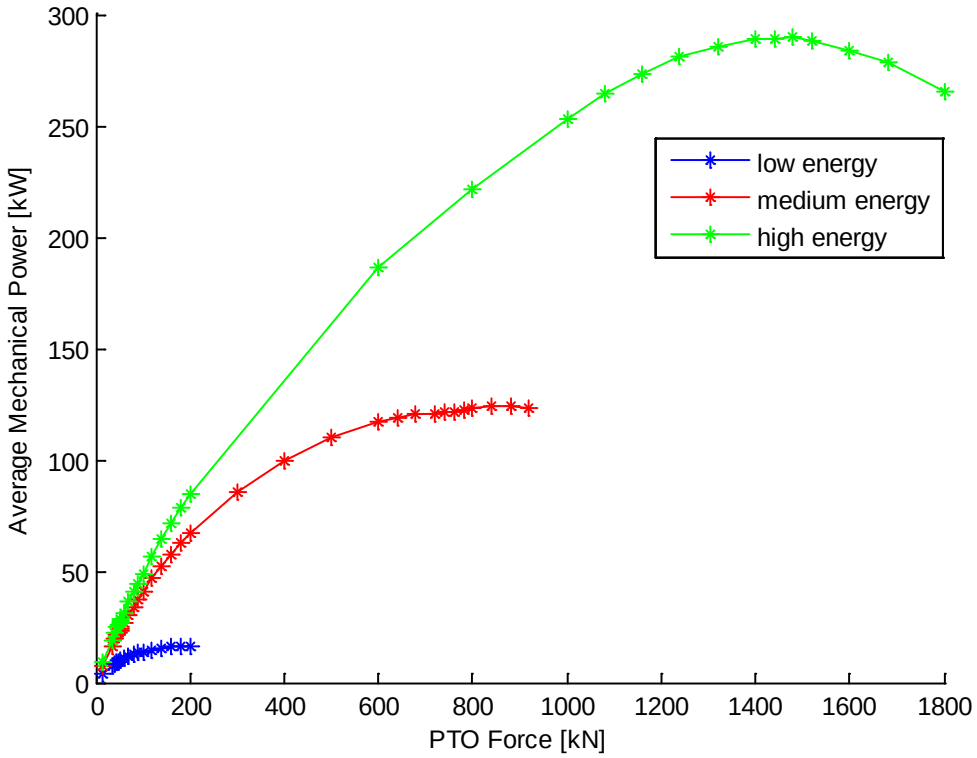

Figure 22 - Diagram Mechanical Power -PTO Force Unidirectional case

On this diagram also a lot of considerations can be made, the most important of these is about the value of the PTO force.
Compared to the previous diagram the PTO force applied is doubled to obtain the same maximum average mechanical power, this happens for every case. Besides, the average power remains close to the maximum value for a large range of PTO forces applied than in the bidirectional case.
The fact that the range of PTO force is large, is very useful and important because it allows obtaining values of mechanical power close to the maximum with different values of PTO force and then with different electric machines can be obtained very similar results.
The last case analyzed is the passive loading in which the trend of the average mechanical power is completely different from the previous diagrams.

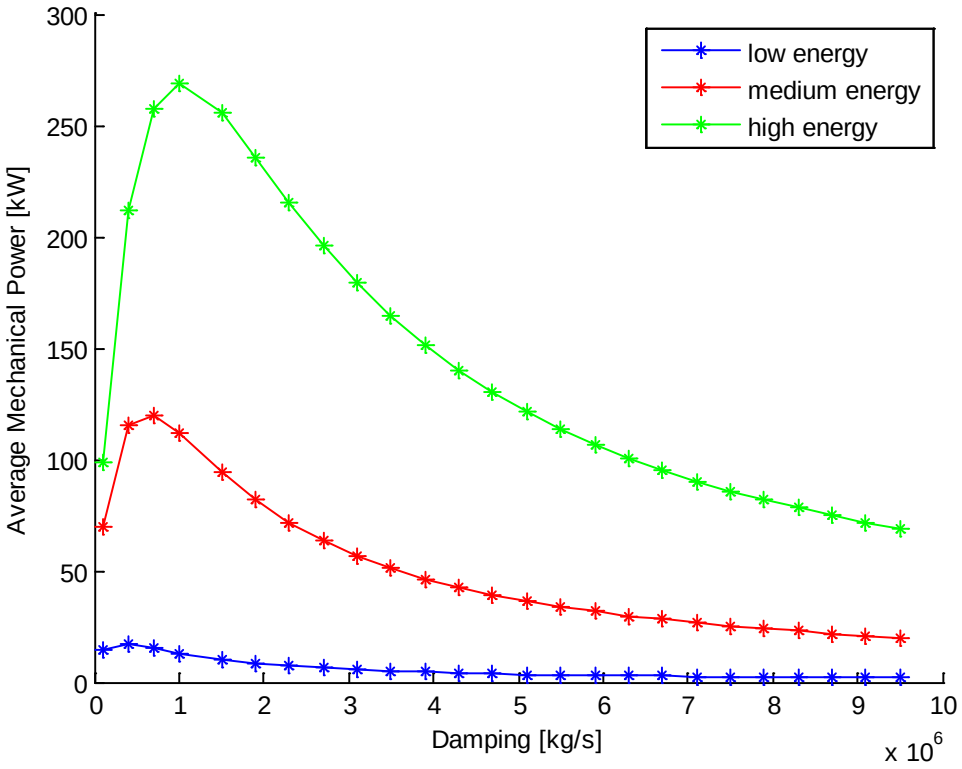

Figure 23 - Diagram Mechanical Power -Damping Passive Loading case

For the passive loading the situation is changed compared to the other cases, because the input of the program are different values of the damping coefficients (B_L) no longer the constant PTO force applied. In the low energy case the maximum average mechanical power is obtained with a B_L equal to 400000 kg/s, in the medium with B_L equal to 700000 kg/s and in the high energy case with B_L equal to 1000000 kg/s. Therefore for sea states with increasing energy, the value of damping coefficient that must be applied to obtain the maximum average mechanical power is increasing.

4.2 Maximum values analysis in bidirectional case

Other important considerations are based on the maximum values of:

- Torque;
- PTO force;
- Mechanical power;
- Buoy position;
- Buoy velocity.

In general it is possible to extract a trend of the buoy velocity and buoy position during all the simulation time but this is not always necessary, because at this stage it is interesting to evaluate only the maximum value of the position and velocity of the buoy. There is a limit for the moving of the buoy and if it is overpassed the model assumes an unnatural and non-linear behavior, that involves useless results.

In the following figures the behavior of torque, mechanical power and PTO force for different values of PTO force applied to the model of bidirectional case is shown. Every ordered value represents the maximum of that quantity.
In this case the input of the program is not the damping coefficient like in the passive loading control, but the PTO force applied constant in module with the same sign as the velocity. Then the diagram with PTO force and torque in order are a straight line because the PTO force applied is constant, therefore that is both the maximum value and the average value.

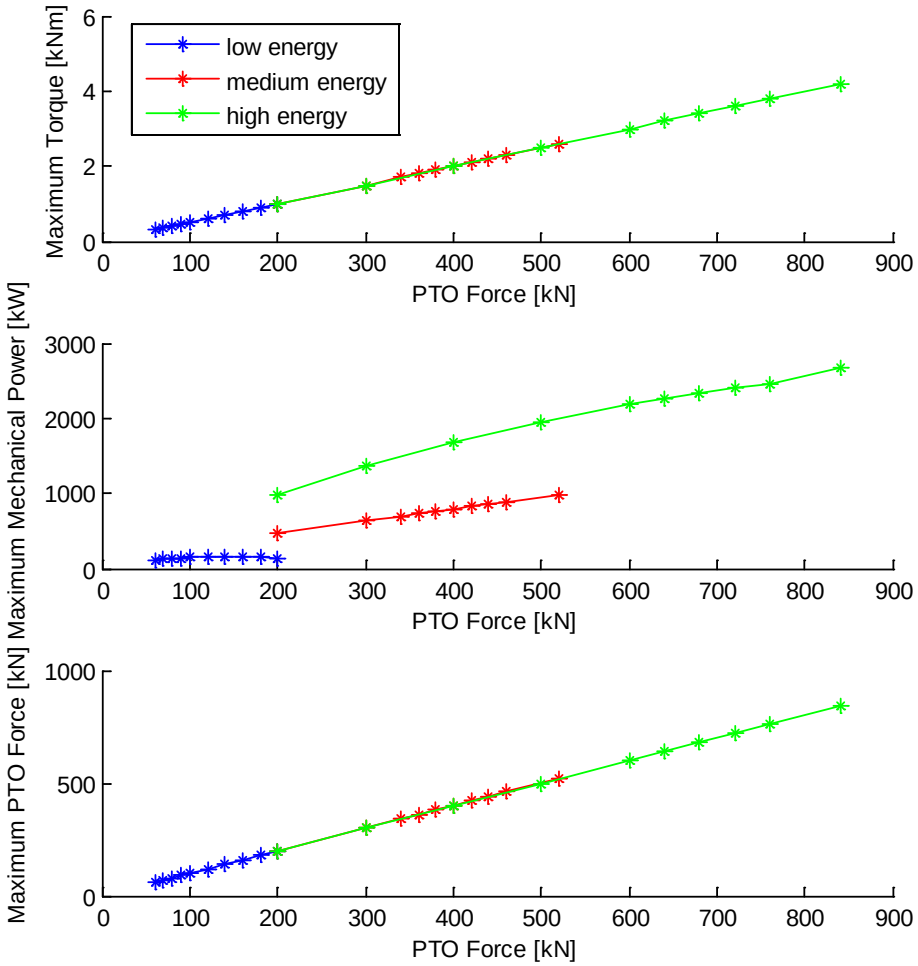

Figure 24 - Diagram Maximum Values of Torque, Mechanical Power, PTO Force in Bidirectional case.

The legend in the previous figure is the same for every diagram. The maximum values are useful to understand better the sizing of the electrical machine. Because if the machine is dimensioned for values of torque and power lower than the maximum values described in the diagrams, probably it will work in overload with serious consequences in performance and life time. With these diagrams a preliminary selection of the electrical machine can be made, or an appropriate control strategy can be selected if the electrical machine is already decided.
Now it is useful to compare the results between the two cases. In the passive loading control when the damping coefficient is higher than one million kg/s, the high energy

sea state requires very high values of torque (over 15 kNm) and PTO force (over 3000 kN) instead in the bidirectional case these values are about one third.
Those values of torque and PTO force are impossible to achieve, because usually the torque for an electrical machine with nominal power of 100 kW is close to 1 kNm, and a machine with nominal torque of 15 kNm is very expensive and useless.
Therefore the electrical machine can be dimensioned for a lower torque applied, with consequence savings, and its range of operation will be limited accordingly. For the low and medium sea state the situation is similar but the difference of values is smaller.
The trend of the maximum mechanical power is completely different in the two cases, respectively passive loading and bidirectional case. In the first one the value of maximum power reaches rapidly the highest value and then decreases, instead in the other case the maximum power increases always when the PTO force applied increases. Anyway the highest value of maximum power reached in the passive loading is higher than the highest value of maximum power in the other case.
An important difference between the two models is that the PTO force and torque in bidirectional case are constant and distinguishing between average and peak value is a non-sense, instead in the passive loading those shows in the diagram represent peak values in module considering the two directions of motion; then the average torque and PTO force applied in the passive loading is lower than the constant values applied in the bidirectional case and the values is close to zero.
Now the maximum values of buoy position and velocity are shown in the following figure.

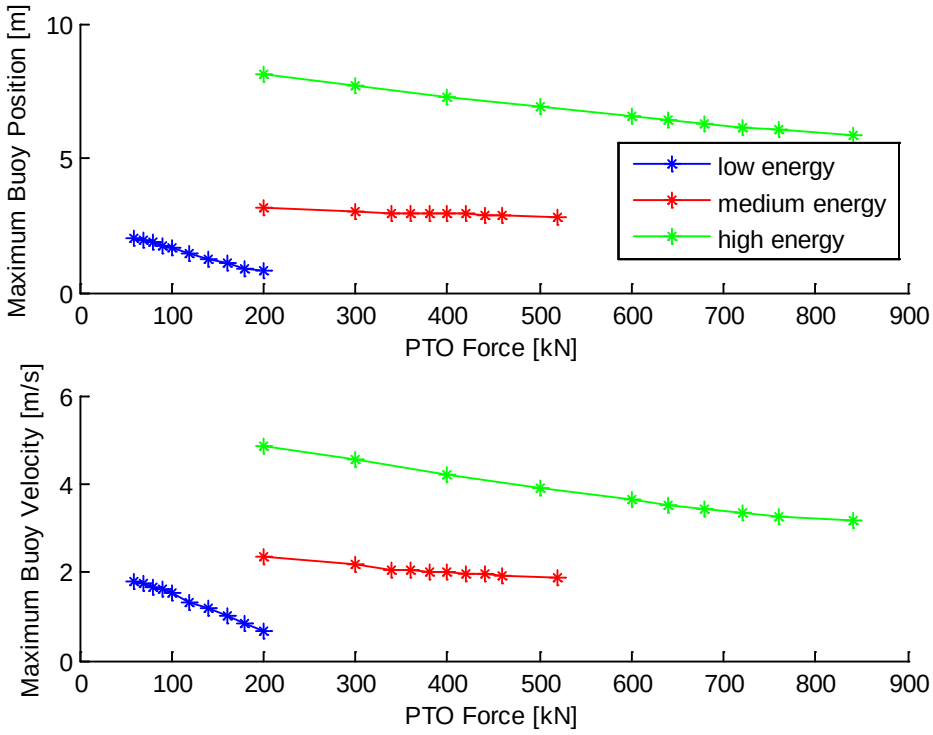

Figure 25 - Diagram Maximum Values of Buoy Position and Velocity in Bidirectional case.

As expected with high values of PTO force applied the buoy displacement and speed are low, but in a realistic model the buoy displacement should not pass 5 meters as maximum value because the buoy cannot exit from the sea.
Compared to the passive loading results the motion and velocity of the buoy are higher, at one point the PTO force applied is too high and impossible to considerer in a realistic model.

4.3 Maximum values analysis in unidirectional case

In the following figure the behavior of torque, mechanical power and PTO force for different values of applied PTO force to the model on unidirectional case is shown. Every ordered value represents the maximum of that parameter.
The input of the program is the PTO force like in the bidirectional case. The applied PTO force is constant in module with the same sign as the buoy velocity, which is considered only when positive. Then the diagrams with PTO force and torque in order are a straight line because the PTO force and the torque are directly proportional, like the bidirectional case.

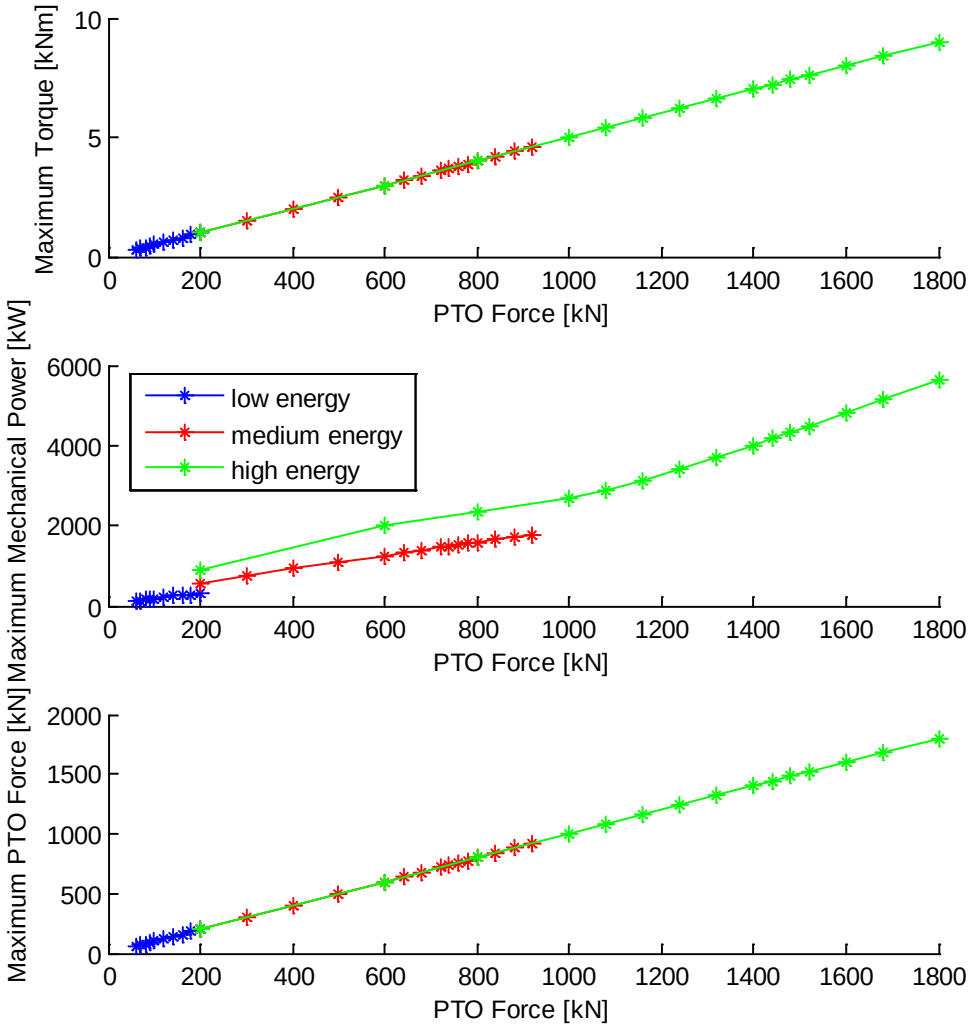

Figure 26 - Diagram Maximum Values of Torque, Mechanical Power, PTO Force in Unidirectional case.

As can be seen the trend of the diagrams is similar to the bidirectional case, the difference is only one: to obtain the same values of average mechanical power, the PTO force and torque applied must be double than the previous case. Therefore if the input force/torque applied is doubled to obtain the same results of the previous case, the maximum mechanical power is double because the PTO force and the maximum mechanical power are proportional for unidirectional and bidirectional cases, with same values of buoy velocity considered.
Like for the other cases, in the following figure there are the plots of maximum buoy position and velocity for the unidirectional case.

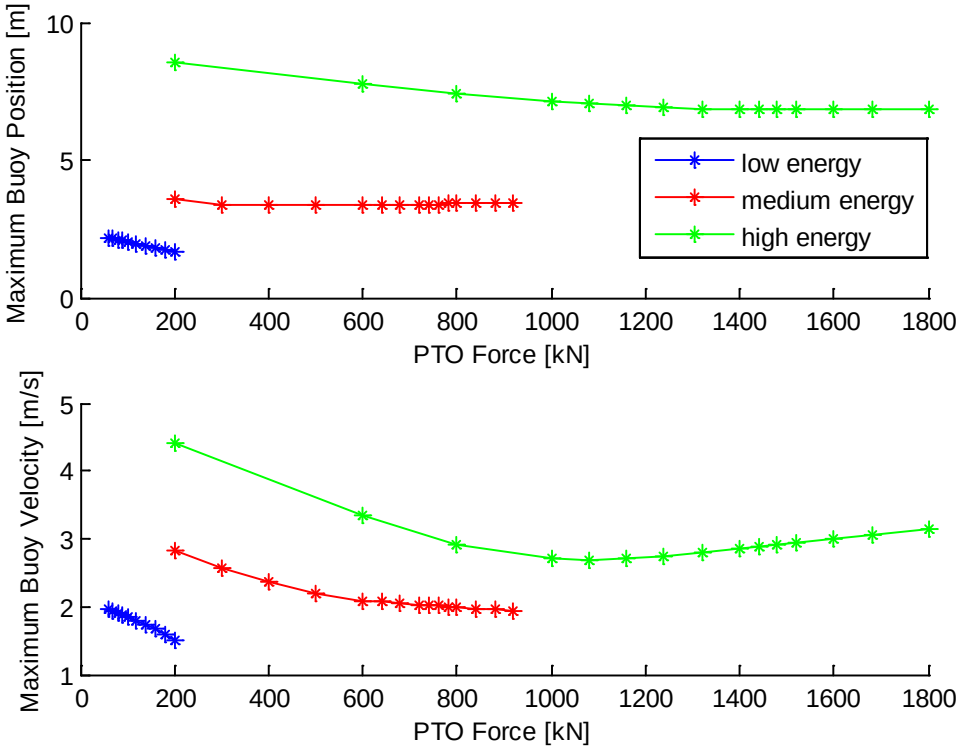

Figure 27 - Diagram Maximum Values of Buoy Position and Velocity in Unidirectional case.

In these diagrams the same considerations of the bidirectional case apply: as can be seen in the high energy sea state the buoy displacement is higher than in the other sea states. This is normal because the incident waves have a higher amplitude compared to the medium and low incident waves.

4.4 Maximum values analysis with passive loading control

In the following figures the behavior of torque, mechanical power and PTO force for different values of damping coefficient applied to the model with passive loading control is summarized. Every ordered value represents the maximum of that parameter.

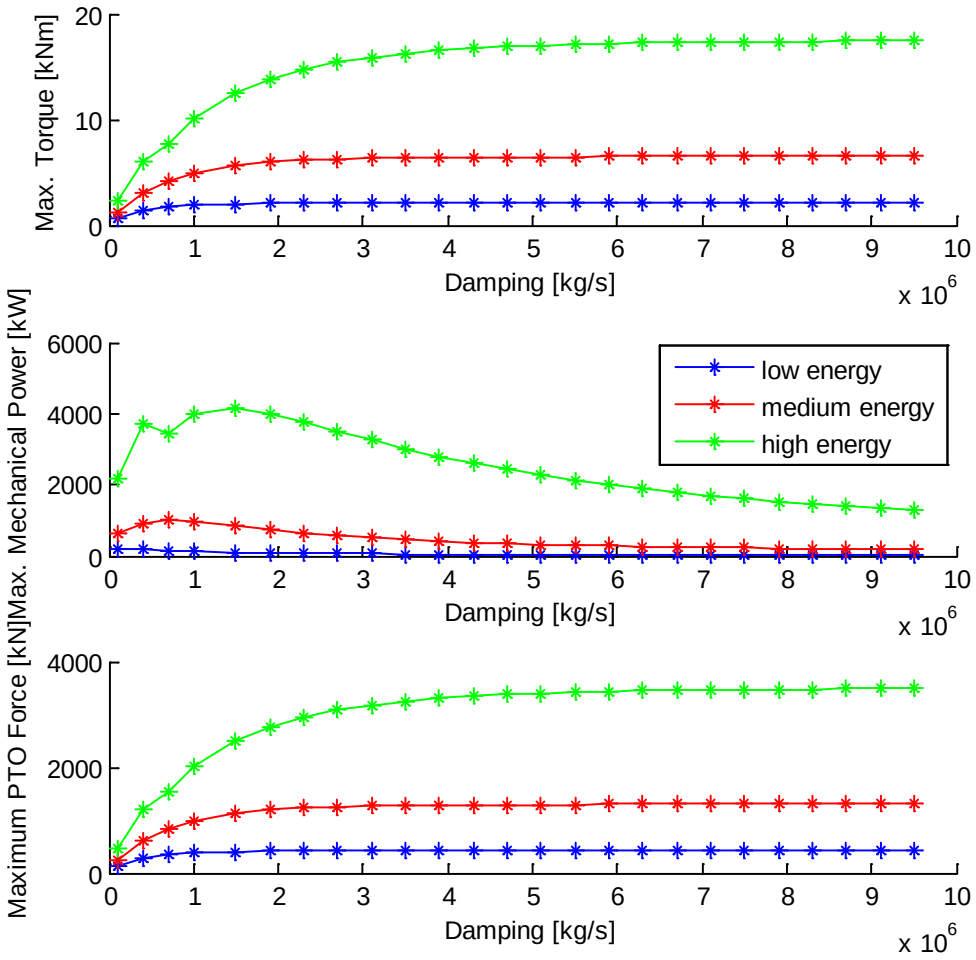

Figure 28 - Diagram Maximum Values of Torque, Mechanical Power, PTO Force with Passive Loading Control.

The legend in the previous figure is the same for every diagram. The things said about the sizing of the electrical machine for the previous case remain valid.
Now it is interesting to see the values of maximum buoy position and velocity in the passive loading control always with the low, medium, high energy cases.

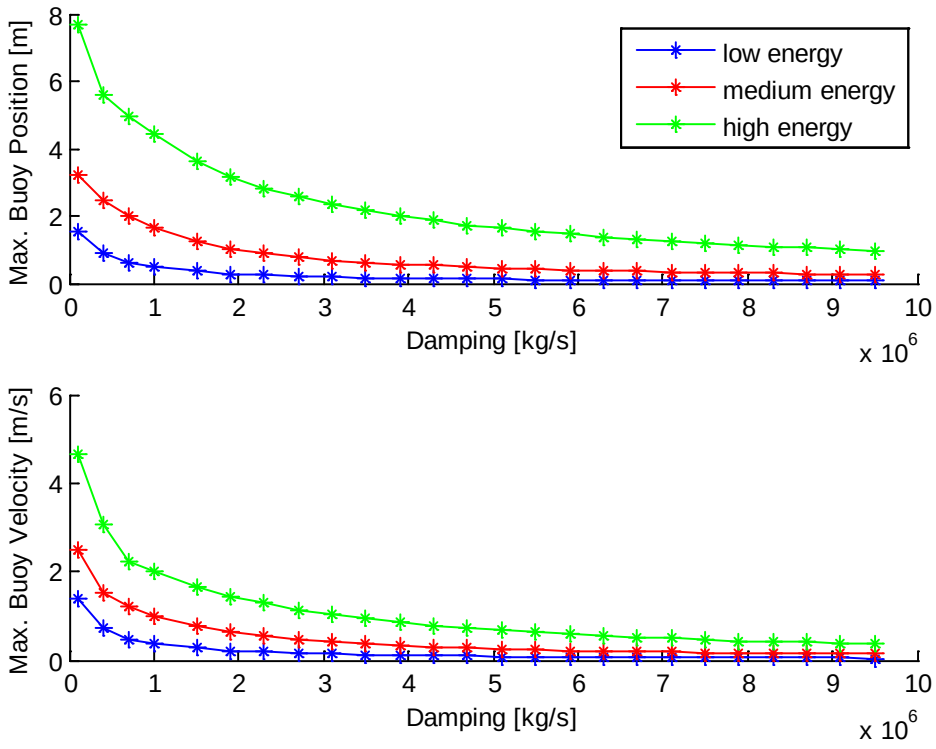

Figure 29 - Diagram Maximum Values of Buoy Position and Velocity with Passive Loading Control.

As can be seen with increased values of damping coefficients the position and velocity of the buoy decreases, this is due to the high values of PTO force applied that force the buoy to have a lower oscillation.

4.5 Final considerations

With these diagrams it's possible to understand better the behavior of the system in different sea states and which strengths and weaknesses the different types of control have. In the Simulink only the hydrodynamic model has been considered, one of the next possible step is to add the electric machine because here only the mechanical power extraction those shows in the diagram without any losses in the PTO.
All the presented solutions of control are valid, but the choice of the better one depends a lot on the energy of the sea state that is considered.
In the following table the main results are summarized.

Table 1 Main Results of the Simulations

		Max Average Power [kW]	PTO Force [kN] - Damping [kg/s]	Max PTO Force [kN]	Max Torque [kNm]	Max Power [kW]	Max Buoy Position [m]	Max Buoy velocity [m/s]	Peak to average power ratios
Low energy sea state	***case1***	17	90	90	0.45	144	1.77	1.6	8.47
	case2		180	180	0.9	288.1	1.76	1.6	16.95
	case3		400000	294.3	1.47	216.6	0.88	0.74	12.74
Medium energy sea state	***case1***	125	440	440	2.2	860.8	2.89	1.96	7.17
	case2		840	840	4.2	1659.5	3.44	1.98	13.28
	case3		700000	838.4	4.2	1004	2	1.2	8
High energy sea state	***case1***	290	720	720	3.6	2396.2	6.17	3.33	8.26
	case2		1480	1480	7.4	4326	6.86	2.92	14.92
	case3		1000000	2000	10	4005.2	4.41	2	13.81

With case 1, 2 and 3 bidirectional, unidirectional and passive loading cases are indicated, respectively. In the fourth column there are the values of PTO force (case 1 and 2) and damping coefficient (case 3) applied to obtain the same maximum average mechanical power, as can be seen in the third column. For the cases 1 and 2 the column of the maximum torque and PTO force are equal to the column of the PTO force used as input (with the respective proportions), because these value are inputs of the program and, as previous said, they are constant.
All the values in the table are referred to the situation which allows extracting the maximum average mechanical power.
Usually the electronic devices are dimensioned for the peak value of power and others parameters, this must be considered because in this case the power electronics equipment are dimensioned for high value of power when the average power is much less than this. It's better that the difference between the peak power and the average power is reduced. In addition the electrical machine that will be installed can't work in overload for too much time. The peak to average power ratios must be as little as possible, because this parameter says how much the maximum power exceeds the average power and then how much the PTO must be oversized.
For the high energy sea state the results obtained are important because it is not cheap to have all the power electronics devices oversized as said before, and this situation needs to analyzed better.
Now the next step that is useful to analyze is what can be done to obtain lower values of peak to average power rations, therefore in the following chapters a lot of limitations are introduced to make the models as realistic as possible and to optimize the applied control strategies.

5. Locations considered and results of the simulations

This chapter is based on the results obtained in the previous simulations which are considered as starting point. Here four different locations are considered and the goal of this chapter is to quantify the energy in MWh that can be extracted in one year for specific values of wave amplitude and energy period or zero crossing period. Another important thing regards the peak power values because, as said in the previous chapter, all the power electronics components are dimensioned for the peak power value.
All the data of the locations are based on real values occurred [11] (general and site related wave data), thanks to this it is possible to compare the results obtained with different models which use the same data for the considered locations.
In the following paragraphs the main relevant technical definitions are introduced and it is explained how and why the locations have been chosen.

5.1 Scatter diagram and choice of the locations

To understand better what is explained in the following paragraphs is useful to define what a scatter diagram is and what its structure is. A scatter diagram is a diagram usually very close to a rectangular matrix which has the energy period *Te* or the zero crossing period *Tz* on the x-axis and the wave amplitude *Hs* on the y-axis.
The relation between *Te* and *Tz* is the following, and further information can be found in [12]:

$$\boldsymbol{Te = 1.2 * Tz} \qquad \textbf{(5.1)}$$

Starting from this general definition it is possible to specify better what every scatter diagram can describe, because there are a lot of different types of scatter with same x- and y- axis but different content. The typical content of the scatter diagram are wave data occurrences, extracted power, and yearly energy. From now on, all the diagrams which contain, for each sea state (each box), the wave data occurrences are called simply “scatter diagrams”, the diagrams which show the extracted power are called “extracted power scatter diagrams” and the diagrams with the yearly energy are called “yearly energy scatter diagrams”. In the following figure there is a scatter diagram which describes the wave data for Emec location.

Hs \ Tz	<3	3,5	4,5	5,5	6,5	7,5	8,5	9,5	10,5	11,5	12,5	13,5	14,5	Sum	Tz ave	dP
0,25		2653	3618	1943	791	356	250	137	31	2				9781	4,89	0,02
0,75		2273	9363	5794	2063	734	182	85	40	2				20536	5,05	0,34
1,25		453	6484	6977	2946	1131	328	106	38		9	7	2	18481	5,48	0,93
1,75		130	2035	7652	2823	1029	352	139	21	0		5		14186	5,81	1,48
2,25			288	5405	3838	1081	319	184	66	9				11190	6,20	2,06
2,75			26	1135	5072	1135	234	137	52	17	2		2	7812	6,65	2,31
3,25			5	137	3278	2002	250	106	35	19	7			5839	7,01	2,54
3,75				14	713	2714	415	92	14	9	2			3973	7,49	2,46
4,25					57	1725	550	94	40	19	0	5	5	2495	7,88	2,09
4,75					7	430	861	118	26	14	5			1461	8,35	1,62
5,25						45	767	144	31	5				992	8,68	1,40
5,75						0	267	255	7	2	5			536	9,05	0,94
6,25					2	5	54	227	14	5				307	9,35	0,66
6,75						5	5	142	80	5				237	9,82	0,62
7,25								66	111		2			179	10,15	0,56
7,75								31	109	2	2			144	10,33	0,53
8,25								7	31	21				59	10,74	0,25
8,75									26	26				52	11,00	0,26
9,25									2	19	5			26	11,62	0,15
9,75										14	2			16	11,63	0,10
10,25										7	2			9	11,72	0,07
10,75											2			2	12,50	0,02
11,25											5			5	12,50	0,05
11,75														0		
Sum	0	5509	21819	29057	21590	12392	4834	2070	774	197	50	17	9	98318		21,46

Figure 30 - Joint probability diagram (*Hs* and *Tz*) for the EMEC location RP5OS 59,00°N;3,66°W (absolute numbers of occurrences, all directions, all year).

This scatter describes how many times in the considered time interval a wave with those particular values of *Hs* and *Te* occurred. There is one of this scatter diagram for each considered location, the last three columns (which are "*Sum*", "*Tz ave*" and "*dP*") are useless for the purposes of this work and can be considered as statistic values. Of these three columns only the value "98318" (which is different for every considered location) needs particular attention because it's the sum of the total occurrences wave data, and through this it is possible to calculate corresponding yearly-percentages.
There are been considered four locations, which are:

- Emec;
- Haltenbanken;
- AUK;
- WaveHub.

For Emec and WaveHub the wave data in [11] is reported in *Tz* and *Hs*, while in Haltenbanken and AUK the wave data is reported in *Te* and *Hs*. This thing is very important because the inputs of the Matlab program to generate the spectra for every sea state are different.
Basically two types of approach are possible:

- in the first one all the sea states are independently generated for every location. In the final step of the calculation the average power extraction results for the sea states in common among the different locations are averaged to obtain one single value as a reference for the considered sea state (which is then considered valid for all the location);

- in the other, in the beginning the sea states in common among the locations are generated only one time and for all the next steps the average power extraction results with the common sea states are the same.

There are not many differences among the two approaches, because the random parameters that can change the generation of the wave profile (corresponding to the sea states) from a specific *Hs* and *Tz*/*Te* have usually negligible effect on the average power extraction [13]. Therefore to obtain a verification of this aspect the first approach is implemented.
At this point it is useful to describe the characteristics of every location, all of those are in Europe and are the most common locations subject of study in the last years for wave energy application testing.

Figure 31 - Map of the Locations

Emec location is situated in the North Atlantic, the acronym Emec stands European Marine Energy Center. This is the location that experiences more different sea state, 130 in total and a lot of those are in common with the other locations.
The second location which has more different sea states is Haltenbanken, this location is situated in Norway in the Norwegian Sea. It's considered one of the most powerful zones for the wave energy because the Norwegian Sea is located in the North Atlantic in a windy zone.

AUK location is in the North Sea and is not as powerful as Haltenbanken. The Wave Hub test site is a project site in the Southwest of England, located 16 km offshore near Cornwall St. Ives Bay.
Of the four locations that are considered in thesis it is important to understand what kinds of programs are implemented to obtain the final result.

5.2 Matlab-Simulink model description

In the beginning for all the sea states of each location, a spectrum using the Bretschneider spectrum equation was created for each *Hs* and *Tz*/*Te*, and starting from this all the wave profiles were elaborated. The result is an array which has in the first row the step time from 0 to 900 seconds and in all the other row (one for each pail *Hs* and *Tz*/*Te*) the excitation force produced by the sea state with those values of wave amplitude and energy period or zero crossing period on the considered buoy. As a result for Emec there are 131 rows, for Haltenbanken 93 rows, for AUK 70 rows and for WaveHub 59 rows.
To create the wave profiles, the matrix of the real wave data in a text file is used as input in the Matlab program, therefore in total there are four matrixes (one for each location) in text file format.
Now it's important to clarify that the previously generated arrays are always used for all the next simulations that require this kind of input. This is an important thing because if the inputs are changed the results obtained are not comparable.
Anyway in this first part only a program in Matlab is necessary to generate such array, and the array with the excitation forces is the input for the next program which is completely automated and uses also a Simulink model.
With this second program the results of the simulations are matrixes which contain the average mechanical power extracted by the point absorber for every sea state, and have as many columns as the values of applied PTO torque and as many rows as the sea state of the considered location. Like in the chapter 4 both bidirectional case and unidirectional case are here implemented, then in total there are eight matrixes from which it is possible to create the diagram of the average mechanical power.
Subsequently another Matlab program is implemented and it gives the diagram of average mechanical power from the previously described matrixes.
The first type of scatter contains in each box the average mechanical power (single value, i.e. considering each location separated from the others), which the considered buoy can extract from that specific sea state. In the following figure there is an example of extracted power scatter diagram.

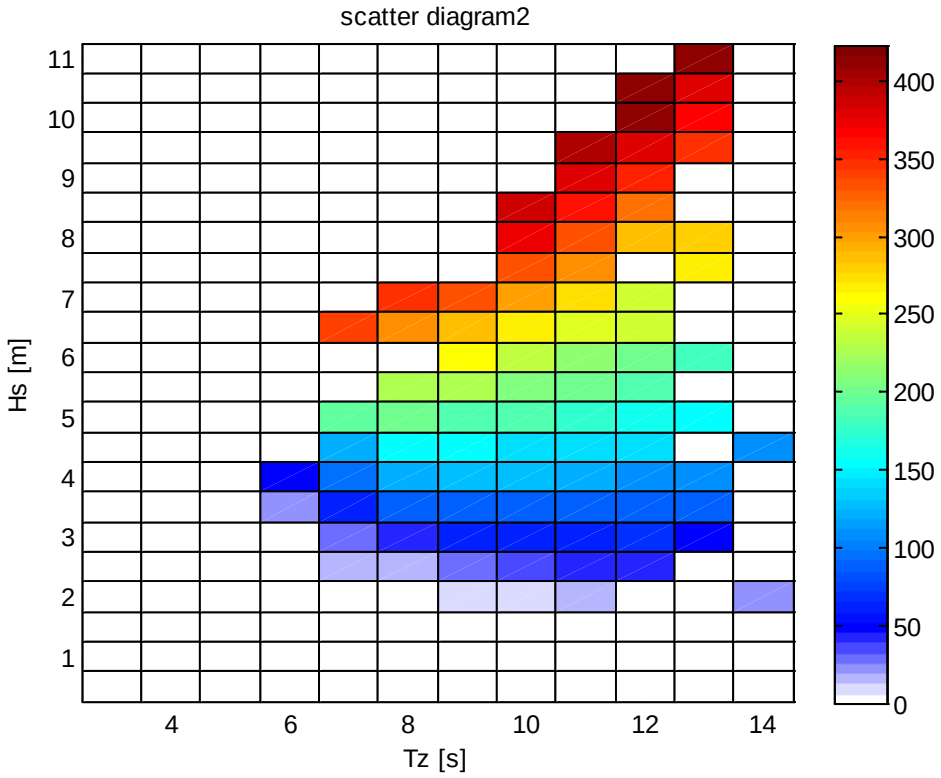

Figure 32 - Extracted power scatter diagram Emec location bidirectional case, applied torque 2 kNm and average power in kW.

In the previous figure the highest values of power are obtained for high values of wave amplitude and zero crossing period as can be expected. Therefore the locations which have a lot of sea states with higher values of *Hs* and *Te*/*Tz* will have high values of extracted power. In general it's not obvious that high values of extracted power match high values of yearly energy, because the yearly energy depends on the wave occurrences data and usually the sea states with higher values of extracted power are the ones that appear less.

The other scatter contains the yearly energy, i.e. the energy that can be extracted in one year from each sea state of that location. The normalized power is the single value of power multiplied for the number of time it appears in the data of measurements divided by the total number of measurements in all the data. The normalized power serves only as intermediate step to obtain the yearly energy scatter diagram. The following figure shows the yearly energy scatter diagram for Emec location.

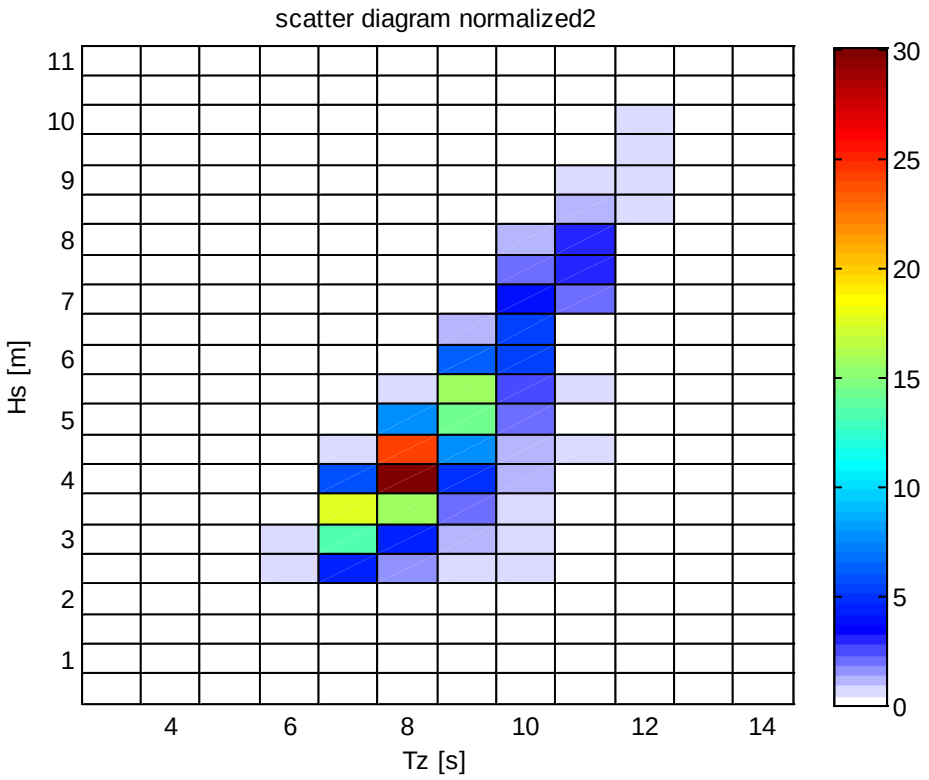

Figure 33 - Yearly energy scatter diagram Emec location bidirectional case, applied torque 2 kNm and energy in MWh.

As can be seen a lot of sea states give a very small contribution to the yearly energy, and in the diagram the values are close to zero. Then as said before, the boxes which have high values of extracted power in this case becomes close to null when they are normalized to obtain the yearly energy scatter diagram. This result depends only to the wave occurrences data, i.e. the boxes with high values of extracted power appear less in the range of time measurement wave data.
In Emec location this situation is more pronounced compared to the other locations but in general this is the trend.

5.3 Results of the simulations

A Matlab program is implemented with five different values of constant torque, considered for both bidirectional and unidirectional case. As can be seen in the following table there are the five values of torque.

Table 2 Applied constant torque [kNm]

Applied constant torque [kNm]
1
2
3
4
5

The choice of these values is not random, because one of the results obtained in the chapter 4 is precisely what value of applied PTO torque is necessary to obtain (in average) the highest values of extracted power, considering the medium energy case. The reference to the medium energy sea state is done because this is the sea state that usually appears more often in terms of wave occurrences and consequently because it gives the highest contribution in the yearly energy scatter diagram.
The values of average mechanical power obtained with these values of applied torque are fine and they are in general typical values for a wave energy site.
One of the important things about the simulation program is that the minimum time step with higher values of torque needs to be small, close to 10^{-6} because the stiffness of the system is high and this is the simplest solution to ensure the stability of the Matlab code. Another way is to increase the tolerance between two consecutive steps but the results can be inaccurate, this is why the first solution is implemented.
In the following table there is a plot with the average power extracted by the point absorber for the sea states occurring at Emec, and for the sea states in common with WaveHub the average value of the power extraction is calculated. These are values of average power that are produced for every sea state in kW with an applied PTO constant torque of 1 kNm in the bidirectional case.

Table 3 Average mechanical extracted power in kW, bidirectional case, values of *Tz* in seconds and *Hs* in meters

Hs\Tz	**4.5**	**5.5**	**6.5**	**7.5**	**8.5**	**9.5**	**10.5**	**11.5**	**12.5**	**13.5**	**14.5**
0.75	0	0	0.01	0.29	0.87	1.46	1.11	2.40	0	0	0
1.25	0.02	0.87	4.87	8.20	10.82	13.20	12.72	0	12.83	11.27	9.97
1.75	0.56	8.83	19.44	24.23	26.91	28.24	26.94	0	21.60	21.42	0
2.25	5.50	27.79	38.68	44.49	43.30	43.08	38.33	38.30	0	0	0
2.75	18.23	50.30	65.34	63.69	62.35	55.91	53.50	48.54	45.03	0	38.87
3.25	34.24	84.19	87.61	83.18	75.37	70.92	67.31	59.77	58.17	0	0
3.75	0	108.37	111.78	105.75	93.68	86.84	78.56	70.12	65.96	0	0
4.25	0	0	137.29	131.28	113.52	101.51	93.27	83.75	0	68.89	66.33
4.75	0	0	168.52	152.09	128.79	118.00	106.75	97.67	88.89	0	0
5.25	0	0	0	174.72	151.03	132.09	121.17	112.66	0	0	0
5.75	0	0	0	0	176.17	148.12	132.42	121.31	109.25	0	0
6.25	0	0	266.30	220.09	191.79	166.65	154.69	138.55	0	0	0
6.75	0	0	0	244.50	218.81	184.72	163.35	145.21	0	0	0
7.25	0	0	0	0	0	201.19	186.80	0	152.55	0	0
7.75	0	0	0	0	0	229.23	193.46	168.56	157.45	0	0
8.25	0	0	0	0	0	234.77	211.54	187.04	0	0	0
8.75	0	0	0	0	0	0	219.76	203.79	0	0	0
9.25	0	0	0	0	0	0	239.04	218.18	192.30	0	0
9.75	0	0	0	0	0	0	0	239.74	203.55	0	0
10.25	0	0	0	0	0	0	0	237.13	211.96	0	0
10.75	0	0	0	0	0	0	0	0	233.58	0	0
11.25	0	0	0	0	0	0	0	0	239.40	0	0

In the previous table the rows or columns which have null values of average power in all boxes are deleted, this is why the zero crossing period starts from 4.5 and the wave amplitude starts from 0.75. The applied torque value is 1 kNm, which is the value that for bidirectional case allows obtaining the highest value of yearly energy.
As can be seen the highest values of power are obtained with high values of wave amplitude and zero crossing period, this result is as expected based on equation (1.1). For increasing values of *Tz* (with the same *Hs* considered) the power does not always increase, i.e. the highest values of extracted power are obtained with relationship between *Hs*/*Tz* close to one. Vice-versa for increasing values of *Hs* (with the same *Tz* considered) the power always increases. Therefore the highest value of extracted power is 266.30 KW and it's obtained with *Tz* = 6.5 and *Hs* = 6.25. The relationship between these values is close to one and in all the matrixes this is the relationship that comes closest to one.
Considering the unidirectional case with applied torque equal to 2 kNm, which is the value that allows obtaining the highest value of yearly energy for the unidirectional, all the previous comments are valid. Then to obtain the same values of yearly energy it is necessary to apply a double value of PTO torque in the unidirectional case compared to the bidirectional case, this is a very important consideration because it affects a lot the choice of the electrical machine size.
Starting from the previous table, it is now possible to derive the extracted power scatter diagram for the considered point absorber but to obtain the yearly produced energy scatter diagram it is necessary to consider every single location because the data of occurrences are different for each one.
An example of extracted power scatter diagram is plotted in the following figure.

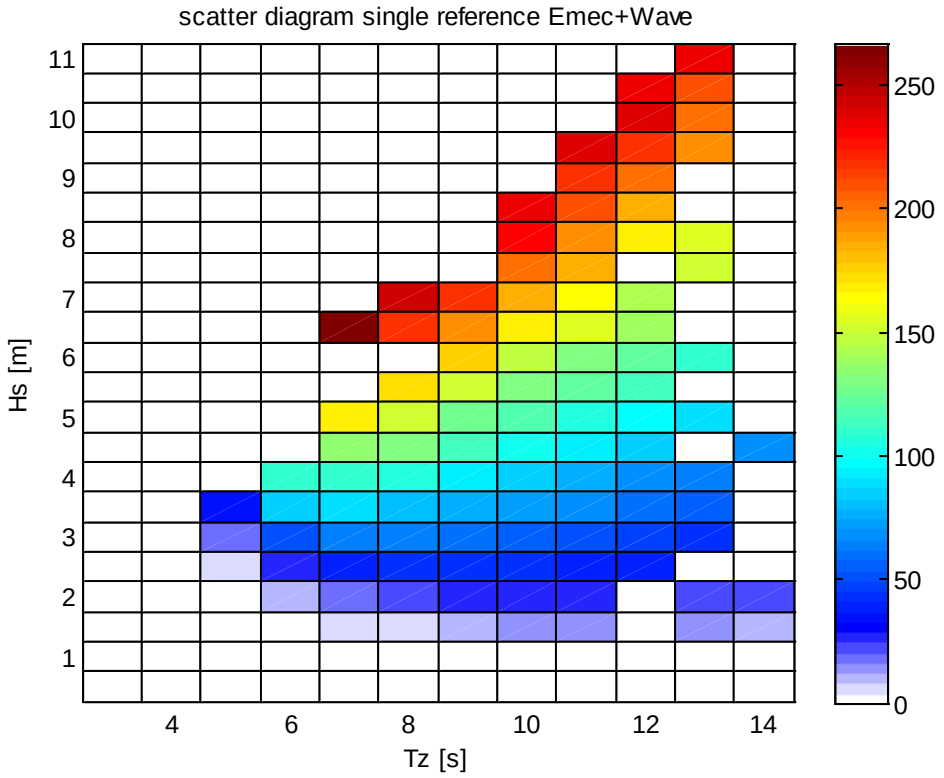

Figure 34 - Extracted power scatter diagram bidirectional case, applied torque 1 kNm and average power in kW.

This is the general scatter diagram for the average power which is considered as reference, in total there are four of this scatter reference diagrams because Emec with WaveHub (which have *Tz* as ordered) and Haltenbanken with AUK (which have *Te* as ordered) for both bidirectional and unidirectional case are considered.
In this diagram for the boxes in common between the locations the average value is calculated and for the boxes not in common only the value that appears in the respective location considered in the figure is shown. Compared to figure 5.3, apart the difference of the applied torque, in figure 5.5 the mean of extracted power considering the locations which have *Tz* in the x-axis (Emec and WaveHub), is shown, while in figure 5.3 the extracted power for sea states which appear in Emec location only is shown. Basically figure 5.5 contains more sea states than figure 5.3 (there are less white boxes compared to figure 5.3), because Emec has a lot of sea states in common with WaveHub but not all of them. Sea states in common between Emec and WaveHub have very similar average power values as expected.
Now it is useful to consider the energy that each location produces in one year and the peak power for every analyzed situation.
The maximum value of energy usually is found in the first column for the bidirectional case and in the second column for the unidirectional case, as can be seen in the following table. The values of torque are in kNm and values of energy are in MWh.

Table 4 Energy extracted in a year in MWh

	Torque=1 kNm	Torque=2 kNm	Torque=3 kNm	Torque=4 kNm	Torque=5 kNm
WaveHub Bidirectional	201.569	150.289	89.944	54.019	31.301
WaveHub Unidirectional	192.441	203.087	183.649	155.089	125.487
Emec Bidirectional	259.183	230.641	170.392	117.003	76.904
Emec Unidirectional	226.773	260.065	253.933	233.101	204.747
AUK Bidirectional	283.938	214.072	136.189	74.769	40.772
AUK Unidirectional	275.257	284.340	252.194	216.161	180.026
Haltenbanken Bidirectional	504.268	500.480	409.190	318.290	229.240
Haltenbanken Unidirectional	404.538	504.740	525.367	505.530	466.860

At this point the keys considerations are the following:

- For sea states with high values of *Hs* and *Tz*/*Te* it's possible to extract, always higher values of average mechanical power increasing the applied PTO torque (this is valid for the five values of torque considered). In particular to obtain the same extracted power in the same sea states, the applied torque in the unidirectional case is close to double compared to the bidirectional case. Therefore with 5 kNm of applied torque the highest values of extracted power are obtained (this is valid for the sea states with high values of *Hs* and *Tz/Te*) both for bidirectional and unidirectional case. For sea states with low or medium value of *Hs* and *Tz/Te* (*Hs* = 1-5 m and *Tz/Te* = 3-10 s) the maximum values of extracted power are obtained in bidirectional case with 1-2 kNm of applied torque and in unidirectional case with 2-4 kNm of applied torque. For values of applied torque higher than these the extracted power decreases. This is very important because the applied torque to obtain the maximum value of yearly energy in a location depends not only on how many times the most powerful sea states (for the applied torque considered) occur in a year but also how many these most powerful sea states are (with this applied torque).
- Then if Haltenbanken location has the higher value of yearly energy in unidirectional case with 3 kNm of applied torque, it means that Haltenbanken has a lot of medium-high energetic sea states which occur in a year and they are maximized with this value of applied torque. While the other locations have on average the most powerful sea states (high values of *Hs* and *Te/Tz*) that do not occur so often in a year and this is why the applied torque to obtain the highest value of yearly energy is lower. Basically the Haltenbanken location has a lot of sea states with medium-high values of *Hs*

and *Te* that appear many times in a year. This is why the yearly energy is maximized with applied torque of 3 kNm in unidirectional case, probably for bidirectional case in Haltenbanken the maximum yearly energy is obtained with 1.5 kNm of applied torque which is not considered in the previous simulations.

- The other locations have the high energy sea states that appear fewer times in a year than at Haltenbanken location, then the sea states that appear more in a year at these locations are those with low-medium energy.

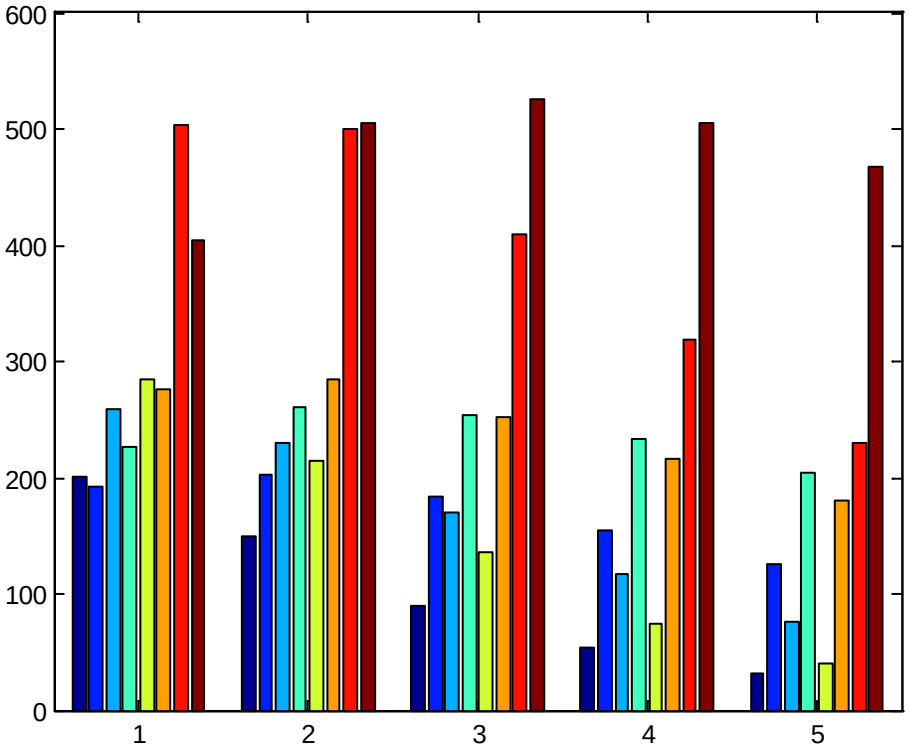

Figure 35 - Bar diagram yearly energy in MWh

In the previous diagram the values of yearly energy that can be extracted for each location are shown. Both bidirectional and unidirectional cases are considered, in the x-axis there is the value of applied torque in kNm and in the y-axis there is the value of the yearly energy in MWh. The bars are in pairs of two, starting to the left respectively bidirectional and unidirectional case for WaveHub, Emec, AUK and Haltenbanken. The Haltenbanken location, as previously said is the location which has the highest values of extracted yearly energy, sometimes happened that the energy extracted in the unidirectional case (considering the same applied torque) in a location is higher than another location but for the bidirectional case this does not happen. This is due to what was said before, i.e. the extracted energy depends on how many the sea states giving the higher value of extracted power for a specific torque are and how often they occur.

In the following table the peak values of power for each situation are summarized. The values of torque are in kNm and the peak power is in kW.

Table 5 Values of peak power in kW

	Torque=1 kNm	Torque=2 kNm	Torque=3 kNm	Torque=4 kNm	Torque=5 kNm
WaveHub Bidirectional	847.845	1592.869	2206.097	2836.249	3547.776
WaveHub Unidirectional	890.119	1695.688	2440.031	3185.729	3883.630
Emec Bidirectional	1580.769	2884.435	3918.072	5285.431	6522.007
Emec Unidirectional	1683.218	2918.123	4239.401	5526.606	6611.375
AUK Bidirectional	1432.096	2410.521	3273.022	4168.655	4679.054
AUK Unidirectional	1591.468	2864.192	3943.865	4821.010	5652.140
Haltenbanken Bidirectional	1728.200	3248.425	4615.340	6044.954	7161.999
Haltenbanken Unidirectional	1802.809	3456.399	5103.086	6496.845	7859.911

The maximum values of peak power is always for the Haltenbanken location considering the same applied torque, this is because Haltenbanken has the most powerful sea states. Those values depend only on the sea state features and are not related with the data of the scatter diagram, and it is not said that the highest values of peak power give the maximum values of extracted energy in a year.
In all of this chapter there is no power limit, this condition is not realistic and for more realistic results it is useful to introduce a power limit which depends on the machine size that is considered.
Another important aspect to consider is that the buoy position is not limited in this chapter, in a good physical model the buoy stays for a half inside the sea and for a half outside the sea at the equilibrium point. Considering the buoy radius and draught (5 meters each) as limit it's unnatural that the buoy passes this 5 m limit of position, because this means that the buoy does not touch the sea anymore (suspended in the air) or it is completely under the sea. In this case the behavior of the buoy would be highly nonlinear and unpredictable, and it would not be correctly represented by the proposed model anymore. To ensure that the buoy respects this physical limit in the next chapter this problem will be considered and a system with limit switch for the buoy position control will be implemented.
Basically these values of extracted energy in a year for the model that is considered are impossible to obtain in a realistic situation, therefore this is like an ideal situation.

5.4 Selective torque control

In this paragraph a new method for maximizing the average extracted power using different values of torque as input is considered. Starting from the previous five values of torque (1, 2, 3, 4, 5 kNm), for each location a table with the average power extracted is built considering all the sea states that appear in the considered location.

So in total for each location there are 5 tables, and every table shows the average mechanical power extracted for a single value of torque considered as input.
It's obvious that for every value of torque used as input the extracted power is different considering the same sea state, then it's possible to apply different value of torque for the different sea states of a location, with the goal of maximizing the power extracted in each sea state.
For every location all the five tables with their respective values of torque applied are considered and a final table for each location is built, in which the sea states have different values of torque applied for maximizing the mechanical power extracted.
In the following figure the final table for the Emec location is shown. This is the legend to understand the results:

Constant torque applied by the PTO
1 kNm
2 kNm
3 kNm
4 kNm
5 kNm

For each box the maximum value of average mechanical power extracted in kW for the bidirectional case is shown. The color of the box is useful to understand immediately which value of torque is used as input to obtain the maximum power value indicated.

Table 6 Average mechanical extracted power in kW (selective control), bidirectional case, *Te* in seconds and *Hs* in meters

Hs/Te	3	4.2	5.4	6.6	7.8	9	10.2	11.4	12.6	13.8	15	16.2	17.4
0.25		0.001294	0.001029	0.000964	0.000923	0.000903	0.000881	0.00089	0.000918	0.000879			
0.75		0.000924	0.000923	0.001084	0.010557	0.236732	1.057965	1.457619	1.105946	2.403322			
1.25		0.000884	0.009165	0.971329	5.106481	8.405708	10.97678	13.0335	12.06234		12.83289	11.27041	9.967212
1.75		0.001064	0.562683	9.105252	20.41728	25.45421	28.20364	29.03815	27.44431			21.42138	
2.25			5.49969	27.68563	37.1023	45.33404	42.63947	42.76087	40.69178	41.09014			
2.75			18.22703	50.29986	64.7323	60.29216	62.4653	64.42102	65.19432	66.99464	52.53888		54.58088
3.25			34.23828	84.18799	86.69252	89.27191	88.5779	92.36468	90.68518	90.37134	88.08919		
3.75				108.3729	111.7778	124.698	129.8281	128.9501	119.5726	114.5958	113.4945		
4.25					137.2878	157.9865	154.8233	150.6649	158.043	162.5017		129.786	138.0928
4.75					168.5228	199.5657	189.2585	205.6127	199.6631	195.2886	194.9466		
5.25						230.2395	271.5097	259.0956	248.7005	221.355			
5.75							296.1224	287.1677	216.7946	283.0193	270.5203		
6.25					337.4481	324.6451	345.1022	326.4744	323.0555	336.268			
6.75						380.0793	442.321	374.1872	402.9007	362.0482			
7.25								466.9106	464.6839		460.7702		
7.75								521.8281	544.0562	451.0823	476.6661		
8.25								564.5678	558.9114	544.0542			
8.75									671.2102	614.9468			
9.25									710.2606	678.1478	661.5104		
9.75										747.2428	692.4038		
10.25										805.9941	732.5726		
10.75											827.9959		
11.25											839.845		

The sea states with low values of *Hs* and *Te* have the maximum average power extracted with high values of torque applied as input.
The same thing happens with the high energy sea states, in which the torque applied to obtain the maximum values of average extracted power is 5 kNm.
For the medium energy sea states the applied torque to obtain the highest power values is included between 2-4 kNm.
All the four considered locations have one of these tables and starting from them it is possible to obtain the extracted yearly energy in MWh.
So in the following table the yearly energy extracted for each location is shown.

Table 7 Extracted energy in a year with selective torque control in MWh

	Yearly average extracted energy (MWh)		
	Selective torque control applied (1-5 kNm)	**Highest value reached without constant torque**	**Percentage gain (%)**
WaveHub Bidirectional	233.789	201.569	15.9846
WaveHub Unidirectional	267.193	203.087	31.5658
Emec Bidirectional	321.886	259.183	24.1926
Emec Unidirectional	345.388	260.065	32.8083
AUK Bidirectional	317.677	283.938	11.8825
AUK Unidirectional	362.187	284.340	27.3781
Haltenbanken Bidirectional	653.183	504.268	29.5310
Haltenbanken Unidirectional	671.900	525.367	27.7012

As can be seen there is a big increase of the energy that can be extracted in a year. In particular for the unidirectional case there is a high percentage gain, close to 30 % for each location, but it's important to remember that in this chapter no constraints are considered.
In the bidirectional case the percentage gain is variable, the minimum value appears in AUK (11.88 %) and the maximum value is in Haltenbanken (29.53 %).
The fact to apply different values of torque as input could be a problem for the electrical machine if the range of the applicable torque is not large, in addition the electrical machine is sized based on the maximum torque value.
It's necessary to compare the additional costs for implementing this new control strategy and the advantages that could be obtained. Especially the cost of the electrical machine must be considered because it can be significant due to the consistent overrating.

In theory the energy that could be extracted from the bidirectional and unidirectional should have the same value if the same locations are considered. Because in the bidirectional case both the directions of the buoy motion are exploited for power production, instead in the unidirectional case only the positive direction of the buoy motion is used. Probably the values of the torque applied are too high for the bidirectional case and the yearly energy extracted doesn't achieve the maximum value which should be close to the highest value of energy extracted in the unidirectional case, always with the same location considered.
This is an important consideration and will be considered in the next chapters.

6. Results of simulations with power limits

As said in chapter 4 (“Results of the simulations with no constraints”), in this paragraphs the results of the same three wave profiles considered in chapter 4 (low energy “sea state”, medium energy “sea state”, high energy “sea state”) are reported but with the introduction in the model of the power limit. Only the bidirectional and unidirectional cases are considered, because the focus of the thesis is to consider PTO with applied constant torque. The power limit is introduced to obtain a more realistic model, because it is useful to understand better the behavior of the power trend. Therefore if, considering the same wave profile, the average extracted mechanical power with 75 kW as maximum limit of the mechanical power, is similar to the average extracted mechanical power obtained with 200 kW as maximum limit of the mechanical power, probably 75 kW of rated power is the best choice for the size of the electrical machine. It’s better because the electrical machine with a smaller rated power (75 kW) is cheaper compared to the larger one, in addition the performance of the electrical machine is better when it works close to the rated power. Then it is possible to obtain money savings and lower losses of power inside the electrical machine because the performance is better, consequently the power converted from mechanical to electrical can be higher with a small size machine.
Considering the results obtained from the different locations it’s possible to choose the better values of power limit, which will be implemented in this chapter. The table 5.2 summarized the average power extracted for each sea state, so starting from this table three values of power limit will be chosen.
In the following figure table 5.2 is revived, the sea states with extracted power lower than 75 kW are colored in yellow, the sea states with extracted power lower than 100 kW are colored in blue (to which the yellow boxes must be added) and the sea states with extracted power lower than 200 kW are colored in green (to which the yellow and blue boxes must be added).

Table 8 Average mechanical extracted power in kW, bidirectional case, values of *Tz* in seconds and *Hs* in meters

Hs\Tz	4.5	5.5	6.5	7.5	8.5	9.5	10.5	11.5	12.5	13.5	14.5
0.75	0	0	0.01	0.29	0.87	1.46	1.11	2.40	0	0	0
1.25	0.02	0.87	4.87	8.20	10.82	13.20	12.72	0	12.83	11.27	9.97
1.75	0.56	8.83	19.44	24.23	26.91	28.24	26.94	0	21.60	21.42	0
2.25	5.50	27.79	38.68	44.49	43.30	43.08	38.33	38.30	0	0	0
2.75	18.23	50.30	65.34	63.69	62.35	55.91	53.50	48.54	45.03	0	38.87
3.25	34.24	84.19	87.61	83.18	75.37	70.92	67.31	59.77	58.17	0	0
3.75	0	108.37	111.78	105.75	93.68	86.84	78.56	70.12	65.96	0	0
4.25	0	0	137.29	131.28	113.52	101.51	93.27	83.75	0	68.89	66.33
4.75	0	0	168.52	152.09	128.79	118.00	106.75	97.67	88.89	0	0
5.25	0	0	0	174.72	151.03	132.09	121.17	112.66	0	0	0
5.75	0	0	0	0	176.17	148.12	132.42	121.31	109.25	0	0
6.25	0	0	266.30	220.09	191.79	166.65	154.69	138.55	0	0	0
6.75	0	0	0	244.50	218.81	184.72	163.35	145.21	0	0	0
7.25	0	0	0	0	0	201.19	186.80	0	152.55	0	0
7.75	0	0	0	0	0	229.23	193.46	168.56	157.45	0	0
8.25	0	0	0	0	0	234.77	211.54	187.04	0	0	0
8.75	0	0	0	0	0	0	219.76	203.79	0	0	0
9.25	0	0	0	0	0	0	239.04	218.18	192.30	0	0
9.75	0	0	0	0	0	0	0	239.74	203.55	0	0
10.25	0	0	0	0	0	0	0	237.13	211.96	0	0
10.75	0	0	0	0	0	0	0	0	233.58	0	0
11.25	0	0	0	0	0	0	0	0	239.40	0	0

The boxes colored in red are the reference values for the power limit choice, which are 75, 100 and 200 kW. These values have been chosen because they allow including many sea states, in particular in all the locations a lot of sea states with low values of extracted power are present. Maybe 200 kW as power limit can be high but one of the goals of this paragraph is also to understand the right values of power limit to be implemented in the locations considered.
In the following table there are the numbers (also in percentage) of the sea states whose energy is fully exploited for each value of power limit.

Table 9 Number of the sea states used for each value of power limit

Value of the power limit (kW)	Number of the sea states	Percentage value
75	53 (yellow)	45.3 %
100	64 (yellow + blue)	54.7 %
200	101 (yellow + blue + green)	86.3 %

As can be seen in the previous table, doubling the value of the power limit (i.e. from 100 kW to 200 kW) the percentage value increases only of 31.6 %. So the higher the value of the power limit is, the lower the increase of the percentage value is.
Anyway considering the data occurrence of the locations it is possible to obtain a table with the percentage occurrence of the exploitable sea states for each value of power limit. In the following table there are the percentage occurrence corresponding at Emec location, considering 1 kNm as torque applied in the bidirectional case.

Table 10 Percentage occurrence for each value of power limit in Emec location

Value of the power limit (kW)	Percentage occurrence
75	83.84 %
100	90.05 %
200	99.81 %

Using a power limit of 75 kW the percentage occurrence is already high, this is a good feedback for the size of the future electrical machine which will be installed. The increase of the percentage occurrence using 100 kW as power limit is only 6,2 %, but the price difference between an electrical machine of 75 kW (rated power) and another one of 100 kW (rated power) is usually contained, so probably 100 kW is the right solution. The last power limit considered (i.e. 200 kW) is useful to understand that a higher limit of power limit is certainly inadequate, because percentage occurrence is already closed to 100 %.
So in this chapter three different limits of the mechanical power are considered, respectively 75 kW, 100 kW and 200 kW. All of the three sea states (wave profiles) are tested in a new Matlab-Simulink program for all the three power limits. The limit of the buoy position is not considered during these simulations, so the buoy can have unnatural behavior. In theory the introduction of the power limit should modify also the buoy position because when the power is close to the limit the program model applies a different PTO force which, when it’s multiplied by the velocity of the buoy,

keeps the power close to the limit, then the hydrodynamic model is modified and also the position of the buoy.

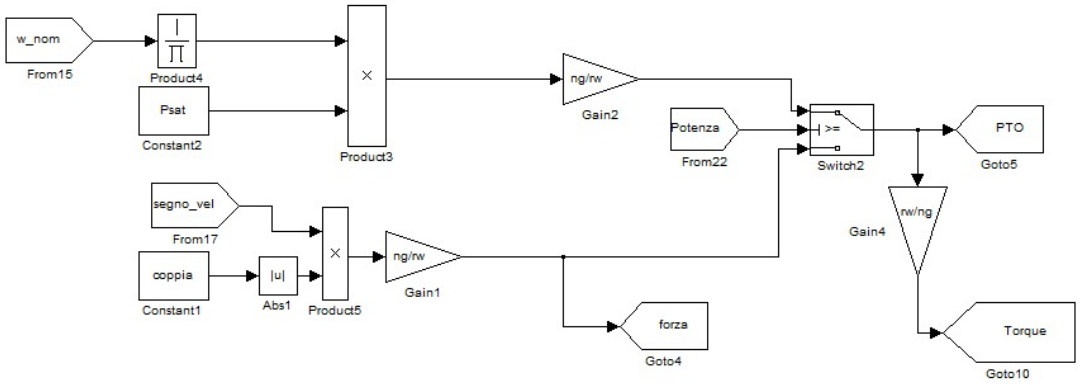

Figure 36 - Simulink block to introduce the power limit

Another important consideration is that the size of the electrical machine is chosen based to the diagram of the average power, although in reality the size of the electrical machine corresponds to a limitation for the maximum power. However we do this because if we work on a corresponding table of peak power, the machine would be excessively oversized. Then we take the average power as a reference, assuming that the machine works most of the time at that value of power (and hence peak power and average are close).

6.1 Bidirectional case with 75 kW of power limit

In this paragraph a power limit of 75 kW is considered in the bidirectional case. In the previous tests (figure 4.4) the trend of the average extracted power with no power limit is shown. In the power limited cases, the average power in the low energy sea state never passes the 75 kW limit, instead the other more energetic sea states always pass this limit when the applied PTO force is higher than 100 kN. Apparently it seems that the system behavior in the low energy sea state isn't changed with the introduction of the power limit, but it is not so. The power limit is a limit for the maximum power, then it's possible that in the unconstrained case and in the low energy sea state the maximum power passes the 75 kW; therefore the average extracted mechanical power becomes lower with the introduction of the power limit.

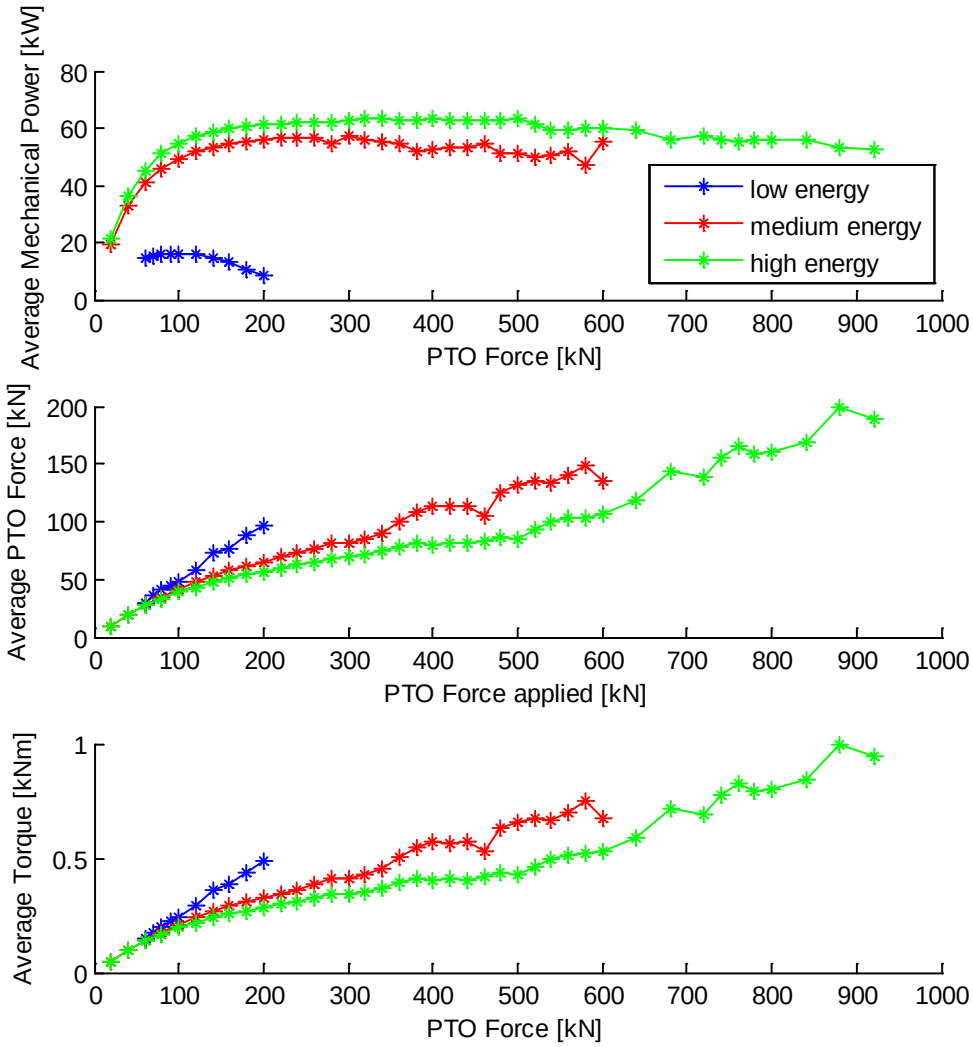

Figure 37 - Average values of power, PTO force and torque in the bidirectional case with 75 kW as power limit

In the previous figure the average power for the low energy sea state is very low, instead for the medium and high energy sea state the average power is very similar. This happens because the maximum power is always close to the limit, in particular when the applied PTO force is higher than 100 kN.
In the diagrams of the average PTO force and average torque, if there had been no limit the trend would have been a straight line, now with the limit the trend is completely changed because the PTO force applied is not always constant. Only in the first steps the trend is like a straight line (PTO force applied lower than 100 kN), because the limit is not passed and the behavior is the same as when there is no power limit.
Now it is interesting to see the values of the maximum power (which are as expect, i.e. maximum power equal to the power limit) and the maximum values of the PTO force and torque. In the following figure these diagrams are shown.

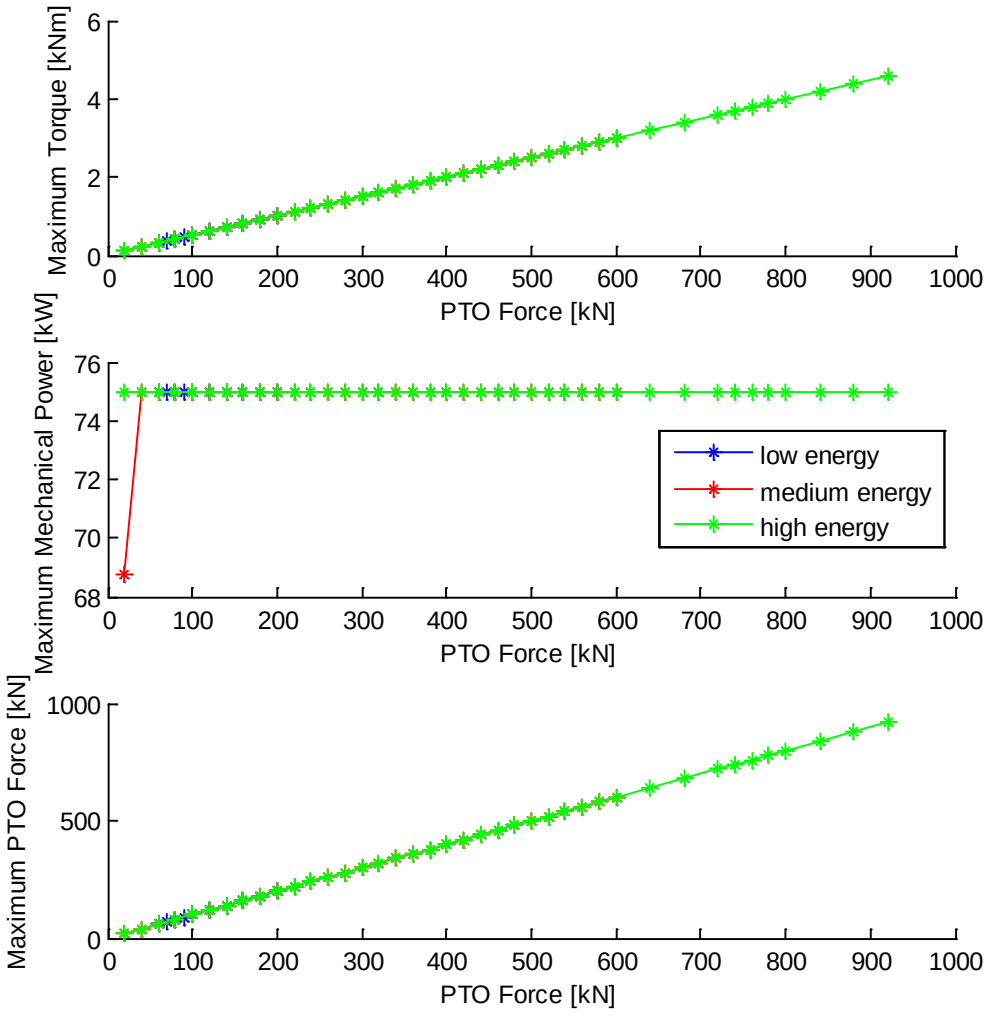

Figure 38 - Maximum values of torque, power and PTO force in the bidirectional case with 75 kW as power limit

As expected the maximum values of PTO force is equal to the constant applied values in every step, because the PTO force applied when the power approaches the limit is always lower than the constant values applied as input in the program. This is why the trend in the diagram of the PTO force is equal to a straight line and the same for the torque diagram with the respective scale of values (the torque is 200 times lower than the PTO force).

In the diagram of the maximum power the maximum values is always equal to the power limit (75 kW), except in the first case of the medium energy sea state where the applied PTO force and the excitation force used as input do not allow to obtaining high values of power. This means that in all of the sea states the maximum power that can be reached is always higher than 75 kW with no constraints.

Seen that the maximum PTO force is always equal to the constant value applied as input, probably the maximum position of the buoy is the same in every step because it usually is with the maximum values of applied PTO force that the maximum values of buoy position are achieved. In particular this should happen in the high energy case.

Since there is a power limit, a possible increase of the buoy velocity (which is not controlled) must match a decrease of the applied PTO force (which is controlled) when the mechanical power is close to the limit, otherwise the limit would be passed.

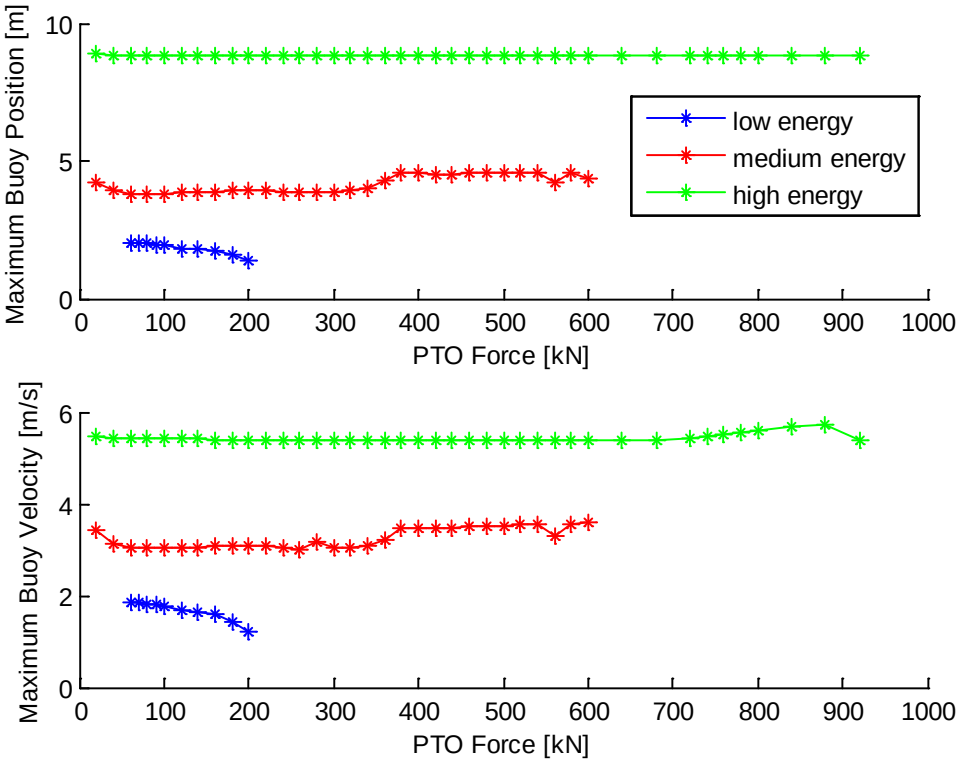

Figure 39 - Maximum values of buoy position and velocity in the bidirectional case with 75 kW as power limit

Just as mentioned before the values of the maximum buoy position for the high energy sea state are always the same, a similar behavior is present also in the medium energy sea state, instead for the low energy sea state the maximum values of the buoy position decreases with the increase of the PTO force applied as input. This thing happens because the average extracted power in the low energy sea state starts to decrease when the applied PTO force is higher than 100 kN.

6.2 Unidirectional case with 75 kW of power limit

In the unidirectional case the average mechanical power should be lower than the bidirectional case, because just one speed direction is considered. This thing happens for every sea state, then the power that can be extracted is close to 50 % - 60 % of the power extracted in the bidirectional case with power limit at 75 kW (and the same applied PTO force), anyway in the following figure the trend of the average power, average PTO force and average torque are shown.

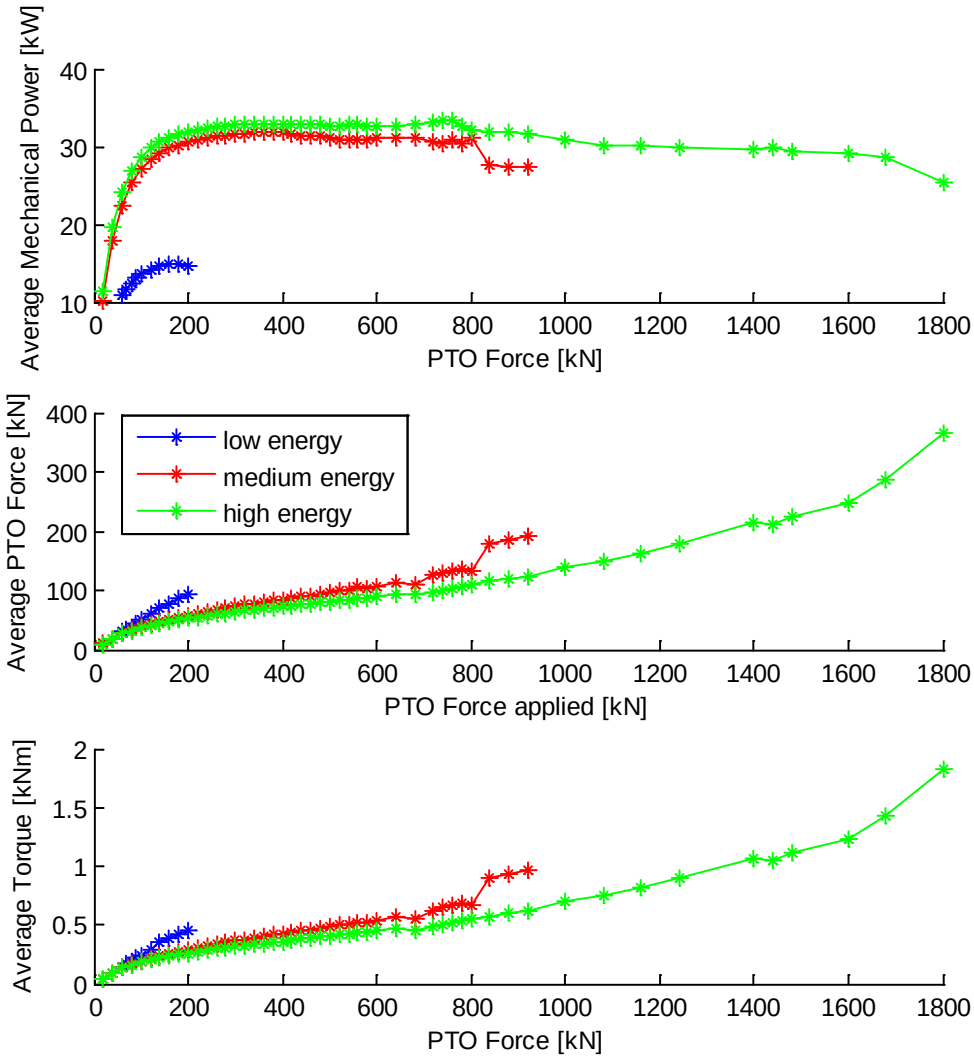

Figure 40 - Average values of power, PTO force and torque in the unidirectional case with 75 kW as power limit

As said before the average power in all the sea state doesn't pass the 60 % of the average power extracted in the bidirectional case (75 kW power limit) with the same reference PTO force. In chapter 4 it has been said that the PTO force applied to obtain the same values of average power must be double in the unidirectional case, here it is not the same because the power limit at 75 kW doesn't allow extracting the same maximum average power for both the cases. Therefore it is possible to apply a double value of PTO force in unidirectional case with 75 kW of power limit but the average power that can be extracted tends to saturate at the 60 % of the maximum average power that can be extracted in the bidirectional case (75 kW power limit). In addition the trend of the average torque and PTO force is not a straight line. This happens, as in the bidirectional case (75 kW power limit), because the maximum power tends often to pass the power limit (75 kW) and the control must intervene to keep the power lower than the limit. When the control to keep the power under the limit intervenes, the applied PTO force is not equal to the constant reference value used as input but it is equal to the power limit divided by the current velocity.

The average PTO force is then modified and its value is smaller than the constant PTO force as input of the program.
Like in the bidirectional case in the following figure the trend of the maximum values of torque, power and PTO force are plotted for the unidirectional case.

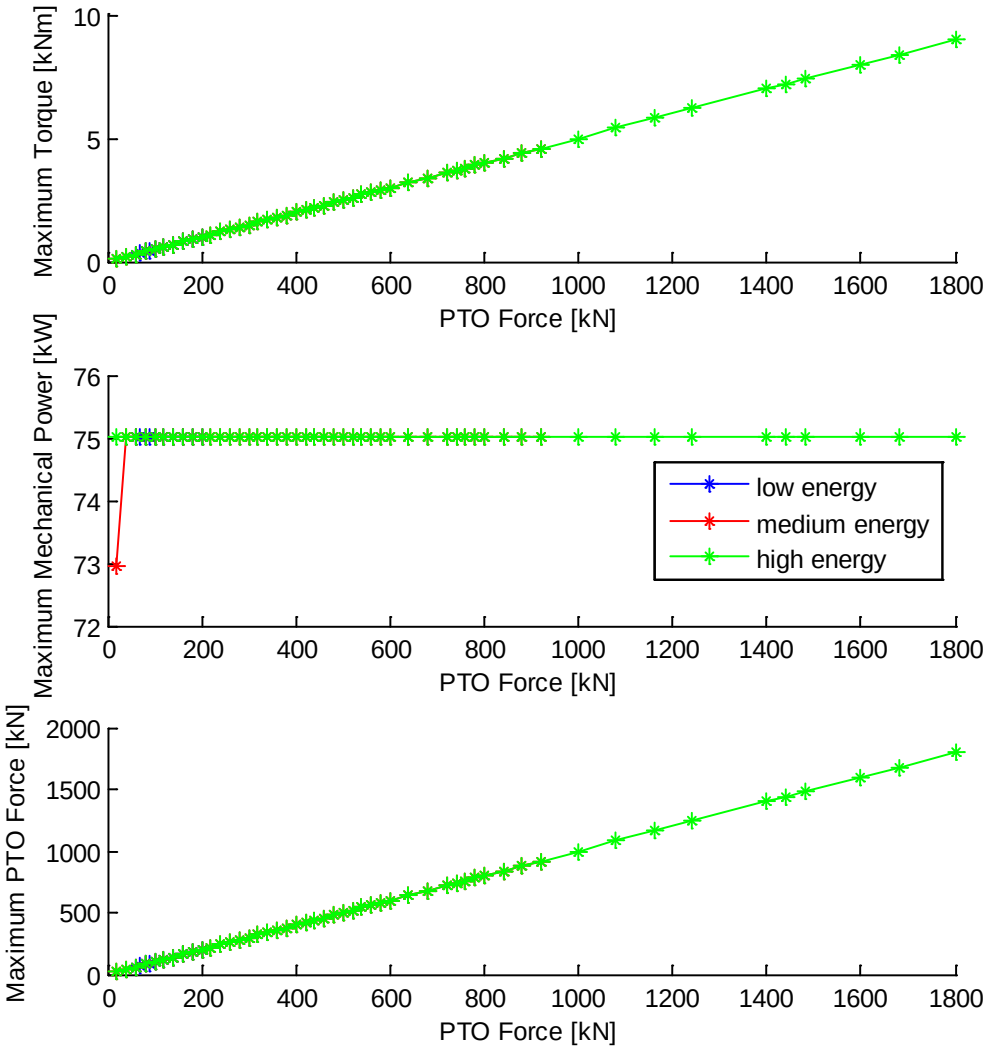

Figure 41 - Maximum values of torque, power and PTO force in the unidirectional case with 75 kW as power limit

The trend of the maximum values is the same as in the bidirectional case (75 kW power limit), and this is obvious. For every constant PTO force applied as input there is almost one time-step during the program in which the respective value of torque, power or PTO force touches the maximum value. For the power the maximum value is the power limit (75 kW), instead for the PTO force the maximum value is the constant value of PTO force applied as input and the same for the torque respecting the rights proportions.
Probably the limit of 75 kW for the power is too low because there are a lot of steps during the simulation which exceed this value. In particular if the electrical machine (with 75 kW of rated power) has a rated torque of 1/2 kNm the equivalent PTO force

is equal to 100/200 kN, the average power considering the average of the three cases is between 20-30 kW which are about 26-40 % of the rated power of the machine.
The values of the maximum buoy position and velocity are the same as in the bidirectional case because the behavior of the two cases is very similar, in the following figure these trends are plotted.

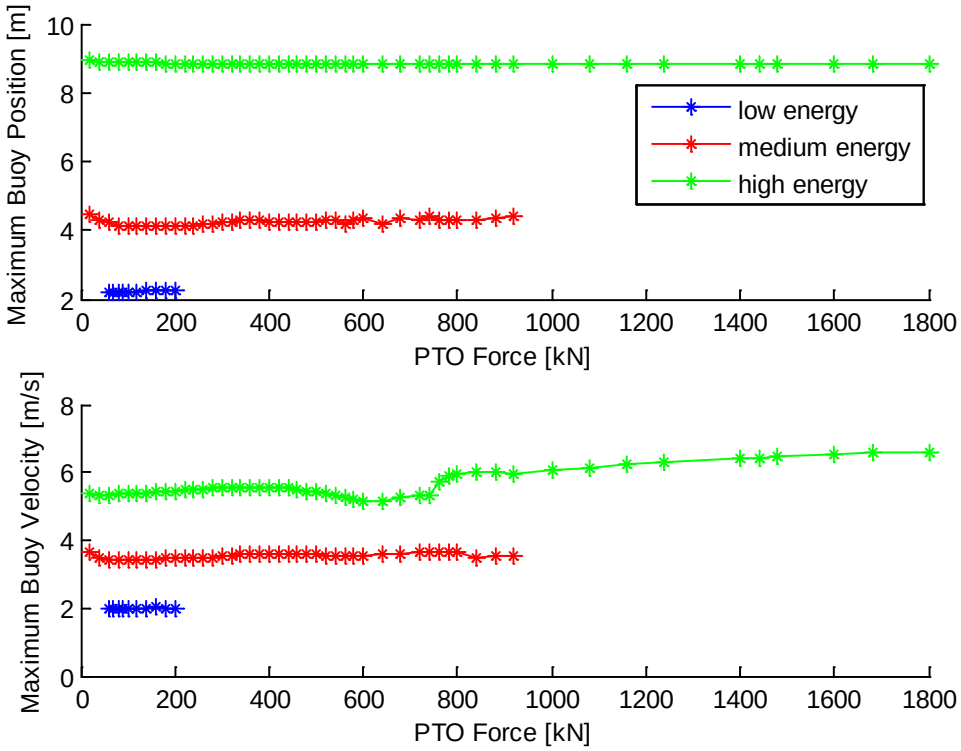

Figure 42 - Maximum values of buoy position and velocity in the unidirectional case with 75 kW as power limit

There are not many differences between the buoy position and velocity in the bidirectional case and in the unidirectional case with power limit, all the things said for the bidirectional case are valid also for the unidirectional case. Compared to the unidirectional case with no power limit, here the maximum velocity remains close to a constant value for every sea state considered, instead in the unidirectional with no power limit the velocity tends to decrease and the same for the buoy position but only for the high and low sea states.

6.3 Bidirectional case with 100 kW of power limit

In this paragraphs the power limit is 100 kW, the implemented program is the same as in the previous cases. Only the value of the power limit is changed. The choice of 100 kW is not random because it's useful to quantify the increase of the average mechanical power compared to the other cases with a power limit of 75 kW.
In the following figure the average values of mechanical power, PTO force and torque are plotted.

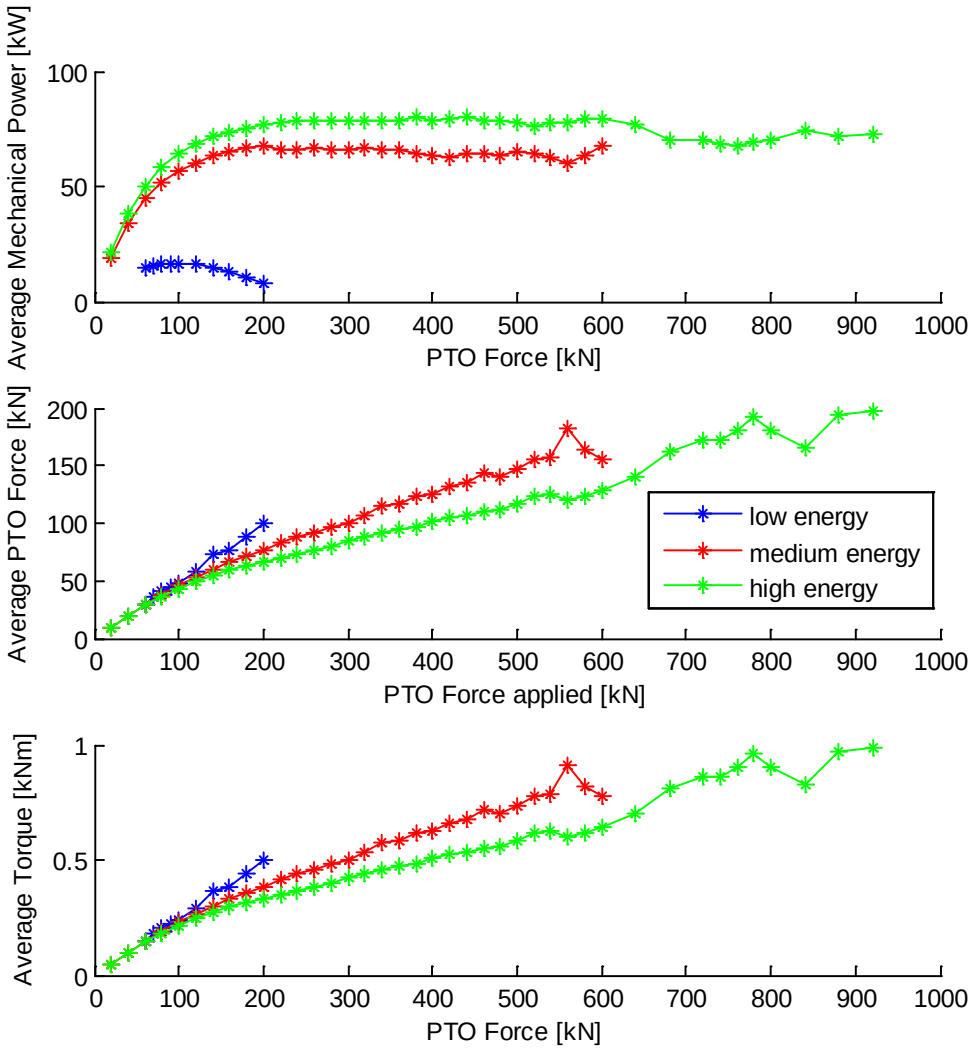

Figure 43 - Average values of power, PTO force and torque in the bidirectional case with 100 kW as power limit

The average power that can be extracted for the medium-high energy sea state grows slightly in particular for the high energy sea state it is close to 80 kW. Then with a higher power limit respectively 25 kW more than the previous limit the increase of the maximum average power in the high energy sea state is close to 20 kW. In the medium energy sea state the increase is lower (about 5 kW) and for the low energy sea state there is no change. Therefore for the considered wave data of a specific location, if the average energy of the sea state is medium-high probably it is better to use a power limit of 100 kW, instead if the average energy of the sea state is low-medium a 75 kW of power limit allows to obtain results close to the results with a 100 kW of power limit. In the next step the power limit will be the rated power of the electrical machine. The trend of the PTO force and torque are similar to the bidirectional case with 75 of power limit and all the things said with 75 kW of power limit remain valid.

The only thing that changes is the maximum values of the power which are always equal to 100 kW in all the PTO force used as input, while in the bidirectional case (75 kW power limit) were equal to 75 kW.
Also for the buoy position and velocity the diagrams have the same trend as in the bidirectional case (75 kW power limit). Therefore only the average values of the power are changed with this different value of power limit used.

6.4 Unidirectional case with 100 kW of power limit

In this paragraph the unidirectional case with 100 kW as power limit is considered, like in the previous paragraph the only thing that changes compared to the unidirectional case (75 kW power limit) is the power limit.
The average power in theory should be the 60 % of the bidirectional case (100 kW power limit), and as said before it's not like the case with no power limit, where it is possible to obtain the same average power between bidirectional and unidirectional case using double values of PTO force in the unidirectional case compared to the bidirectional. There is a limit of the maximum average power that can be extracted, and this limit is shown in the following figure.

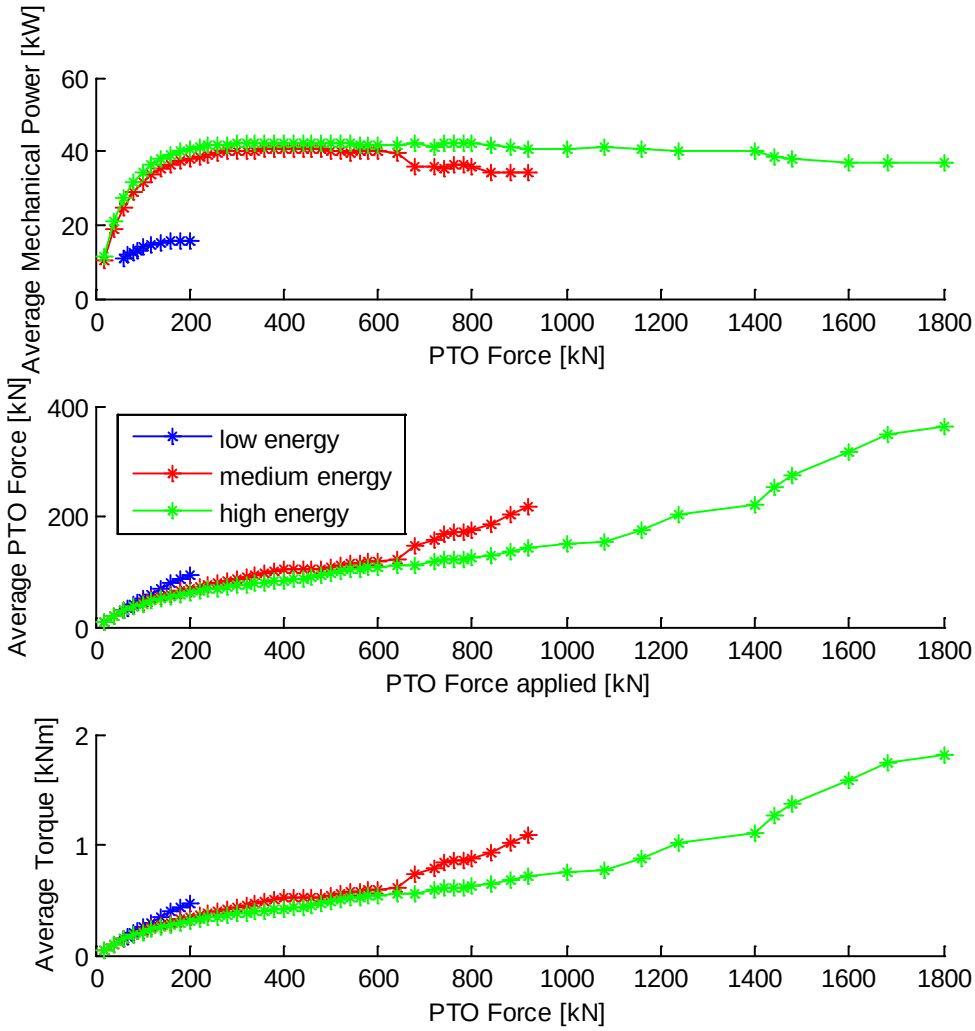

Figure 44 - Average values of power, PTO force and torque in the unidirectional case with 100 kW as power limit

The maximum average power is close to 45 kW for the medium-high energy sea states, while in the bidirectional case (100 kW power limit) it was close to 80 kW. Then the same thing happens in the unidirectional and bidirectional case with 75 kW as power limit, in these cases the power is 35 kW (unidirectional) and 60 kW (bidirectional).

In the unidirectional case an increase of 25 kW of power limit, allows achieving 10 kW more of average power (considering the maximum values), instead in the bidirectional case an increase of 25 kW of power limit, allows achieving 20 kW more of average power always considering the maximum values. The sea states with medium-high energy have a greater advantage with the increase of the power limit, instead the low energy sea state is not affected by this increase of power limit.

So, there isn't an absolute better solution for the choice of the power limit (PTO sizing), all depends on the considered site for deployment, i.e. on the scatter diagram (wave data occurrences) of the considered location. Usually if the location has a lot of sea states with high energy, a higher power limit can be chosen.

About the average PTO and torque, all the things said before remain valid and the trend are very similar. For the maximum values of torque, power, PTO force, buoy position and velocity the trends are the same as in the previous cases. It's important to specify that here very high values of applied PTO force are considered and as a result also high values of torque are obtained. This is because an ideal situation in which it's possible to apply whatever values of PTO force is considered.

6.5 Bidirectional case with 200 kW of power limit

In this paragraph all of the three sea states are considered and the power limit is 200 kW. With this value of power limit in theory the high energy sea state should increase the average mechanical power extracted, because it is the wave profile in which the maximum power takes the higher values. The power limit is double compared to the previous analysis case, therefore it's expected that the low energy sea state remains the same as in the previous case (100 kW power limit) and the medium and in particular the high energy sea state can extract higher values of average mechanical power.
In the following figure the trend of the average power, average applied PTO force and torque are shown.

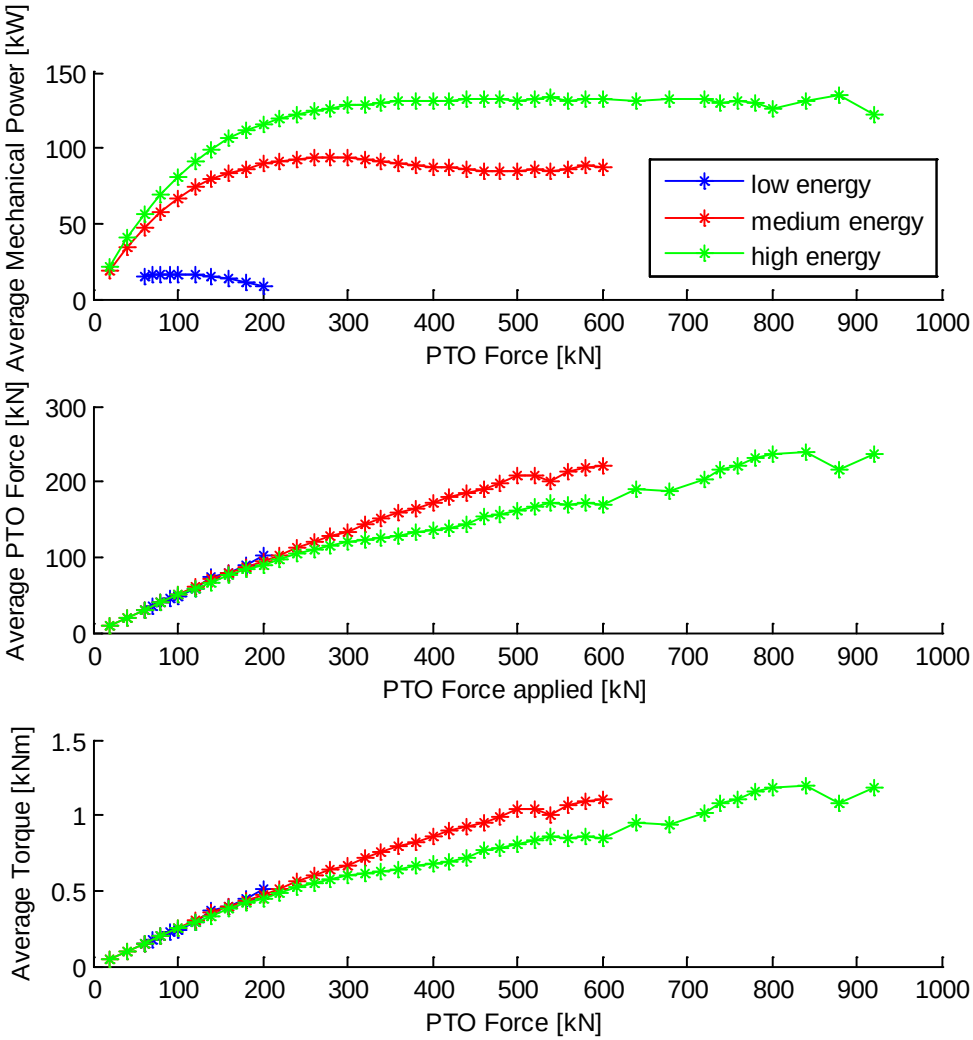

Figure 45 - Average values of power, PTO force and torque in the bidirectional case with 200 kW as power limit

The maximum value of the average power is close to 140 kW and it's obtained in the high energy sea state, the medium energy sea state has a maximum average power close to 95 kW, while the low energy sea state keeps the same trend as in the previous case (with the same condition, i.e. PTO force applied, bidirectional case ecc..). As expected the high energy sea state is more favored by the increase of the power limit.

The average PTO force and torque have the same trend as in the previous cases (75/100 kW), but the values are higher.

Compared to the previous case the low energy sea state doesn't pass the maximum value of power i.e. the power limit, as can be seen in the following figure.

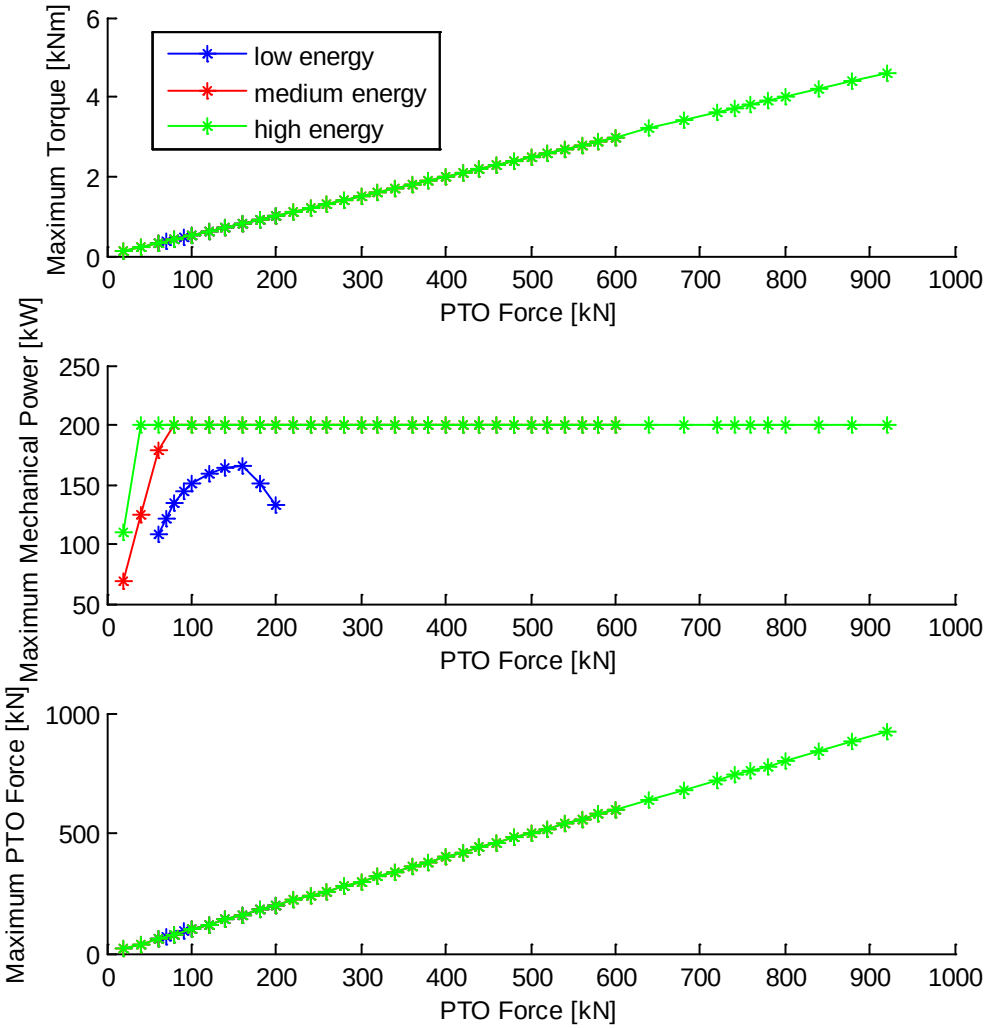

Figure 46 - Maximum values of torque, power and PTO force in the bidirectional case with 200 kW as power limit

Just as said before the low energy sea state doesn't pass the power limit as maximum power, the same thing happens with the first 3 tests of the medium energy sea state in which the applied PTO force are low. The maximum values of PTO force are the same of the applied PTO force and for the torque it's the same with the correct proportion.
The trend of the maximum values for the buoy position and velocity never change and it's the same as in the case 75 kW as power limit.

6.6 Unidirectional case with 200 kW of power limit

For the sake of completeness, also for the 200 kW power limit the unidirectional case is considered. The maximum average power should be about the 60 % of the average maximum power in the bidirectional case (200 kW power limit). In the unidirectional case the maximum average power is the 60 % because only one direction of the buoy velocity is considered.

In the following figure the trend of the average power, average applied PTO force and average torque are shown.

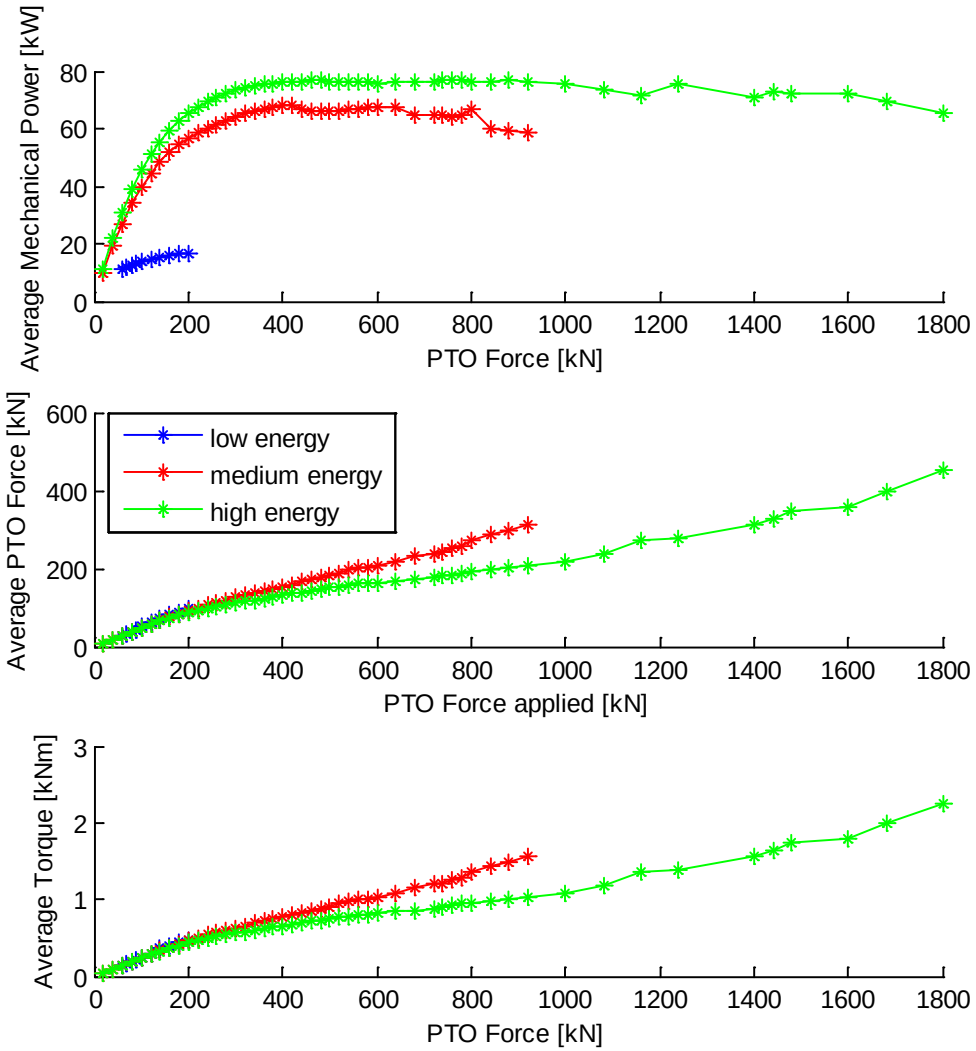

Figure 47 - Average values of power, PTO force and torque in the unidirectional case with 200 kW as power limit

As expected the maximum average power can be extracted in the high energy sea state and it is close to 85 kW, which is the 60 % of the maximum average power that can be extracted in the bidirectional case with the same value of power limit. Both the trend of the average PTO force and torque are similar to the previous case, the only thing that changes is that the maximum values are higher.
The maximum power has the same trend as in the bidirectional case in which the low energy sea state never reaches the maximum value (i.e. the power limit), the medium and high energy sea states are the same compared to the previous case (bidirectional).
The maximum buoy position and velocity are always the same for every situation considered, probably the buoy position and velocity profiles in the time change but the maximum values achieved are always the same.

6.7 Considerations and summary table

Table 11 Main results of simulations test

Power limit [kW]	Case	Energy sea state	Maximum average power [kW]	PTO force ref.[kN]	Capacity factor	Average torque [Nm]	Maximum power [kW]	Maximum buoy position [m]	Maximum buoy velocity [m/s]
75	Bidirectional	Low	16.243	90	0.2166	221.554	75	1.9737	1.7875
		Medium	57.053	300	0.7607	408.204	75	3.879	3.0285
		High	63.333	400	0.8444	401.6176	75	8.8387	5.3938
	Unidirectional	Low	14.969	180	0.1996	428.5363	75	2.2516	2.0112
		Medium	31.837	360	0.4245	402.8818	75	4.2761	3.6020
		High	33.450	760	0.4460	522.2151	75	8.84	5.7422
100	Bidirectional	Low	16.415	90	0.1641	222.3644	100	1.8493	1.6648
		Medium	67.914	200	0.6791	385.5576	100	3.8312	3.0252
		High	80.264	380	0.8026	482.7572	100	8.7922	5.351
	Unidirectional	Low	15.654	180	0.1565	439.0824	100	2.1526	1.9215
		Medium	40.547	480	0.4055	526.0281	100	4.0897	3.4173
		High	42.472	760	0.4247	609.5125	100	8.7977	5.6036
200	Bidirectional	Low	16.504	90	0.0825	222.7844	144.05	1.7639	1.6005
		Medium	93.750	280	0.4686	634.1521	200	3.56	2.7296
		High	135.62	880	0.6781	1074.7	200	8.6127	5.1579
	Unidirectional	Low	16.429	180	0.0821	444.4515	200	1.8482	1.6695
		Medium	67.989	400	0.3401	768.9668	200	3.8452	3.0527
		High	77.177	760	0.3859	922.5406	200	8.6356	4.6967

In the previous table all the main results of the simulations with the power limits are presented. The average PTO force in the bidirectional case is calculated considering only the positive values of applied PTO force (=>0), because the PTO force is applied in both the directions and the average considering both the directions is obviously close to zero. For the average torque in the bidirectional case it is the same with the appropriate scale of values (i.e. average torque is 200 times lower than the average PTO force). In the unidirectional case the PTO force is applied only in the positive direction and the average PTO force is calculated considering these positive values.
The capacity factor is calculated dividing the average power by the power limit (rated size). It achieves the highest values in the high energy sea state in particular for the bidirectional case. Increasing the value of the power limit the capacity factor decreases, so a small size of electrical machine allows obtaining high values of capacity factor and as a consequence a better exploitation of the PTO.
In the low energy sea state the value of the maximum average mechanical power doesn't change so much when the power limit changes. Thus for a location which has a lot sea states with low energy, a small size machine is the better choice. This is valid for both bidirectional and unidirectional case, the maximum average power extracted being always close to 16 kW.
In the medium energy sea state the maximum average power extracted in the bidirectional case is in most cases twice as much as in the unidirectional case. With the increase of the power limit the differences between the bidirectional and unidirectional case are reduced. In particular the difference in the value of the maximum average extracted power between the two cases tends to decrease a lot.
The sea state which has more advantages by the increase of the power limit is the high energy sea state, the maximum average power with 200 kW as power limit is equal to 135.62 kW which is the highest value of average of power of all the simulations. In all of the cases considered the average torque values are under 1 kNm, and for the low energy sea state with 75 kW as power limit (bidirectional case) it reaches the minimum value which is equal to 221.554 Nm.
The goal of the chapter is to understand better how the value of the power limit (size of the PTO) can change the average mechanical power extracted, without considering at this stage the maximum buoy position limit, which will be introduced in the following. Thus the buoy position is not fully realistic, because in all the tests with the high energy sea state the maximum buoy position constraint is always broken. The position of the buoy is important, but it doesn't affect so much the average power extracted because all along the simulation time the limit of the buoy position is sporadically passed.

6.8 Trends over time of power, torque, buoy velocity and position

In order to understand better the behavior of the main system parameters, their time evolution should be considered. In particular the power, torque, buoy velocity and position because these parameters are very affected by the constraints introduced in to the model.
In this paragraph the high energy sea state is considered in three different situations:

- The first analyzed situation is without constraints into the model, i.e. there are no power limit and buoy position limit.

- In the second situation there is only the power limit (100 kW) and the buoy position limit is not considered.
- In the last there are both the power limit (100 kW) and the buoy position limit (~5 m).

Only the high energy sea state is considered since only in this sea state the buoy position exceeds the buoy radius (5 m), while in the low and medium energy sea states the buoy position doesn't pass 4.3 meters which is a non-critical value and a system to control the buoy position would be useless.
A new model in Simulink is implemented to control the buoy position. Basically the new subsystem, introduced in the previous model including the power limit, is like a limit switch system (mass-spring-damper) which intervenes only when the buoy position is close to pass the fixed limit (4.8 m). When the buoy position is close to 4.8 m a new (spring type) force is introduced in to the hydrodynamic system which counteracts the buoy displacement and allows reducing the buoy maximum position, therefore the buoy position is always less than 5 meters. If the buoy position is naturally under the 4.8 m limit, the contribution of this new force is equal to zero. The buoy position is considered in absolute value, so for the system working in both the directions of the buoy motion.
In the following figure the new model in Simulink for the buoy position control is shown.

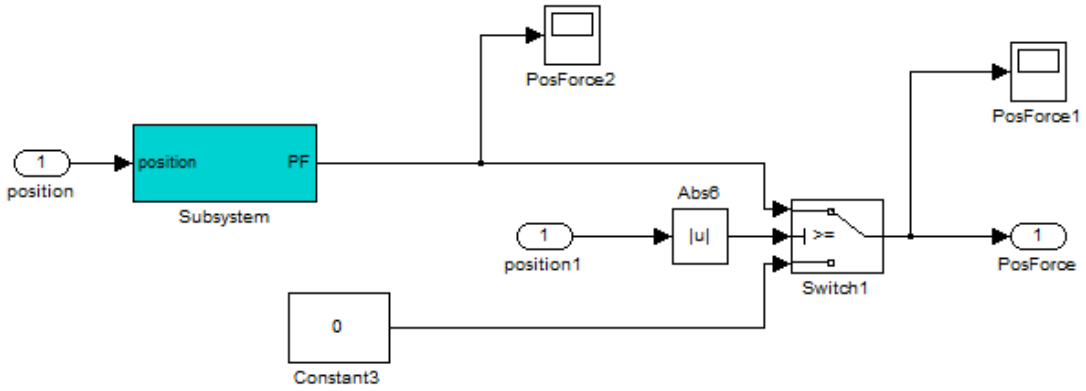

Figure 48 - Simulink for the buoy position controls

The subsystem in the previous figure is shown in the following figure.

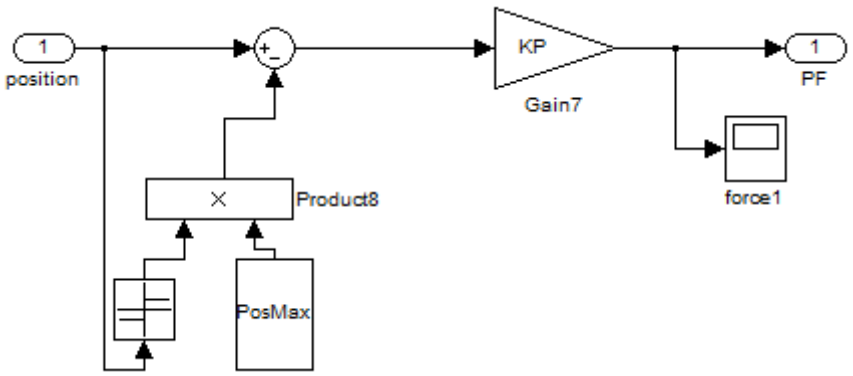

Figure 49 - Simulink subsystem to calculate the force introduced by the buoy position control

In the subsystem shown in figure 6.14 the force is calculated as real buoy position minus maximum position (which is fixed at 4.8 m), and this difference is multiplied by a coefficient (KP = 700*10^6 N/m). This force is considered as a force introduced by a mechanical system (end-stop system) so it does not affect the total applied PTO force. So only the power limit control influences the trend of the PTO force.
In all the simulations for the bidirectional case the reference PTO force is equal to 380 kN and for the bidirectional case is equal to 760 kN, these values of PTO force are changed when the system to control the buoy position intervenes. The choice to apply always the same PTO force is not random because using the same input it's possible to compare the results in all the different situations. The PTO force values chosen are the values that allow achieving the higher values of average extracted power. The simulation time is always 900 seconds.
In the following figure the trend of power and torque are plotted for the three considered cases in the bidirectional case.

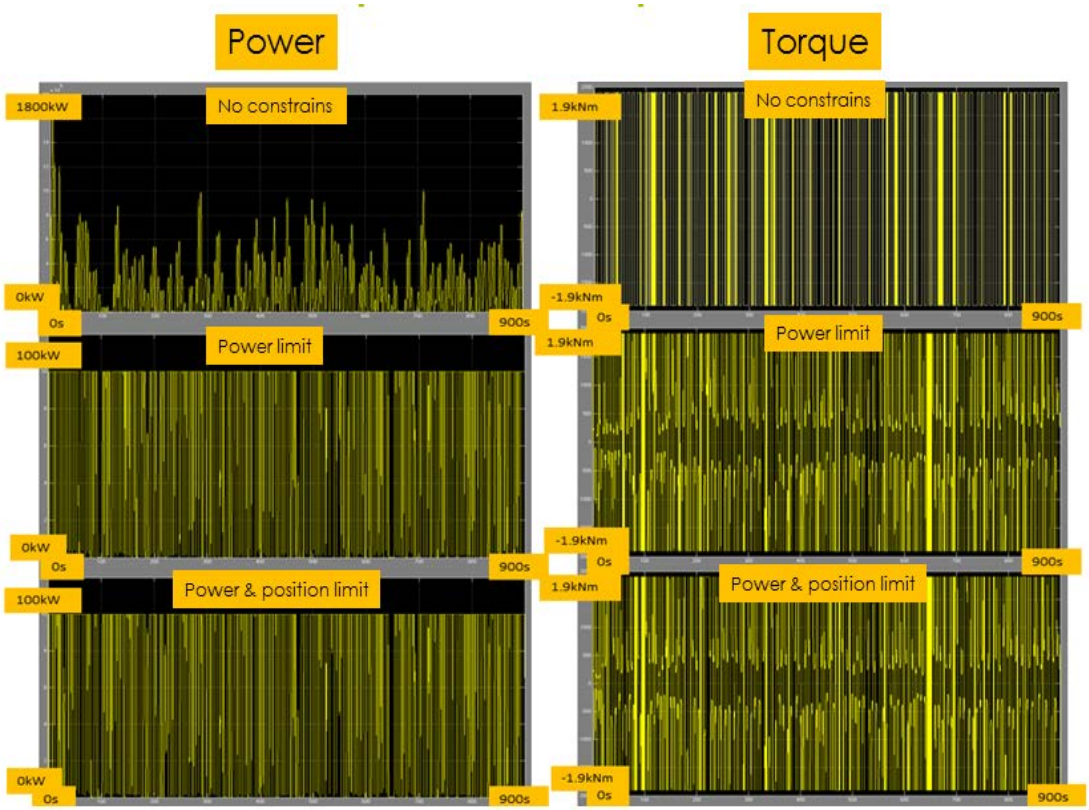

Figure 50 - Trend over time of power and torque

On the left there is the trend of the power and on the right there is trend of the torque. The figures in the first line are the trend with no constraints in the model, the two figures of the second line are the trend with only the power limit (100 kW) and the last two figures are the trend with both the power limit (100 kW) and the buoy position limit (~5 m).

In the simulation with no constraints the peak power is close to 1600 kW and the applied torque is always constant (1.8 kNm) with the sign concordant with the speed of the buoy. For the cases with costraints the maximum power is equal to the limit (100 kW) and the trend is completely different compared to the case with no constraints, because the force applied by the subsystem to control the power and the force applied by the subsystem to control the buoy position introduce a nonlinear behavior in to the model.

To understand better what nonlinear behavior means, in the following figure the trend of the power (from 100 to 200 seconds of simulation) and the torque (from 96 to 100 seconds of simulation) are shown, but only for the case with constraints.

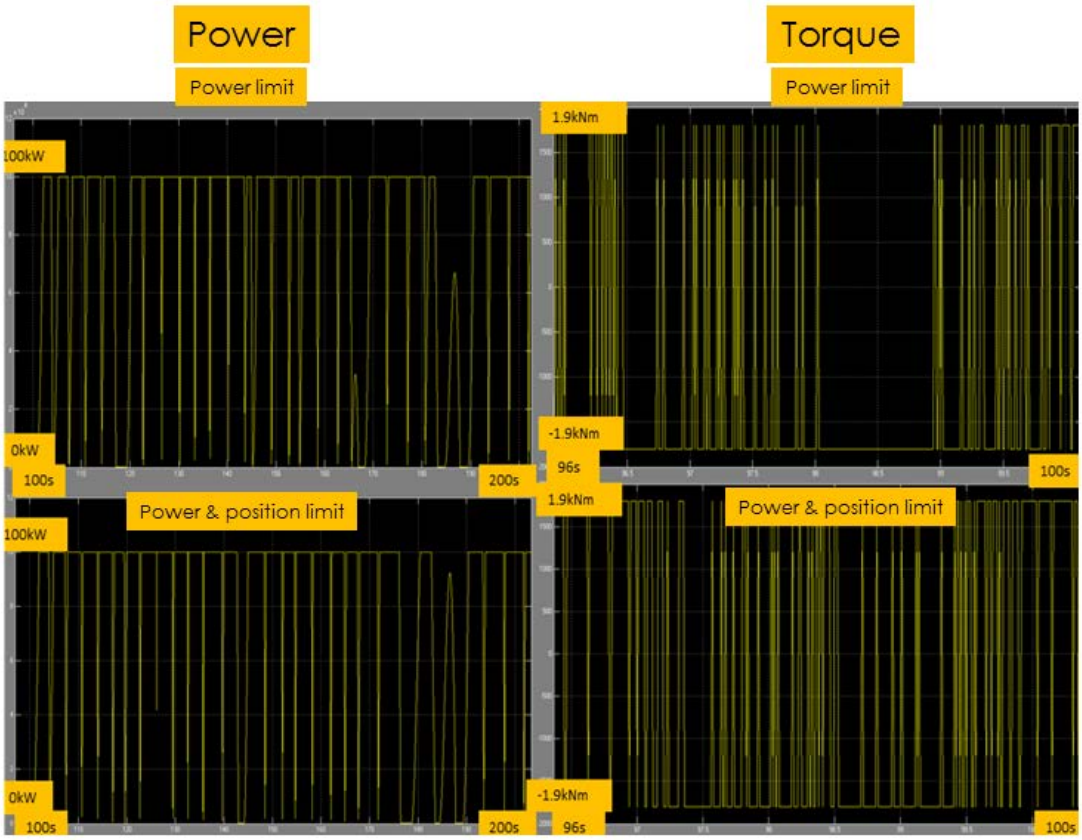

Figure 51 - Zoom of the trend over time of power and torque

On the left there is the trend of the power and on the right there is the trend of the torque, the images of the first line are of the case with only the power limit constrain and the last two for the case with both the power limit and the buoy position limit.
The applied torque has a strong nonlinear trend, which is especially caused by the force applied to keep the power under the limit. The trend of the applied torque is not very different between the two cases, because the applied force to control the buoy position works sporadically (the buoy position limit is passed only seldom).
In the following figure the trends over time of the buoy position and velocity are shown with the same structure of the previous figures.

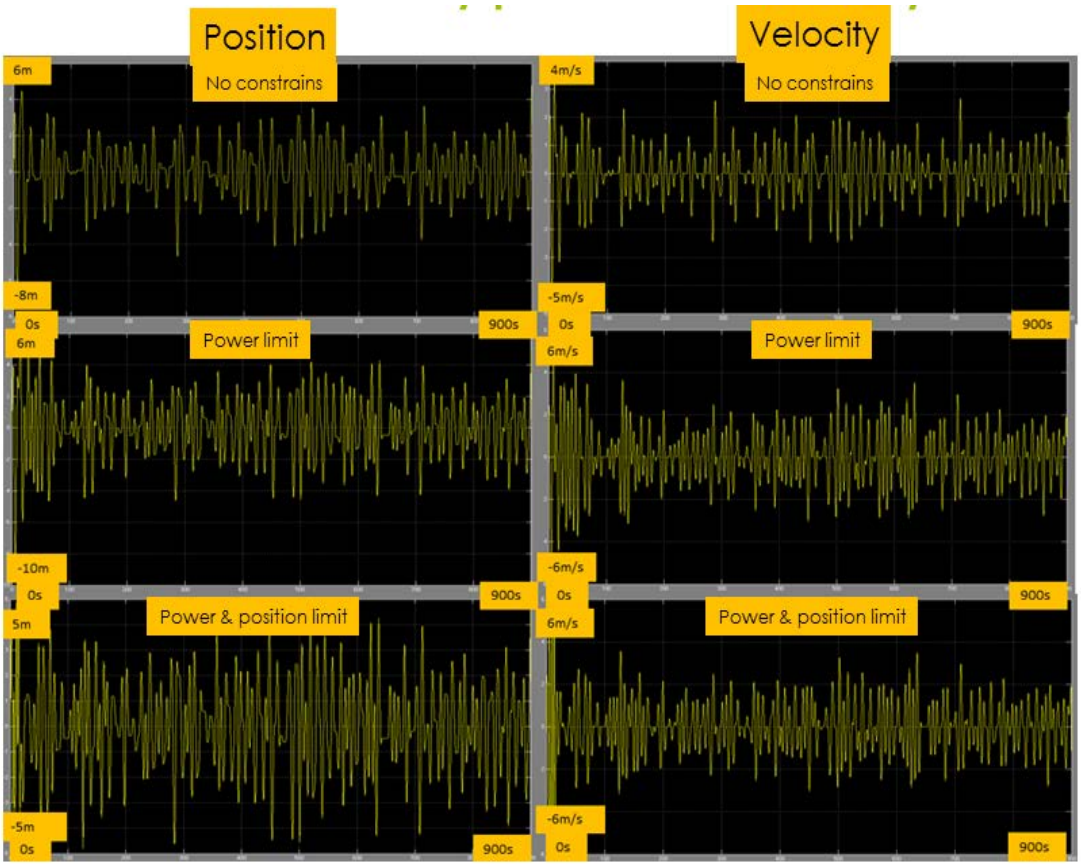

Figure 52 - Trend over time of buoy position and velocity

On the left there is the buoy position trend and on the right the buoy velocity trend for all the 900 seconds of the simulation time.
The maximum value of the buoy position when there is no buoy position control is close to 8 meters, in the case with the buoy position control the buoy position is always under 5 meters. The buoy position limit rarely is passed when there is no buoy position control, therefore the average power is only a little bit lower in the case with all the constraints compared to the case with only the power limit constrain.
In the unidirectional case there is always the same trend for each parameter, so the considerations made for the bidirectional case remain valid.

6.9 Comparison of results

Table 12 Main results of the simulations

		Energy sea state	PTO force Reference [kN]	Capacity factor	Average power [kW]	Maximum power [kW]	Peak to average power ratios
No constraints	**Bidirectional**	**Low**	90	-	16.504	144.05	8.73
		Medium	200	-	99.858	471.33	4.72
		High	380	-	220.81	1686.8	7.64
	Unidirectional	**Low**	180	-	16.511	288.1	17.45
		Medium	480	-	109.9	1102.3	10.03
		High	760	-	221.88	2339.1	10.54
Power limit (100 kW)	**Bidirectional**	**Low**	90	0.1641	16.415	100	6.09
		Medium	200	0.6791	67.914	100	1.47
		High	380	0.8026	80.264	100	1.25
	Unidirectional	**Low**	180	0.1565	15.654	100	6.39
		Medium	480	0.4055	40.547	100	2.47
		High	760	0.4247	42.472	100	2.35
Power limit (100 kW) & buoy position control	**Bidirectional**	**Low**	90	0.1641	16.415	100	6.09
		Medium	200	0.6791	67.914	100	1.47
		High	380	0.7881	78.808	100	1.27
	Unidirectional	**Low**	180	0.1565	15.654	100	6.39
		Medium	480	0.4055	40.547	100	2.47
		High	760	0.4085	40.847	100	2.45

In the previous table there are the main results of the simulations. For the model with the power limit and the buoy position control only the high energy sea state is considered, because in the low and medium energy sea states the buoy position doesn't need to be controlled (the maximum value is close to 4.3 meter). The peak to average power ratios is calculated dividing the peak power by the average power. The lowest values of the peak to average power ratios are obtained in the bidirectional case with the high energy sea state, respectively in the case with the power limit and the case with power limit and buoy position control.
The capacity factor is calculated dividing the average power by the power limit (rated size), as can be seen in the previous table only in the bidirectional case the capacity factor has a relevant value (close to 0.80) for medium-high energy sea states. In all of the others cases the capacity factor is low and 0.50 as value is passed sporadically.
The applied PTO force for both bidirectional and unidirectional case is always the same, so the results are comparable. The average power extracted in the bidirectional case with power limit and buoy position control (high energy sea state) is lower than the average power extracted in the same case considering only the power limit, this effect is due to the fact that for higher values of buoy position and velocity the power extracted is higher.

7. Considered locations with constraints

Starting from the results obtained in chapter 5 some new simulations are made, in which the power limits and the buoy position control are introduced. The same locations as in chapter 5 are considered and the results will be compared with the results without constraints, in particular in a specific analysis about the yearly energy extracted.
The buoy position control is implemented to maintain the buoy position between -5 and +5 meters, like the buoy position control used in the previous chapter.
Two different values of power limit are considered i.e. 100 kW and 150 kW, these two values are selected based on the results of the previous chapter. A power limit of 200 kW is considered too high, so a lower size of the electrical machine to be installed has been preferred.
In this chapter the results obtained are more realistic and for a better comparison of the results with the simulations without constraints, the same values of torque applied have been chosen (i.e. 1, 2, 3, 4, 5 kNm).
All the extracted power scatter diagrams and the yearly energy scatter diagrams have the same structure shown in chapter 5, so the goal of the chapter is to show the new values of yearly energy extracted in both the power limits (100 and 150 kW) considered and in the end an analysis about the results obtained without constraints and with constraints.

7.1 Results of the simulations with 100 kW as power limit

For all the locations considered some simulations were run for both bidirectional and unidirectional cases. The choice of 100 kW as power limit was widely explained at the beginning of chapter 6.
The following figure is a plot of the average power extracted by the point absorber for the sea states occurring at Emec and WaveHub, and for the sea states in common the average value of the power extraction is calculated. These are values of average power that are produced for every sea state in kW with an applied PTO constant torque of 1 kNm in the bidirectional case.

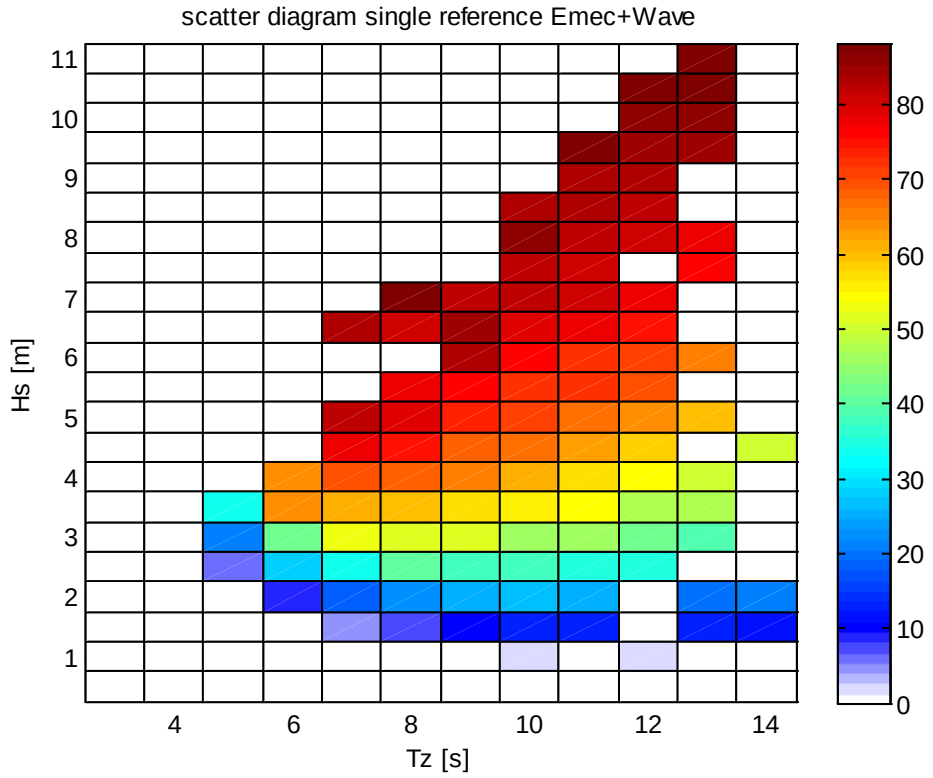

Figure 53 - Extracted power scatter diagram bidirectional case, applied torque 1 kNm and average power in kW (100 kW as power limit).

The power limit isn't passed obviously, and the maximum average power is significantly reduced. In figure 5.5 the maximum average power reached was more than 250 kW, while with the limit introduced the maximum average power is close to 90 kW and it is obtained again in sea states with high values of H_s and T_z (on the top of figure 7.1).

All the average powers are reduced compared to same situation without constraints, but here there is a saturation acting in the sea states with the highest values of H_s and T_z and this effect is introduced by the power limit. So for the sea states with high energy a lot of power is lost because the average values of the power are significantly reduced.

For the low energy sea states the power limit introduced is not relevant, because the peak power of the mechanical power that can be extracted in these sea states is lower than 100 kW. So if the power limit is higher than the peak power, the system operation is unaffected and the average power is not modified.

In the following figure a yearly energy scatter diagram for Emec location in the bidirectional case with a torque applied of 2 kNm is shown.

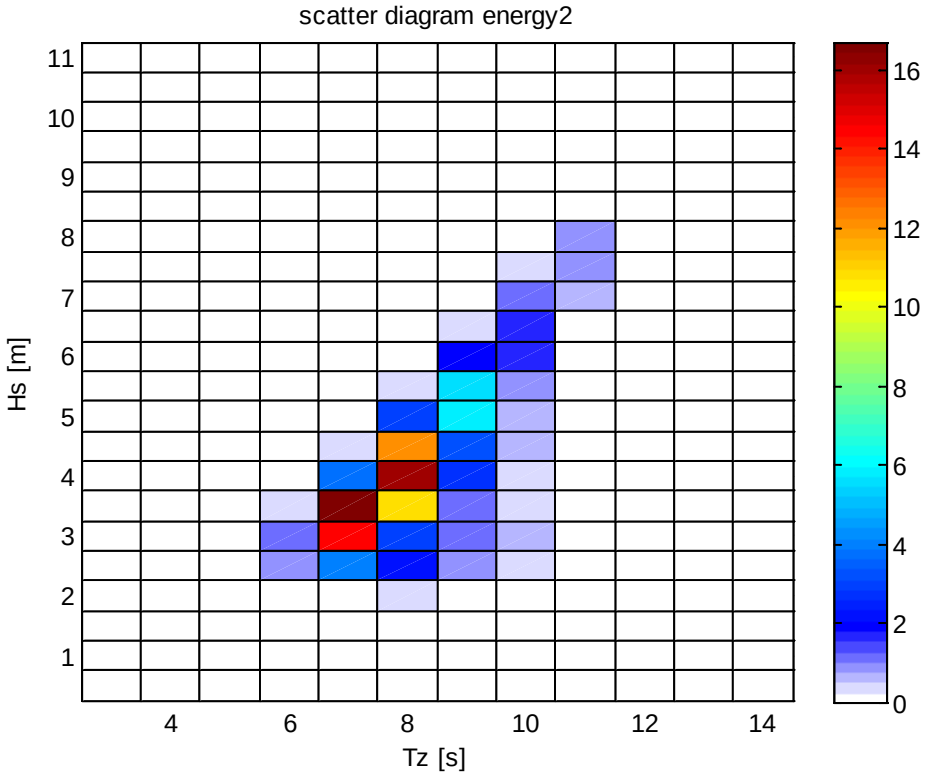

Figure 54 - Yearly energy scatter diagram Emec location bidirectional case, applied torque 2 kNm and energy in MWh (100 kW as power limit).

The yearly energy that can be extracted in these situations is obviously lower than the yearly energy that can be extracted without constraints, considering the data occur.
In the simulations without constraints the yearly energy that can be extracted is close to 30 MWh, here it is halved but however the same sea states give the higher values of energy.
So the maximum average power without constraints is 250 kW and with 100 kW as power limit is 90 kW. The maximum yearly energy without constraints is 30 MWh and with 100 kW as power limit is 16 MWh. Even if the yearly energy extracted with 100 kW as power limit is lower than the case with no constraints but the maximum average power extracted is much reduced, with a consequent money saving considering the PTO that should be installed.
Now it is useful to show the results of the yearly energy extracted for all the locations.

Table 13 Energy extracted in a year in MWh

	Torque=1 kNm	Torque=2 kNm	Torque=3 kNm	Torque=4 kNm	Torque=5 kNm
WaveHub Bidirectional	163.015	102.065	63.814	36.728	19.028

WaveHub Unidirectional	149.801	126.511	101.695	79.191	64.834
Emec Bidirectional	184.278	128.717	97.697	77.104	40.354
Emec Unidirectional	150.018	130.933	107.984	92.942	71.470
AUK Bidirectional	201.018	122.884	83.843	66.838	28.939
AUK Unidirectional	169.416	142.319	114.225	101.069	77.498
Haltenbanken Bidirectional	314.300	236.687	173.902	135.240	88.202
Haltenbanken Unidirectional	229.152	211.018	187.194	160.372	142.059

The energy extracted in each location is significantly reduced, in particular when the torque applied is high. This happens because the medium-high energy sea states give the most important contribution with high values of torque applied, but the power limit reduces this contribution and in particular for the unidirectional case this has a strong impact. In the end of the chapter there is a table with the comparison of the results.
Probably with lower values of torque applied the power extracted in both the cases would be higher, this is possible because the fixed limit of 100 kW is more favorable at the sea states with low-medium energy (i.e. with low values of wave amplitude and energy period).

7.2 Results of the simulations with 150 kW as power limit

As said before this power limit has been chosen because 100 kW as power limit could be a too low limit for the medium-high energy sea states, so to understand the behavior of these sea states some simulations with a 150 kW power limit have been run.
In the following table there is a plot with the average power extracted by the point absorber for the sea states occurring at Emec (for the sea states in common with WaveHub the average value of both the power extractions is considered). These are values of average power that are produced for every sea state in kW with an applied PTO constant torque of 1 kNm in the bidirectional case.

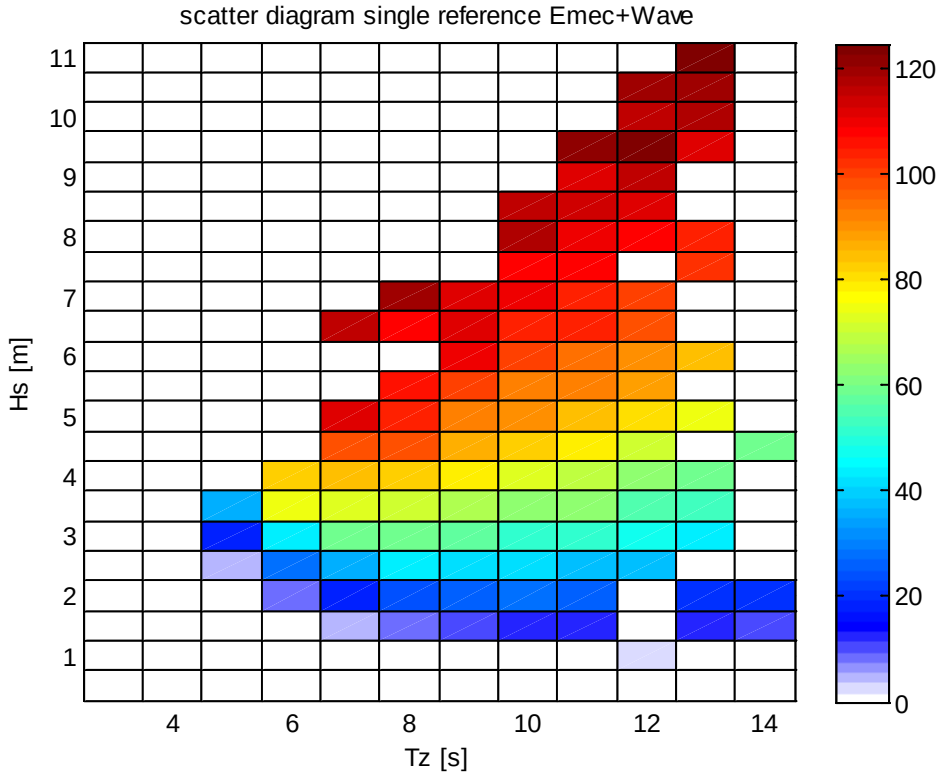

Figure 55 - Extracted power scatter diagram bidirectional case, applied torque 1 kNm and average power in kW (150 kW as power limit).

The maximum average power that can be extracted is close to 120 kW, which is 30 kW higher than the maximum average power that can be extracted with 100 kW as power limit. As a result an increase of 50 kW in the power limit gives an increase of 30 kW considering the maximum average power extracted.
It's necessary to evaluate for each considered locations what is the gain in the average power extracted compared to an increase of power limit. Also in the other locations the behavior is the same as in Emec, so probably 100 kW as power limit (power rated of the electrical machine) is the better choice.
Not all the sea states have a benefit with the increase of the power limit because a lot of sea states have a peak power lower than the power limit, so an increase of the power limit is useless for these sea states.
In the following figure a yearly energy scatter diagram for Emec location in the bidirectional case with a torque applied of 2 kNm is shown.

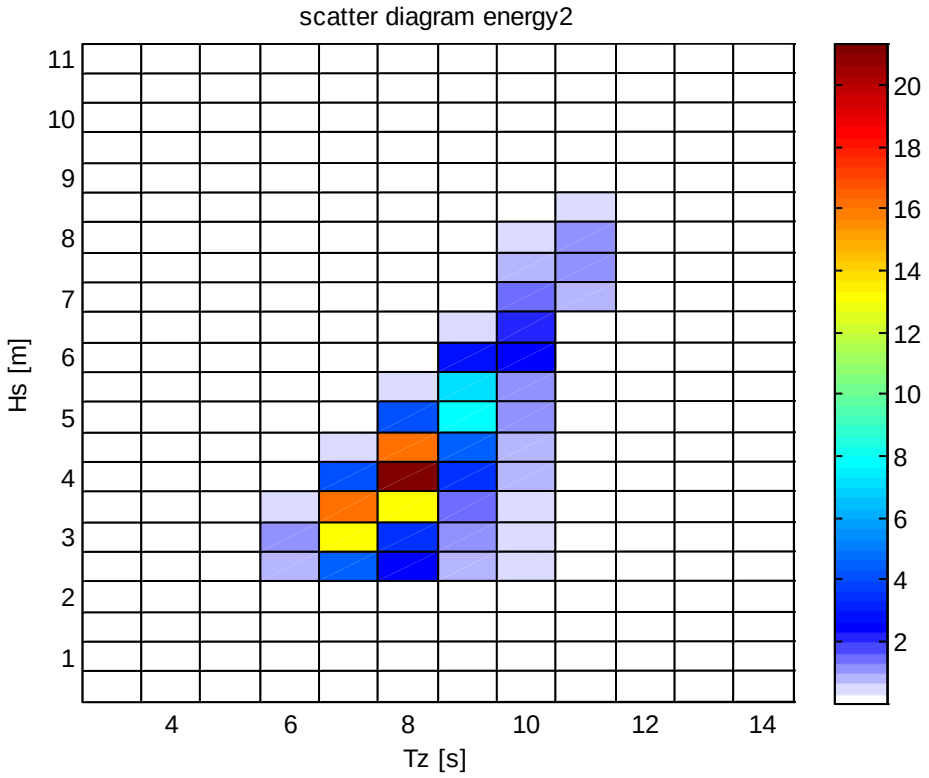

Figure 56 - Yearly energy scatter diagram Emec location bidirectional case, applied torque 2 kNm and energy in MWh (150 kW as power limit).

The maximum yearly energy extracted for Emec with a power limit of 150 kW is a little bit increased compared to Emec with a power limit of 100 kW, but the difference for the maximum value is only 6 MWh. In all the locations there is the same trend for the yearly energy, so also here a 100 kW power limit gives better result compared to 150 kW.
The sea states that give the higher values of extracted power are obviously the same for both the power limits.
As in the previous paragraph with 100 kW as power limit, also here a table with yearly energy extracted for each location in both bidirectional and unidirectional case is shown.

Table 14 Energy extracted in a year in MWh

	Torque=1 kNm	Torque=2 kNm	Torque=3 kNm	Torque=4 kNm	Torque=5 kNm
WaveHub Bidirectional	182.333	113.501	60.195	42.669	25.947
WaveHub Unidirectional	171.163	149.487	123.341	92.683	73.121
Emec Bidirectional	215.269	153.108	109.782	78.687	51.717

Emec Unidirectional	179.369	162.478	134.425	111.922	94.894
AUK Bidirectional	228.902	143.622	96.993	65.412	33.930
AUK Unidirectional	204.932	176.602	142.232	113.137	97.794
Haltenbanken Bidirectional	378.566	290.936	206.886	164.349	125.210
Haltenbanken Unidirectional	283.717	269.484	236.917	207.899	178.029

Haltenbanken location is always the location with the highest values of yearly energy extracted. Also here lower values of applied torque should be allowed to obtain higher values of yearly energy extracted, but however these results are useful for a comparison with the case without constraints.
The lower values of yearly energy are in WaveHub considering the same value of the applied torque for all the locations, in particular when the applied torque 5 kNm the energy that can be extracted decreases a lot. This happens because the sea states that give the highest contribution are the medium energy sea states, which are the majority of all the data considered.

7.3 Comparison of results

In order to understand better the results obtained, a table with the percentage gain of the yearly energy has been built. The reference values are the yearly energy extracted without constraints.

Table 15 Percentage gain in the yearly energy extraction compare to the case with no constraints

	Torque=1 kNm			Torque=2 kNm			Torque=3 kNm			Torque=4 kNm			Torque=5 kNm		
	No limit	**100 kW**	**150 kW**	**No limit**	**100 kW**	**150 kW**	**No limit**	**100 kW**	**150 kW**	**No limit**	**100 kW**	**150 kW**	**No limit**	**100 kW**	**150 kW**
WaveHub Bidirectional	201.569	-19.13	-9.54	150.289	-32.09	-24.48	89.944	-29.05	-33.07	54.019	-32.01	-27.70	31.301	-39.21	-17.10
WaveHub Unidirectional	192.441	-22.16	-11.06	203.087	-37.71	-26.40	183.649	-44.63	-32.84	155.089	-48.94	-40.24	125.487	-48.33	-41.73
Emec Bidirectional	259.183	-28.90	-16.94	230.641	-44.19	-33.62	170.392	-42.66	-35.57	117.003	-34.10	-32.75	76.904	-47.53	-32.75
Emec Unidirectional	226.773	-33.85	-20.90	260.065	-49.65	-37.52	253.933	-57.48	-47.06	233.101	-60.13	-51.99	204.747	-65.09	-53.65
AUK Bidirectional	283.938	-29.20	-19.38	214.072	-42.61	-32.91	136.189	-38.44	-28.78	74.769	-10.61	-12.51	40.772	-29.02	-16.78
AUK Unidirectional	275.257	-38.45	-25.55	284.340	-49.95	-37.89	252.194	-54.71	-43.6	216.161	-53.24	-47.66	180.026	-56.95	-45.68
Haltenbanken Bidirectional	504.268	-37.67	-24.93	500.480	-52.71	-41.87	409.190	-57.50	-49.44	318.290	-57.51	-48.37	229.240	-61.52	-45.38
Haltenbanken Unidirectional	404.538	-43.36	-29.87	504.740	-58.19	-46.61	525.367	-64.37	-54.90	505.530	-68.28	-58.87	466.860	-69.57	-61.87

In the previous table all the results of the simulations about the locations are shown, obviously the values of the yearly energy extracted (MWh) are higher in the case without constraints. The percentage variation is always negative because the fixed power limit (100, 150 kW) can't be passed, so the mechanical power is always lower than the limit. The columns in yellow have the reference values of the yearly energy in MWh without constraints, all of the others columns are in percentage.
Usually the higher is the energy that can be extracted in a location is, the higher the percentage variation (considering the absolute value) is, probably because the high energy sea states are very limited by the power limit and the contribution of these sea states is less. As said on the previous chapter in the bidirectional case the torque applied should be probably lowered, to obtain better results from the point of view of energy-extraction.
There is no linear behavior about the trend of the yearly energy extracted i.e. if the torque applied increases it's not said that the percentage variation increases or decreases, everything depends on the sea states occurring at the considered location. So to understand better this important thing, in the following figure the trend of the percentage variation for Haltenbanken location in the bidirectional case with 100 kW power limit is shown.

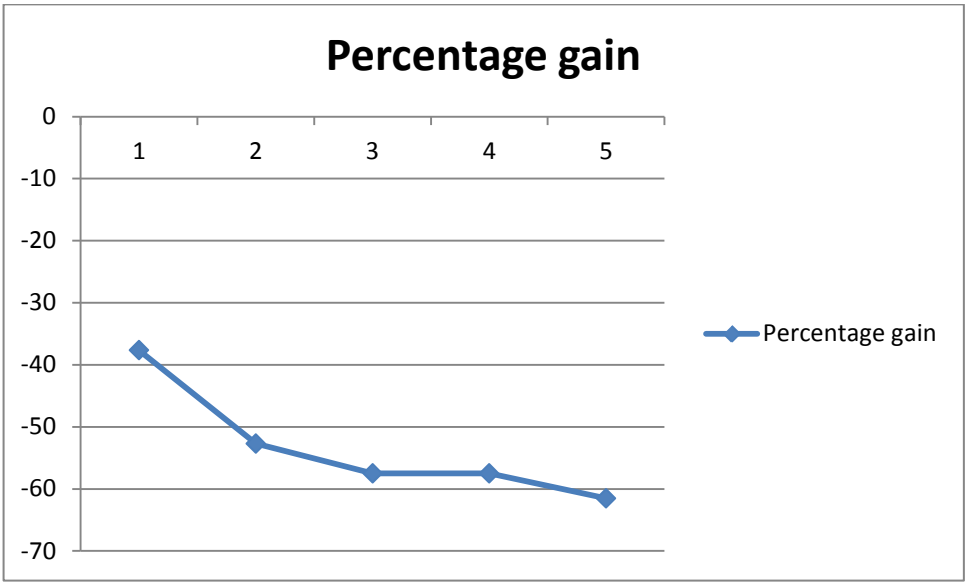

Figure 57 - Percentage variation for Haltenbanken location (100 kW)

However usually the percentage variation (in absolute value) increases with the increases of the torque applied.
The power limit has a lower effect when the torque applied is lower. This behavior is because low values of torque applied the low-medium energy sea states give the highest contribution. The best choice for a future electrical machine is 100 kW as rated power, because with an increases of 50 kW of power limit only a ~10 % increase of the yearly energy can be achieved.

7.4 Selective torque control

As made in paragraph 5.4 also here the optimal value of the constant torque control is considered for the locations with constraints, taking into account the already

mentioned power and position constraints. The process to achieve the results is the same as said at paragraph 5.4, anyway the values of the yearly energy will be certainly lower than in the case with no constrains. Only for the power limit of 100 kW the selective torque control is implemented, because this is the selected rated power for the future electrical machine installed. The buoy position control is also considered and the maximum buoy displacement is fixed to 5 m (considering the absolute value).
In the following figure the final table to Emec location is shown. This is the legend to understand the results:

Constant reference torque applied by the PTO
1 kNm
2 kNm
3 kNm
4 kNm
5 kNm

For each box the maximum value of the average mechanical power extracted in kW for the bidirectional case is shown. The color of the box is useful to understand immediately which value of torque is used as input to obtain the maximum power value.

Table 16 Average mechanical extracted power in kW (selective control), bidirectional case, *Te* in seconds and *Hs* in meters

Hs/Te	3	4.2	5.4	6.6	7.8	9	10.2	11.4	12.6	13.8	15	16.2	17.4
0.25		0.001294	0.001029	0.000964	0.000923	0.000903	0.000881	0.00089	0.000918	0.000879			
0.75		0.000924	0.000923	0.001084	0.010557	0.236732	1.057965	1.457619	1.105946	2.403322			
1.25		0.000884	0.009165	0.971329	5.109006	8.349011	10.96361	12.86023	12.03281		12.83687	11.2671	9.855908
1.75		0.001064	0.562683	9.08277	20.29881	25.04442	27.33522	28.06236	26.58483			20.78973	
2.25			5.594789	30.03584	32.75868	39.84244	37.03226	37.1717	34.18476	35.66959			
2.75			21.48686	42.51442	50.03317	47.34079	51.87633	44.53452	47.91387	45.35487	39.05679		38.5166
3.25			34.39376	64.74963	62.94797	61.91149	58.04302	53.10236	53.8656	53.23628	50.515		
3.75				64.36286	69.12923	69.45535	73.76276	63.42896	58.62335	55.07299	55.81852		
4.25					77.33024	78.44274	69.19631	68.87971	66.45469	66.20442		53.75811	57.53416
4.75					84.741	78.60623	76.4555	74.73879	75.15735	69.21189	65.32806		
5.25						82.28914	80.23798	70.10641	74.83391	72.73308			
5.75							83.93597	79.47951	77.69811	70.75673	70.32197		
6.25					83.86367	83.50837	87.62341	83.17516	80.33355	78.44713			
6.75						89.93807	84.91133	82.76477	81.70892	81.116			
7.25								86.77829	85.38904		81.99798		
7.75								90.07812	84.82822	85.1139	80.3581		
8.25								87.69634	85.9063	84.68503			
8.75									85.24107	89.29066			
9.25									91.24877	90.45923	86.16967		
9.75										85.49535	88.62374		
10.25										88.73157	88.86772		
10.75											89.47856		
11.25											90.61165		

The maximum value of the average extracted power is close to 91 kW, it's a high value considering that the power limit is 100 kW. The first two rows of the table give a very small contribution to the total power extracted because the values of *Hs* and *Te* are very little, so the most important sea states are obviously those which have high values of *Hs* and *Te*.
For high values of *Hs* and *Te* the maximum power is not extracted with 5 kNm of torque reference as happened in table 5.5, but the values of the torque reference are always between 2-4 kNm. This is an important consideration because it means that it is not useful to use high values of applied torque, anyway the perfect range of the torque reference to achieve the maximum extracted power is between 2 and 4 kNm.
All the four considered locations have one of this tables and starting from this it is possible to obtain the corresponding extracted yearly energy in MWh.
So in the following table the yearly energy extracted for each location are shown.

Table 17 Extracted energy in a year with selective torque control in MWh

	Yearly average extracted energy (MWh)		
	Selective torque control applied (1-5 kNm)	**Highest value reached without constant torque**	**Percentage gain (%)**
WaveHub Bidirectional	164.005	163.015	0.6073
WaveHub Unidirectional	155.966	149.801	4.1155
Emec Bidirectional	185.967	184.278	0.9165
Emec Unidirectional	154.601	150.018	3.055
AUK Bidirectional	201.310	201.018	0.1453
AUK Unidirectional	172.283	169.416	1.6923
Haltenbanken Bidirectional	316.427	314.300	0.6767
Haltenbanken Unidirectional	236.913	229.152	3.3868

There is a very small increase of the yearly energy extracted, the effect of the constraints is to reduce the gap (of yearly energy extracted) between the selective torque control and the highest value reached without selective torque control. Therefore if the selective torque control is difficult to implement, probably there is not enough gain to reward the time and money spent to implement the selective torque control, but it can be recommended if it only requires a software modification in the control algorithm. It's important to remember that in this chapter there is the

power limit fixed at 100 kW. Anyway the higher gain is achieved for the unidirectional case but is always less than 5 %. Compared to the same case without constraints, here the highest values of the yearly energy extracted are achieved in the bidirectional case. This happenes for the constraints introduced into the model, which do not allow achieving high values of yearly energy extracted in the unidirectional case.
Therefore the peak power can be maximum 100 kW; but in the unidirectional case the peak power, with no constraints, is always higher than the peak power for the bidirectional case, then the average power is reduced in particular in the unidirectional case. As can be seen in table 5.4, which shows the peak power with no constraints, the unidirectional case achieves very high peak power. The introduction of the power limit in the model involves a big reduction for the power that can be extracted in the unidirectional case. This is why the average power for the unidirectional case (with constraints) becomes lower than the average power in the bidirectional case (considering the same input), while, considering the model without constraints, the opposite happened.

8. Modeling and control of a permanent magnet synchronous generator (PMSG)

To transform the energy from mechanical to electrical a permanent magnet synchronous generator (PMSG) has been chosen. This kind of generator has three mains characteristics [14]:

1. High efficiency;
2. High power density;
3. High torque-to-inertia ratio.

Another important characteristic of this kind of generator is that there are no copper losses in the rotor, because the rotor field is excited by permanent magnets. As there is no need for brushes or slip rings the PMSG is significantly smaller in size than a conventional synchronous machine.
There are two types of this machine, and they can be distinguished based on the different position of the permanent magnets. The first one is called *surface mounted permanent magnet machine* and the second one is called *interior mounted permanent magnet machine* [15], [16].
The d-axis is defined as through the center of the magnetic pole, while the q-axis is perpendicular (90 electric degrees) to the d-axis.

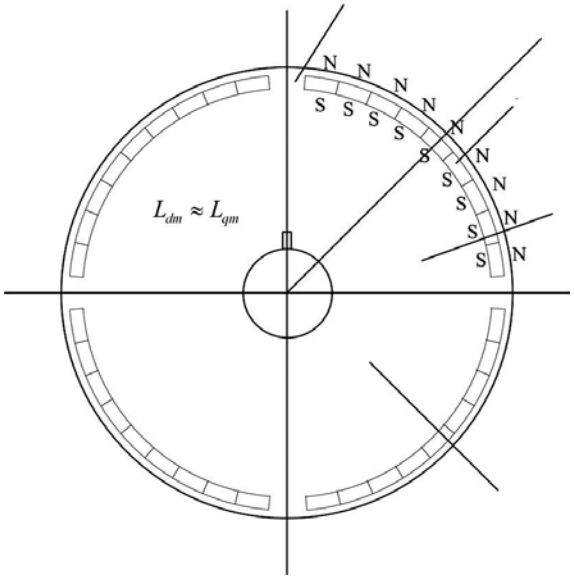

Figure 58 - Surface PM rotor (four poles)

For a surface mounted permanent magnet machine the inductances for both axes are the same, as the permanent magnetic material can be considered to have a relative permeability near unity [17], [18].
In this thesis the PMSG is a surface mounted with 4 poles ($2p = 4$), in the following table there are the main characteristics of the generator.
The steps to calculate the parameters of the generator are in appendix B, in the following table there are the main results.

Table 18 Rated generator data

Quantity	Value
Nominal power, P_n	100 kW
Nominal torque, T_n	636 Nm
Nominal voltage, U_n	400 V
Nominal current, I_n	152 A
Nominal frequency, f_n	50 Hz
Nominal speed, n_n	1500 rpm
Numbers of poles, $2p$	4
Permanent magnet flux, Ψ_{pm}	1.15 Vs
Stator resistance, R_S	0.0722 Ω
Stator leakage inductance, L_S	3.441 mH

8.1 PMSG Equations

In order to get a dynamical model for the electrical generator that easily allows us to define the generator control system, the equations of the generator are projected on a reference coordinate system rotating synchronously with the magnet flux.
So the magnet flux has only real component and this induce a simplification in the equations of stator voltages. The reference *d-q* system is rotating with the electromechanical velocity ω_e, and the real axis coincident with the rotor polar axis.
The dynamic model of the surface-mounted permanent-magnet generator in the magnet flux reference system is [19], [20]:

$$\boldsymbol{u_d = -R_S i_d - L_S \frac{di_d}{dt} + L_S \omega_e i_q} \quad \textbf{(8.1)}$$

$$\boldsymbol{u_q = -R_S i_q - L_S \frac{di_q}{dt} - L_S \omega_e i_d + \omega_e \Psi_{pm}} \quad \textbf{(8.2)}$$

where L_S and R_S are the generator inductance and resistance, respectively, ω_e is the generator speed (rad/s), and Ψ_{pm} is the magnet flux. The above equations show how to control current components by means of the applied voltage.
The electromagnetic torque is given by [19]:

$$\boldsymbol{T = \frac{3}{2} p \Psi_{pm} i_q} \quad \textbf{(8.3)}$$

where p is the pole pair number. Equation (8.3) shows that the generator torque may be controlled directly by the quadrature (q-axis) current component.

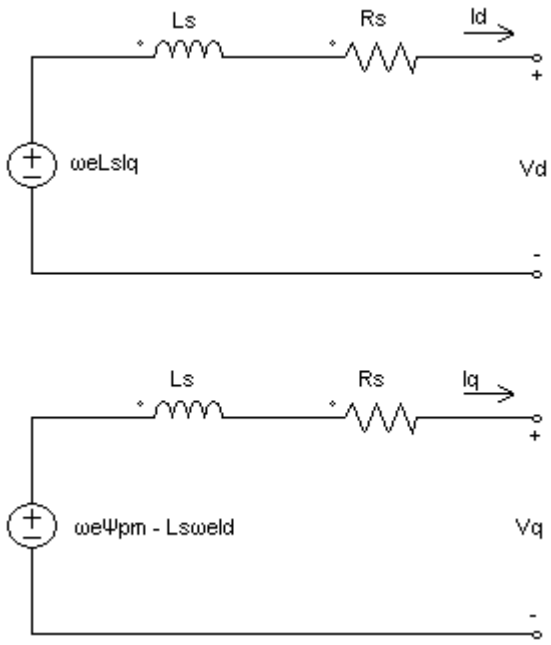

Figure 59 - Equivalent *d* and *q* axes generator circuit

Starting from the previous equations a Matlab-Simulink model is implemented, in which the inputs of the model are the U_q, U_d voltages and the mechanical speed. The mechanical speed is the buoy velocity multiplied by the gear ratio (equal to 20) and divided by the pinion radius (0.1 m).
In order to understand better the bond between mechanical and electromechanical speed, is useful to show the following equations:

$$\omega_m = \frac{2\pi}{60} n_n \quad \left[\frac{rad}{s}\right] \tag{8.4}$$

$$\omega_e = 2\pi f \quad \left[\frac{rad}{s}\right] \tag{8.5}$$

$$\omega_m = \frac{\omega_e}{p} \quad \left[\frac{rad}{s}\right] \tag{8.6}$$

In which n_n is the mechanical speed in rpm, ω_m is the mechanical speed in rad/s, ω_e is the electromechanical speed in rad/s and f is the frequency in Hz. It should be noted that the mechanical speed and the electromechanical speed are linked by the pole pairs number.
In the following figure the Simulink model for the PMSG is shown.

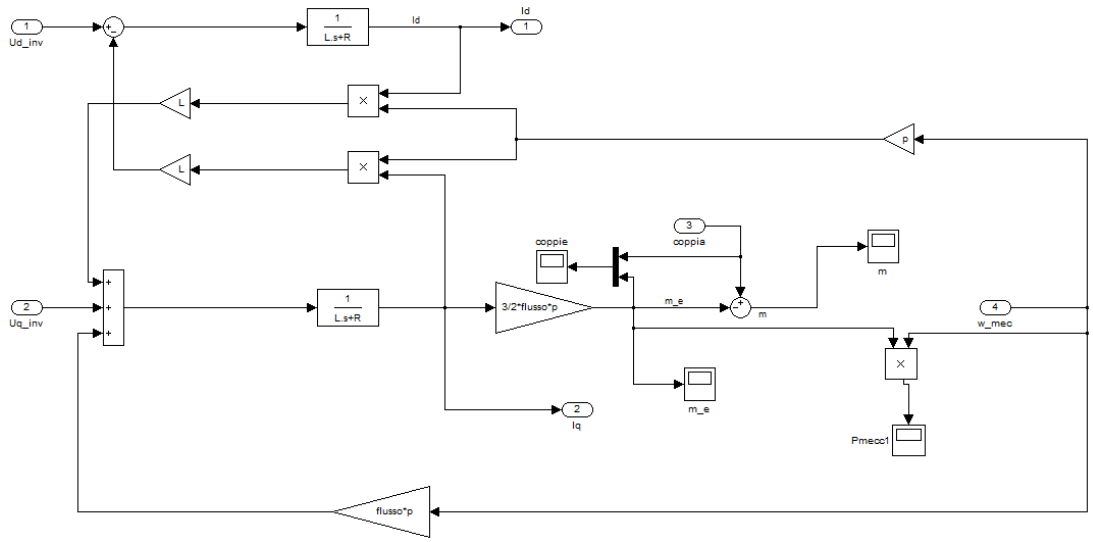

Figure 60 - Simulink model of a PMSG

The mechanical speed is directly set by the hydrodynamic model, so is not necessary to implement a control for the speed loop.
The outputs of the PMSG model in Simulink are the two currents i_d and i_q. These two currents are used as measured currents in the current control loop.

8.2 Current control

The project of the current controllers is complicated because the two rings (*d* and *q* axis) are not independent, but theyaffect each other because of the cross-coupling present between *d* and *q* axes of the machine because of terms $\omega_e L_s i_q$ and $\omega_e L_s i_d$. It's possible to eliminate the cross-coupling between the two axes by inserting at the output of the controllers a cross-coupling term opposed to the cross-coupling inherent in the machine [21].
Usually the high dynamic response requested by the synchronous drives needs a force compensation appearing in the electromotive q-axis. This is achieved by adding to the current controller output a signal proportional to the i_q electromotive force inside the motor [21].
Now the *d* and *q* current loop are independent on each other and the equations in *d-q* are the following:

$$\boldsymbol{u_d = -R_S i_d - L_S \frac{di_d}{dt}} \tag{8.7}$$

$$\boldsymbol{u_q = -R_S i_q - L_S \frac{di_q}{dt}} \tag{8.8}$$

The transfer functions from *i* to *u* can therefore be written as:

$$\boldsymbol{\frac{i(s)}{u(s)} = \frac{\frac{1}{R_S}}{1+\frac{L_S}{R_S}s}} \tag{8.9}$$

These current loops are controlled by PI regulators. The transfer block of the PWM system (G_c) is set to be unit, like in the decoupling of the axes. This is a fair simplification for the comparably slow wave energy converter system.
The open loop transfer function is the following:

$$G_{OL} = K_P \frac{1+T_i s}{T_i} \frac{\frac{1}{R_s}}{1+\frac{L_s}{R_s}s} \tag{8.10}$$

The parameters of PI regulators are tuned according to [21], so $T_i = \frac{L_s}{R_s}$ cancelling out the electrical time constant.

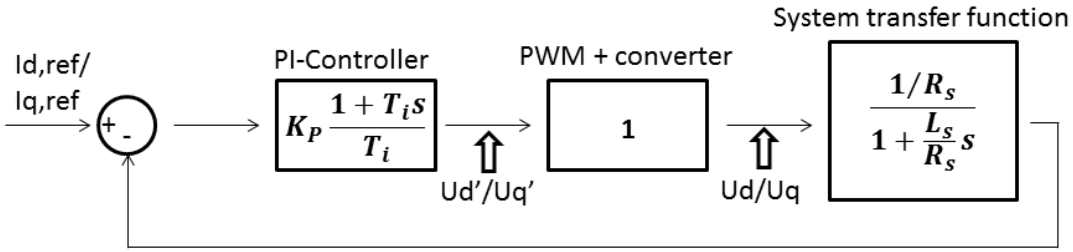

Figure 61 - Block diagram of current control loop. Notably the PWM + converter block is represented by a unity gain.

Now the open loop transfer function can be written as follow:

$$G_{OL} = K_P \frac{1+T_i s}{T_i} \frac{\frac{1}{R_s}}{1+\frac{L_s}{R_s}s} = K_P \frac{\frac{1}{R_s}}{\frac{L_s}{R_s}s} = K_P \frac{1}{L_s s} \tag{2}$$

The gain K_p is determined by evaluating the term for the closed loop transfer function. Imposing the value of the closed loop transfer function equal to unity, a value for K_p can be approximated.

$$G_{CL}(\omega) = \frac{G_{OL}}{1+G_{OL}} = \frac{K_p}{L_s j\omega + K_p} = 1 \tag{8.12}$$

The value of K_p must be much greater than $L_s\omega$ ($K_p >> L_s\omega$). The maximum value of bandwidth of the current ring is set to 5000 *rad/s*, and the value of L_s is equal to 3.441 *mH*. So it's considered a value of K_p equal to 10 sufficiently large for all operation areas.

8.3 Torque control

For wave energy applications a large fluctuation in the speed can be expected, so the electrical machine could work in over-speed and as a consequence it is necessary to weaken the magnetic field [14]. Choosing an electrical machine with rated speed equal to the maximum speed that can be achieved by connecting the electrical machine to the WEC is not the best option, since the maximum speed is achieved only sometimes during system operation.
It's not possible to control directly the field produced by the permanent magnets, and the control of the field is different compared to a double excited electrical machine.

The d-axis current is fixed at zero when the speed of the machine is under the rated speed. In this way, under constant torque operation, it is possible to control the torque only with the q-axis current.
However, in order to weaken the magnetic field a d-axis current is needed, having both signs for the bidirectional case. Instead in the unidirectional case only a negative d-axis current is needed, because only the positive speed is considered. This is called Field-Weakening Control, and in this thesis it is implemented as written in [14] but with some modifications.

Field-Weakening Control
There are a lot of different constraints in the PTO system. The maximum voltage and current, the limit of torque and speed of the PMSG, the maximum voltage and current of the inverter. When the speed increases the first limitation in which the system incurs is due to the maximum torque of the generator. The speed of the generator in general can be in both directions so it's necessary to consider the absolute value of the speed and the d-axis current will has the same sign of the real speed. Therefore for over-speed (positive) the d-axis current will be negative instead for over-speed (negative) the d-axis current will be positive.
When the saturation of torque is achieved the q-axis current is constant and equal to the maximum value that can be set.
The second saturation point occurs when the maximum power of the generator is achieved, so the maximum induced voltage of the generator has been reached. In this situation for further increase in speed, the induced voltage will have to be kept constant. The current and voltage can be represented by the following equations:

$$\boldsymbol{i_d}^{\boldsymbol{2}} + \boldsymbol{i_q}^{\boldsymbol{2}} \leq \boldsymbol{i_{max}}^{\boldsymbol{2}} \tag{8.13}$$

$$\boldsymbol{u_d}^{\boldsymbol{2}} + \boldsymbol{u_q}^{\boldsymbol{2}} \leq \boldsymbol{u_{max}}^{\boldsymbol{2}} \tag{8.14}$$

Starting from equations (8.1) and (8.2) the steady-state equations can be expressed as:

$$\boldsymbol{v_d} = \boldsymbol{R_S i_d} - \boldsymbol{\omega_e L i_q} \tag{8.15}$$

$$\boldsymbol{v_q} = \boldsymbol{R_S i_q} + \boldsymbol{\omega_e}(\boldsymbol{L i_d} + \boldsymbol{\Psi_{pm}}) \tag{8.16}$$

By substituting (8.15) and (8.16) into (8.14), one can get the following voltage constraint in terms of the stator current variables:

$$\left(\boldsymbol{i_d} + \frac{\boldsymbol{\omega_e^2 L_S \Psi_{pm}}}{\boldsymbol{R_S^2 + \omega_e^2 {L_S}^2}}\right)^{\boldsymbol{2}} + \left(\boldsymbol{i_q} + \frac{\boldsymbol{\omega_e R_S \Psi_{pm}}}{\boldsymbol{R_S^2 + \omega_e^2 {L_S}^2}}\right)^{\boldsymbol{2}} \leq \frac{\boldsymbol{V_{max}^2}}{\boldsymbol{R_S^2 + \omega_e^2 {L_S}^2}} \tag{8.17}$$

In order to maximize the power extraction, one wants to maintain the torque as high as possible. In other words the q-axis current has to be as high as possible and the d-axis current has to be always zero. When the speed increases the voltage is forced to

be kept as high as possible and the contribution for maintaining the maximum torque is given by the d-axis current, only when the speed passes the rated speed.
The inputs of the control block are the speed of the generator which is direct connected with the buoy velocity and the reference torque. The reference torque is calculated by controlling the sing of the buoy velocity, to have always a constant sign of the mechanical power.

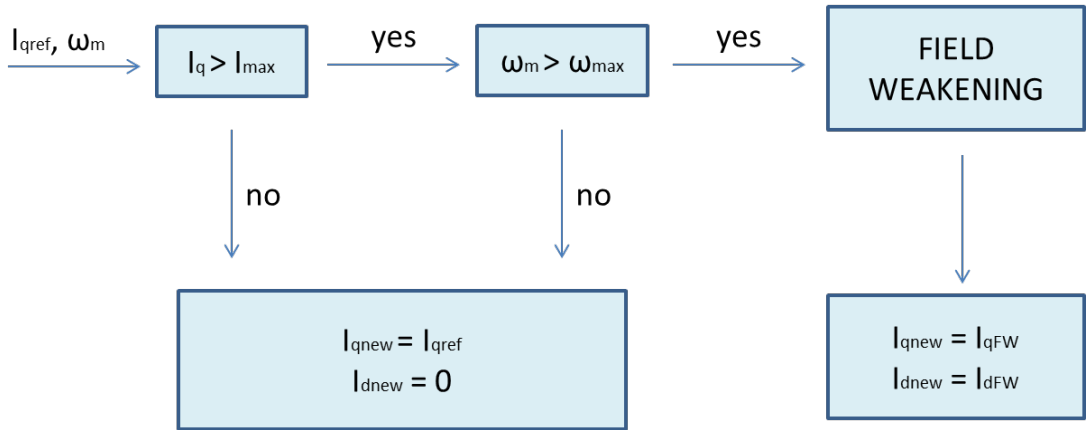

Figure 62 - Flowchart representing the idea behind the torque control determination of the reference currents

The maximum allowed speed at which the field weakening starts to be applied is written in [14], where $i_q = i_{max}$. It depends on the generator characteristics and is calculated as follow:

$$\omega_{max} = \frac{-2R_S I_{max}\Psi_{pm} + \sqrt{(2R_S I_{max}\Psi_{pm})^2 - 4(\Psi_{pm}^2 + L_S I_{max}^2)(R_S^2 I_{max}^2 - V_{max}^2)}}{2(\Psi_{pm}^2 + L_S{}^2 I_{max}^2)} \qquad \textbf{(8.18)}$$

All the equations which will be written in the following paragraph are from the paper of Ching-Tsai Pan, Jenn-Horng Liaw [14]. The implementation of the robust field weakening control is a little bit changed compared to the original, because both the directions of the motion need to be considered to achieve the correct operation also in the bidirectional case. Also it's not necessary a minimum value for the i_q current, because the reference current can be both positive and negative.
Combining equations (8.13) and (8.17) one can express the voltage constraints solely as function of speed and d-axis current:

$$\left(i_d + \frac{\omega_e^2 L \Psi_{pm}}{R_S^2 + \omega_e^2 L^2}\right)^2 + \left(\pm\sqrt{I_{max}^2 - i_{d,ref}^2} + \frac{\omega_e R_S \Psi_{pm}}{R_S^2 + \omega_e^2 L^2}\right)^2 \leq \frac{V_{max}^2}{R_S^2 + \omega_e^2 L^2} \qquad \textbf{(8.19)}$$

Rearranging the previous equation in order to calculate an expression for the d-axis current, the result is the following equation:

$$i_{d1,2ref} = \frac{-b \pm \sqrt{b^2 - 4ac}}{2a} \qquad \textbf{(8.20)}$$

Where *a*, *b*, *c* are given by the following expressions:

$$\boldsymbol{a = 4\left(i_{d,cen}^2 + i_{q,cen}^2\right)}$$

$$\boldsymbol{b = 4i_{d,cen}\left(\frac{V_{max}^2}{R_S^2 + \omega_e^2 L^2} - \left(I_{max}^2 + i_{d,cen}^2 + i_{q,cen}^2\right)\right)}$$

$$\boldsymbol{c = \left(\left(I_{max}^2 + i_{d,cen}^2 + i_{q,cen}^2\right) - \left(\frac{V_{max}^2}{R_S^2 + \omega_e^2 L^2}\right)\right)^2 - 4i_{q,cen}^2 I_{max}^2}$$

The values of $i_{q,cen}$ and $i_{d,cen}$ represent the coordinates of the center of the voltage constraint circle expressed by equation (8.17).

$$\boldsymbol{i_{d,cen} = -\frac{\omega_e^2 L \Psi_{pm}}{R_S^2 + \omega_e^2 L^2}}$$

$$\boldsymbol{i_{q,cen} = -\frac{\omega_e R_S \Psi_{pm}}{R_S^2 + \omega_e^2 L^2}}$$

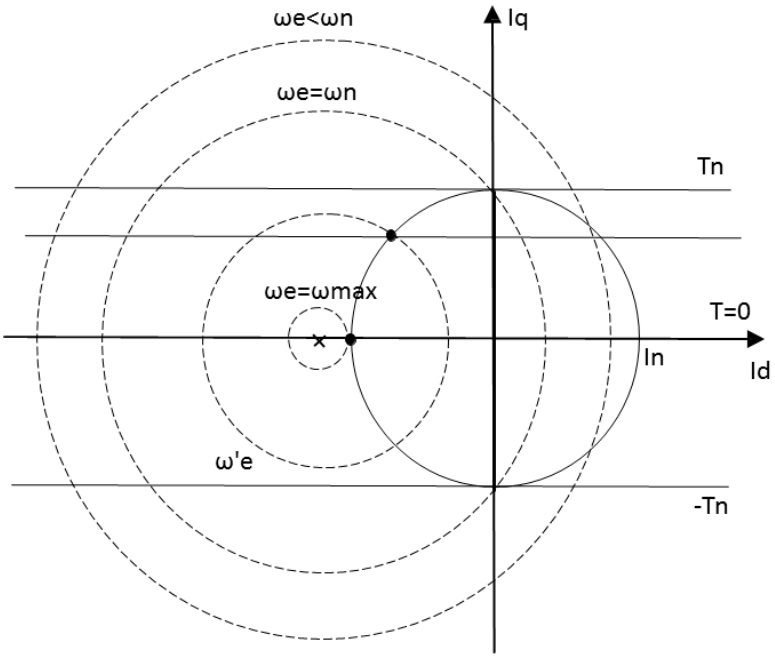

Figure 63 - Operating limits of the PMSG

The determinant b^2-$4ac$ is positive for all the values in the field weakening operation area, as a consequence the value of the d-axis current depends to the sign of the velocity motion as follow:

$$i_{d,ref} = \frac{-b+\sqrt{b^2-4ac}}{2a} \quad if \quad \omega_e > 0 \tag{8.21}$$

$$i_{d,ref} = \frac{-b-\sqrt{b^2-4ac}}{2a} \quad if \quad \omega_e \leq 0 \tag{8.22}$$

So the new q-axis current can be updated, and it is calculated as follow:

$$i_{q,ref} = \sqrt{I_{max}^2 - i_{d,ref}^2} \tag{8.23}$$

All the previous equations are implemented in a Simulink block called *FIELD WEAKENING*. The outputs of the block are the updated *d* and *q* axes current.

9. Wave – to – Wire modeling

In this chapter a Matlab-Simulink model with the hydrodynamic system and the electrical generator, including the electrical drives is considered. Both the constraints (i.e. power limit and buoy position control) are implemented in the model, so this is the final model in which the three usual sea states are tested (low energy, medium energy, high energy).
The model allows calculating the global efficiency of the system to convert the mechanical power into electrical power considering different values of torque applied as input, in particular a real-time blocks to calculate the generator losses is implemented in which the copper losses, the iron losses and the mechanical losses (called also additional losses) are calculated.
Both the bidirectional and the unidirectional cases are considered and the values of the input torque are obtained by the previous simulations results. The generator tested in nominal condition (rated speed and torque constants) has efficiency close to 94% considering all the possible losses. Obviously in the considered wave energy application the speed of the generator is not constant and in the bidirectional case it is in both directions, so the efficiency would be lower than in nominal condition. However the electric drive is implemented as realistic as possible and the reference torque is perfectly followed.

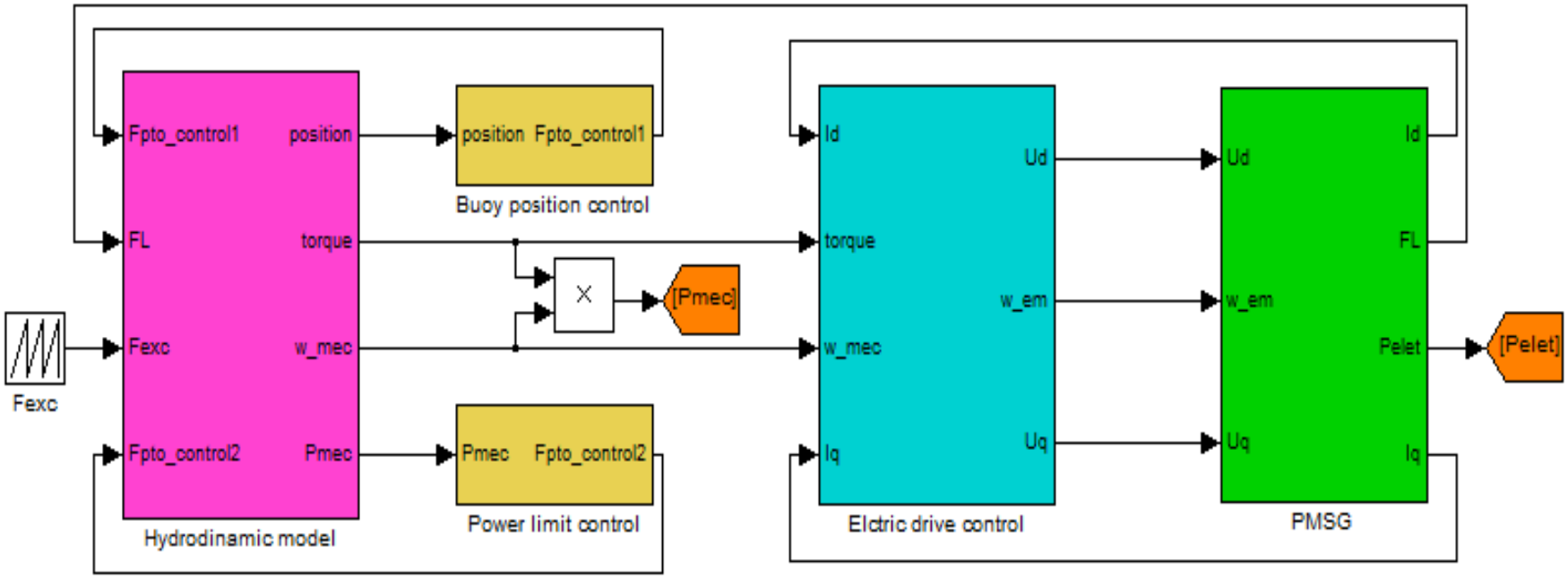

Figure 64 - Final Simulink model

9.1 Electrical power and PMSG losses

As said before it is very important to calculate the efficiency of the conversion from mechanical to electrical power. The generator losses are however difficult to determine in particular when the PMSG is not a standard machine or is used under continuously variable operating conditions and there are no diagrams to show the trends of the losses. So all the generator losses are calculated in real-time, in particular the copper losses (Joule losses), the iron losses (hysteresis plus eddy-current losses) and the mechanical losses (additional losses).
The equation to calculate the electrical power considering only the copper losses is the following [21]:

$$\boldsymbol{P_{eletrical} = \frac{3}{2}\left(u_d i_d + u_q i_q\right)} \quad [W] \tag{9.1}$$

The equation (9.1) is implemented in Simulink but it's not the actual electrical power produced because it does not automatically take into account the iron and mechanical losses.
Measurements of iron losses in magnetic material are traditionally made with sinusoidal flux density of varying frequency and magnitude [22]. The total iron-loss density p_{iron} is commonly expressed in the following form for sinusoidal varying magnetic flux density B (the magnetic flux density is not perfectly sinusoidal in the actual solution, but the approximation should not significantly affect the result so it can be accepted) with angular frequency ω_m [23]:

$$\boldsymbol{p_{iron} = p_h + p_e = k_h B^{\beta} \omega_m + k_e B^2 \omega_m^2} \quad \left[\frac{W}{m^3}\right] \tag{9.2}$$

where p_h and p_e are the hysteresis and the eddy-current loss density, respectively, k_h and k_e are hysteresis and eddy current constants, and β is the Steinmetz constant, all of which depend on the lamination material. These constants can be obtained by curve fitting from manufacturer's data. Typical values for grades of silicon iron laminations used in small and medium induction motors, with the stator frequency given in radians per second, are in the ranges k_h = 40-55 , β = 1.8-2.2, and k_e = 0.04-0.07. The term p_{iron} must be multiplied by the volume of the iron machine, this value is fixed at 0.0510 m^3.
The mechanical losses are difficult to evaluate because the environment where the PMSG is working can influence the losses. To consider also these losses the following equation is implemented in a real-time model in Simulink [24]:

$$\boldsymbol{p_{add} = c_1 A_n \sqrt{n}} \quad [W] \tag{9.3}$$

Where c_1 = 0.4-0.6, A_n is the nominal apparent power calculated as $\frac{P_n}{cos\varphi}$ and n is the generator speed in rpm.
In the model the following constant parameters values are used:

Table 19 Generator losses constant parameters values

Quantity	Value
Hysteresis constant, k_h	48

Eddy current constant, k_e	0.055
Steinmetz constant, β	2
Magnetic flux density, B	0.8 T
Iron volume, *Volume*	0.0510 m^3
Mechanical constant, c_1	0.5
Nominal apparent power, A_n	105.26 kVA
Load factor, $cos\varphi$	0.95

The trends of the different powers losses are very different each other's, in particular the additional losses have more weight compared to the other power losses. In the model the lost power calculated as difference between the mechanical power and the electrical power has a trend a little bit different compared to the power losses calculated separately from each other and subsequently added. This happens because the parameters (i.e. U_d, U_q, I_d and I_q) used to calculate the electrical power have a small delay due to the electric drive, so the power lost can be negative when, in that specific instant, the mechanical power is lower than the electrical power. Anyway the trends are only slightly different because this happens sporadically and the values of the total power losses have a difference less than 5 %, so both the results are reliable.
To calculate the efficiency of the generator the electrical power is calculated as in equation (9.1) and subsequently the additional and iron losses are subtracted. So the efficiency is calculated as follows:

$$\boldsymbol{\eta = \frac{P_{electrical}}{P_{mechanical}}} \qquad \textbf{(9.4)}$$

In the following figure the trends of the power losses are shown for the bidirectional case in the high energy sea state with 400 Nm as torque input.

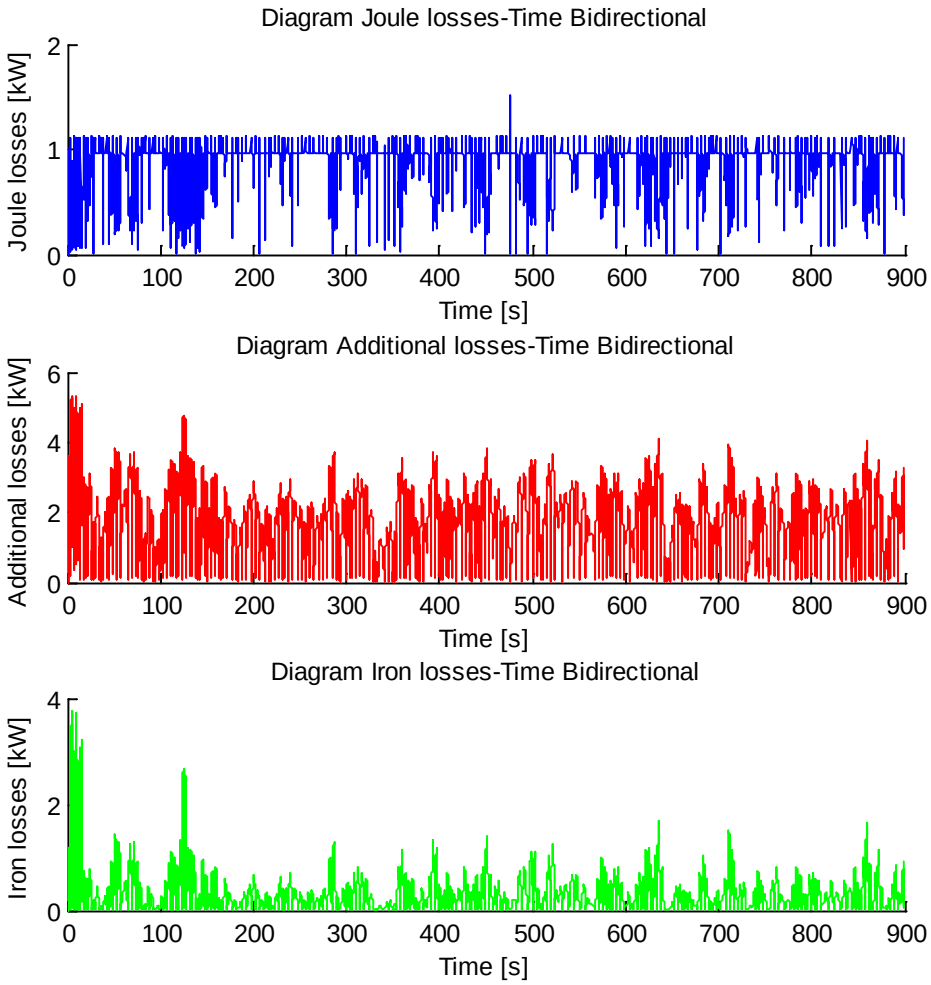

Figure 65 - Powers lost diagrams

9.2 Results of the simulations considering the final model

Considering the most important results of the simulations (i.e. mechanical power, electrical power, power losses and efficiency of the generator) some diagrams are presented for both bidirectional and unidirectional cases.
For all the simulations the power limit is fixed at 100 kW and the maximum buoy position (considering the absolute value) is fixed at 5 m. The generator considered is that described in chapter 8.
To understand better the trends of the considered variables, each diagram has the same inputs. In the following figure there are the main diagrams for the bidirectional case.

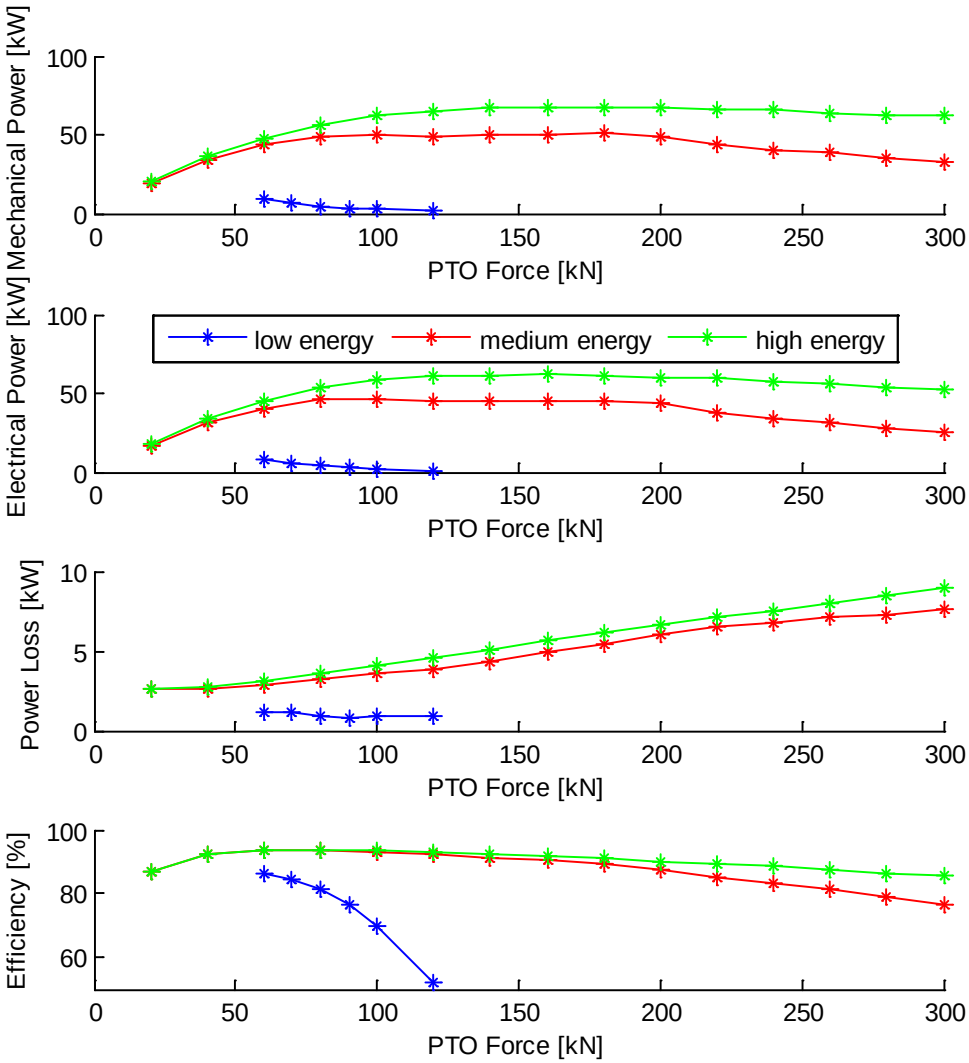

Figure 66 - Main diagrams for the bidirectional case

The mechanical power has quite the same trend as the figure 6.8, considering the same values of power limit and maximum buoy position. Obviously the electrical power has the same trend but different values because the power loss is subtracted from the mechanical power.

The efficiency, considering the low energy sea state, decreases very quickly because the value of the power loss is close to the mechanical power used as input for the generator. For the medium and high energy sea states the maximum value of the efficiency is close to 93 % and it is achieved for values of torque reference as input lower than 700 Nm (140 kNm). This happens because the generator works close to the rated torque and also because the power lost is small in percentage compared to the mechanical power. Decreasing the mechanical power used as input involves an increase of the percentage power lost (compared to the mechanical power), because some losses are always present for all working points of the machine (i.e. mechanical losses, iron losses, eddy current losses).

The lowest value of the efficiency is close to 54 % and is achieved in the low energy sea state for 600 Nm (120 kNm) as torque reference, but also for the medium and high energy sea states it is possible to get lower values of the efficiency if the torque reference is increased.
As for the bidirectional case also for the unidirectional case the same variables are shown in the following figure.

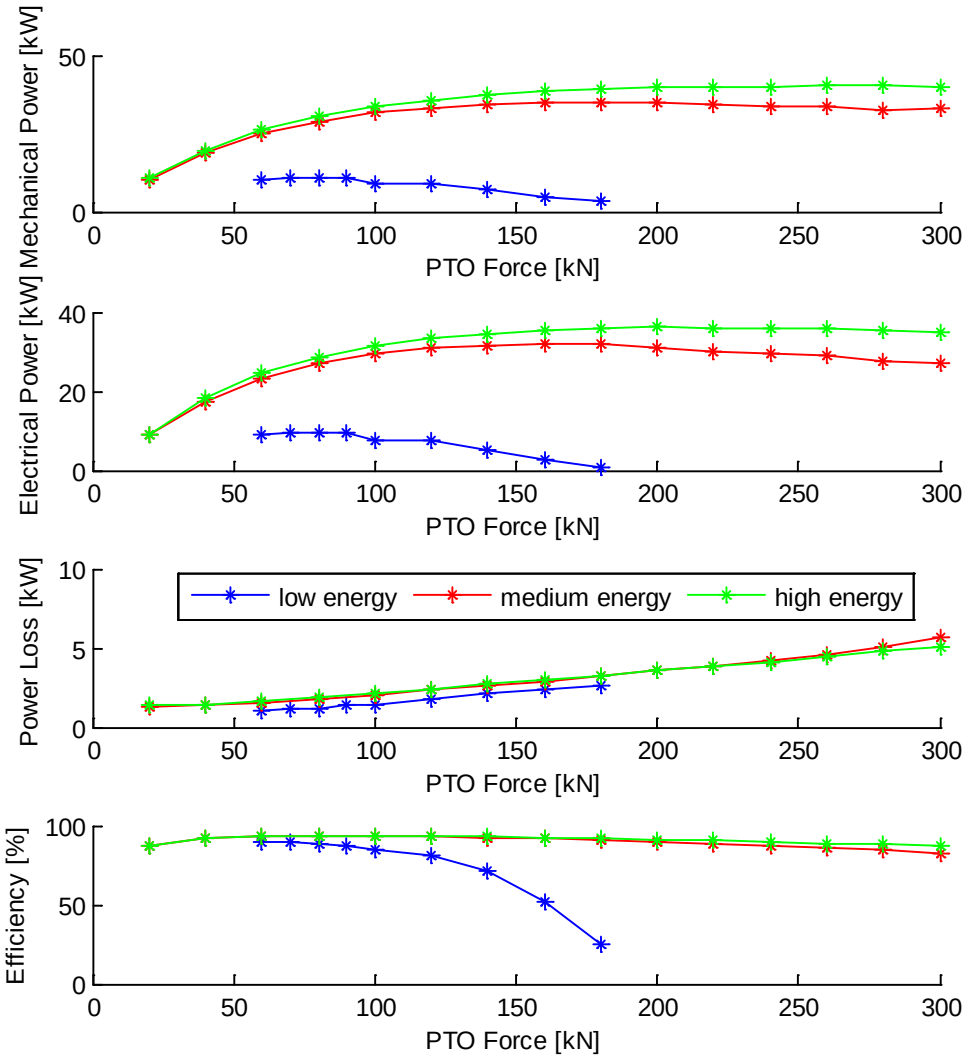

Figure 67 - Main diagrams for the unidirectional case

In the unidirectional case the efficiency decreases faster compared to the bidirectional case (considering the same values of applied torque). This is due to at the lower values of the mechanical power which increases the percentage weight of the power losses. Anyway is possible to achieve high values of the efficiency (η > 90 %) as in the bidirectional case for values of the torque reference lower than 900 Nm (180 kNm). The power lost increases with the increase of the torque reference. In the following table there are the main results for the medium energy sea state in both bidirectional and unidirectional cases.
In the unidirectional case the average power is always lower than in the bidirectional case (considering the same input), this happens because the introduction of the power

limit fixed the peak power at 100 kW with a high reduction of the average mechanical power that can be extracted in both the cases, but in particular for the unidirectional case which has the highest values of peak power (without the power limit).

Table 20 Main results of the simulations for the medium energy sea state

Considered case	Torque ref. [Nm]	Mechanical power [kW]	Electrical power [kW]	Power lost [kW]	Efficiency [%]
Unidirectional	100	10.150	8.823	1.3264	86.9314
	200	18.854	17.445	1.4091	92.5261
	300	24.910	23.333	1.5765	93.6710
	400	28.928	27.127	1.8010	93.7741
	500	31.648	29.586	2.0616	93.4857
	600	33.207	30.875	2.3322	92.9769
	700	34.076	31.463	2.6135	92.3305
	800	34.820	31.896	2.9244	91.6013
	900	35.029	31.810	3.2198	90.8083
	1000	34.648	31.101	3.5470	89.7626
	1100	34.121	30.235	3.8854	88.6129
	1200	33.790	29.587	4.2031	87.5611
	1300	33.431	28.891	4.5392	86.4220
	1400	32.559	27.521	5.0382	84.5262
	1500	32.743	27.013	5.7298	82.5005
Bidirectional	100	19.126	16.564	2.5624	86.6029
	200	34.037	31.381	2.6555	92.1981
	300	43.267	40.393	2.8745	93.3565
	400	49.092	45.832	3.2599	93.3597
	500	50.328	46.743	3.5851	92.8765
	600	49.363	45.500	3.8628	92.1747
	700	49.777	45.412	4.3651	91.2307
	800	50.333	45.427	4.9054	90.2540
	900	50.657	45.191	5.4658	89.2103
	1000	49.289	43.221	6.0679	87.6890
	1100	44.278	37.761	6.5173	85.2810
	1200	40.375	33.590	6.7852	83.1945
	1300	38.350	31.216	7.1340	81.3978
	1400	34.681	27.429	7.2516	79.0905
	1500	32.786	25.173	7.6134	76.7787

Considering the same values of the torque reference, the efficiency is always lower in the bidirectional case. This happens because the velocity in the bidirectional case is in both directions and the power losses depend very much on the velocity. For the high energy sea state the trends of all the variables are closed to the trends of the medium energy sea state.

Anyway the higher the torque reference is the higher the power losses are, in particular the Joule losses because they depend on the square of the current reference (i.e. torque reference).
To better understand the trend of the efficiency, the trends of the efficiency in both the cases for all the considered sea states are plotted in the following figure.

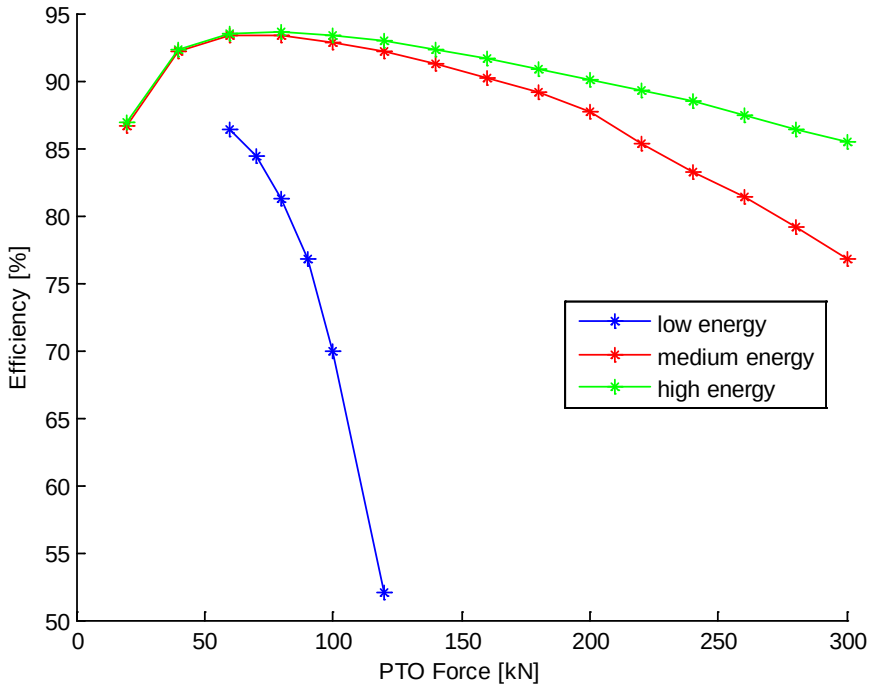

Figure 68 - Generator efficiency in the bidirectional case

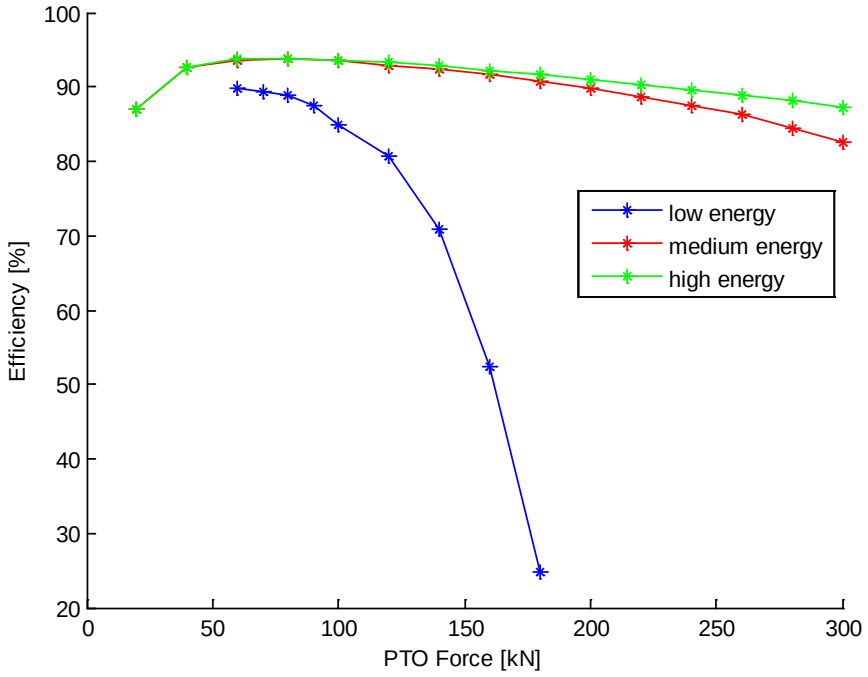

Figure 69 - Generator efficiency in the unidirectional case

10. Conclusions and further works

10.1 Conclusions

This thesis is focused on the comparison of the performance of two types of point absorber WECs called bidirectional and unidirectional, characterized by different power extraction strategies. In the former, both the directions of the buoy motion are used to produce power, while in the latter only the positive direction of the buoy motion is exploited for power production. Another important goal was to evaluate the effect of a straightforward control strategy using a constant torque (force) applied by the PTO system, i.e. the PMSG works with constant torque, whose performance are evaluated for both the types of devices.
Considering the hydrodynamic system based on Cummins equation with irregular waves as input, the average mechanical power that can be extracted from the WEC is calculated. Once the mechanical power is calculated (without constraints) with the same method in both cases, some constraints are added into the model and the mechanical power is recalculated (with constraints). The two constraints considered are:

- The power limit;
- The buoy position control.

The above constraints allow more realistic results, but these two constraints influence the value of the PTO force (torque), as they act on it. For this reason, the torque applied as input becomes only a reference value, while the real applied torque can be different.
Subsequently, a realistic PMSG and electric control drive (including torque control, field weakening etc.) are implemented in the model and tested for the three reference sea states, with the purpose of understanding the behavior of the generator with these new types of inputs (constant torque and bidirectional/unidirectional speed).
The three sea states considered as reference are the low energy, the medium energy and the high energy sea states. Anyway, the following real locations are considered, in order to obtain results as realistic as possible:

- WaveHub;
- Emec;
- AUK;
- Haltenbanken.

The results obtained from the locations are very interesting. Haltenbanken is the most powerful location: in the bidirectional case, the yearly energy that could be extracted (considering the mechanical power) is 314.300 MWh, assuming a 100 kW as power limit and a maximum buoy displacement of ±5 m. Considering different values for the controls it is possible to increase or decrease the yearly energy extracted, the maximum value achieved in Haltanbanken is 316.427 MWh with the selective torque control (assuming a 100 kW as power limit and a maximum buoy displacement of ±5 m). Finally, it can be concluded that the bidirectional (without considering the

electrical machine) is the best system, as it allows achieving higher values of yearly energy produced with lower values of reference torque.
Considering also the electric drive and the PMSG (with all the constraints), the PTO of the bidirectional system has lower efficiency compared to the one operating in the unidirectional system, but the electrical power output is still higher (using the same value of torque reference as input). Therefore the bidirectional case, in spite of two directions of the motion, is the best solution but the reference input torque must be close to the rated torque of the electrical machine to obtain high values of efficiency.

10.2 Further works

As a future extension of the present work, carrying out the following tasks is recommended:

- In this thesis two constraints are considered in the model: the power limit and the buoy position control. The introduction of the constraints affects the value of the PTO force and introduces also a nonlinearity in the system, but the advantages are higher than the disadvantages. To improve the behavior of the WEC also a new system control for the buoy velocity should be introduced, to ensure that it is kept within a certain range.
- The trend of the torque applied should be as linear as possible to limit abrupt differences of torque applied to the electrical machine. It's necessary to smooth the trend of the PTO force (torque) to have as linear as possible system behavior. This should improve the global efficiency of the WEC and also reduce the stiffness of the system with a consequent decrease of the cluster memory used.
- The field weakening implemented in the Simulink model is adapted from another application in which the constant torque applied must be positive and greater than zero. There is no problem with this control but it should be further optimized for this kind of application (i.e. torque and velocity with both the signs). In particular the algorithm of the field weakening e.g. a reference program in Matlab or C++ code could be written and eventually used for all of this kind of applications.
- Update all the hydrodynamics parameters values of the WEC. Some parameters should be changed with the increases or decreases of the mechanical power extracted, so a real time dynamic model in Matlab-Simulink should be implemented to calculate the real values of the parameters for different range of power as output.
- Introduction of an inverter with PWM technology and update all the current and voltage limits of the electric drive control with fully realistic values. In the model the inverter's gain considered is equal to one and the inverter is substituted with a time responding delay. The limits of the current and voltage are fixed in the model considering the nominal current and voltage of the PMSG.
- The PMSG should be connected to the AC grid; considering HVDC power transport from the offshore platform to the onshore system grid could be also interesting. Anyway this kind of applications can be implemented only when

the power extracted is high and the distance from the offshore to the onshore is hundreds kilometers considering a wave farm.

- Simulation of the locations with the final Simulink model to calculate the real electrical power that can be extracted from the waves. In the thesis this step has not been implemented because the cluster used for the simulation had not enough memory and in particular for the low energy sea states the program requires a lot of time to reach the solution. This probably happens for the high stiffness of the system and the step-size must be restricted with a consequent increase of the memory used.

Bibliography

[1] Clémente, "Wave energy in Europe: current status and prospective," 2002.

[2] H. Andrews e N. Jelly, Energy Science: Principles, Technologies and Impacts, Oxford: Oxford University Press, 2007.

[3] L. Alberti, E. Tedeschi, N. Bianchi, M. Santos and F. Alessandro, "Effect of the generator sizing on a wave energy converter," *The International Journal for Computation and Mathematics in Electrical and Electronic Engineering,* vol. 32, no. 1, pp. 233-247, 2013.

[4] M. Sidenmark, A. Josefsson, A. Berghuvud e G. Broman, «The Ocean Harvester - Modelling, Simulation and Experimental Validation,» Uppsala, 2009, pp. 421-425.

[5] A. F. de O. Falcao, «Wave energy utilization: A review of the technologies,» *Renawable and Sustainable Energy Reviews,* n. 14, pp. 899-918, 2010.

[6] W. Cummins, «The impulse response function and ship motions,» *Schiffstechnik,* n. 1662, pp. 101-9, 1962.

[7] J. Falnes, Ocean Wave Energy and Oscillating Systems: Linear Interaction Including Wave-energy Extraction, Cambridge: Cambridge University Press, 2002.

[8] E. Tedeschi, M. Carraro, M. Molinas e P. Mattavelli, «Effect of Control Strategies and Power Take-Off Efficiency on the Power Capture From Sea Waves,» *IEEE TRANSACTIONS ON ENERGY CONVERSION,* pp. 1-11, 2011.

[9] E. Tedeschi, M. Carraro, M. Molinas e P. Mattavelli, «Analysis of Power Extraction from Irregular Waves by All-Electric Power Take Off,» *IEEE,* pp. 2370-2377, 2010.

[10] E. Tedeschi e M. Molinas, «Wave-to-wave buoys control for improved power extraction under electro-mechanical constraints,» *Suitable Energy Technologies (ICSET), 2010 IEEE International Conference,* 2010.

[11] K. Nielsen e T. Pontes, «Report T02-1.1 OES IA Annex II Task 1.2 Generic and Site-related Wave Energy Data,» September 2010.

[12] M. W. H., «Sea Spectra Revisited,» *Marine Technology,* vol. 36, n. 4, pp. 211-227, 1999.

[13] P. Ricci, J. Saulnier, A. d. O. Falcao e M. Pontes, «Time-Domain models and Wave Energy Converters Performance Assessment,» in *Proceeding of the 27th International Conference on Offshore Mechanics and Artic Engeering*

(OMAE08), Estoril, Portugal, June 15-20, 2008.

[14] P. Ching-Tsai e L. Jenn-Horng, «A robust field-weakening control starategy for surface-mounted permanent-magnet motor drives,» *IEEE TRANSACTIONS ON ENERGY CONVERSION*, vol. XX, n. 4, pp. 701-709, December 2005.

[15] I. Boldea, Synchronous Generators, Polytechnical Institute, Temisoara, Romania: Taylor & Francis Group, 2006.

[16] M. M.S., B. H. e L. Louze, «Sliding Mode Control (SMC) Of Permanent Magnet Synchronous Generators (PMSG),» *Energy Procedia*, pp. 43-52, 2012.

[17] M. Carpaneto, M. Marchesoni e G. Vallini, «Practical Implementation of a Sensorless Field Oriented PMSM Drive with Output AC Filter,» *International Symposium on Power Electronics, Electrical Drives, Automation and Motion*, pp. 318-323, 2010.

[18] S. L. Herman, Electric Motor Control, Cliffon Park, NY: Delmar, 2010.

[19] M. Chinchilla e S. Arnandes, «Control of Permanent-Magnet Generators Applied to Variable-Speed Wind-Energy Systems Connected to the Grid,» *IEEE TRANSACTIONS ON ENERGY CONVERSION*, vol. 21, n. 1, pp. 130-135, March 2006.

[20] R. Monajemy e R. K. Fellow, «Control and Dynamics of Constant-Power-Loss-Based Operation of Permanent-Magnet Synchronous Motor Drive System,» *IEEE TRANSACTIONS ON INDUSTRIAL ELECTRONICS*, vol. 48, n. 4, pp. 839-843, AUGUST 2001.

[21] S. Bolognani, Dispense di azionamenti elettrici, Padova, 2005.

[22] C. Chris Mi, G. R. Slemon e R. Bonert, «Minimization of Iron Losses of Permanent Magnet Synchronous Machines,» *IEEE TRANSACTIONS ON ENERGY CONVERSION*, vol. 20, n. 1, pp. 121-127, March 2005.

[23] C. Mi, G. R. Slemon e R. Bonert, «Modeling of Iron Losses of Permanent-Magnet Synchronous Motors,» *IEEE TRANSACTIONS ON INDUSTRY APPLICATIONS*, vol. IIV, n. 3, pp. 734-741, May-June 2003.

[24] G. Someda, Elementi di costruzione di macchine elettriche, Bologna: Casa Editrice Prof. Riccardo Pàtron, 1954.

Appendix A

Simulink model

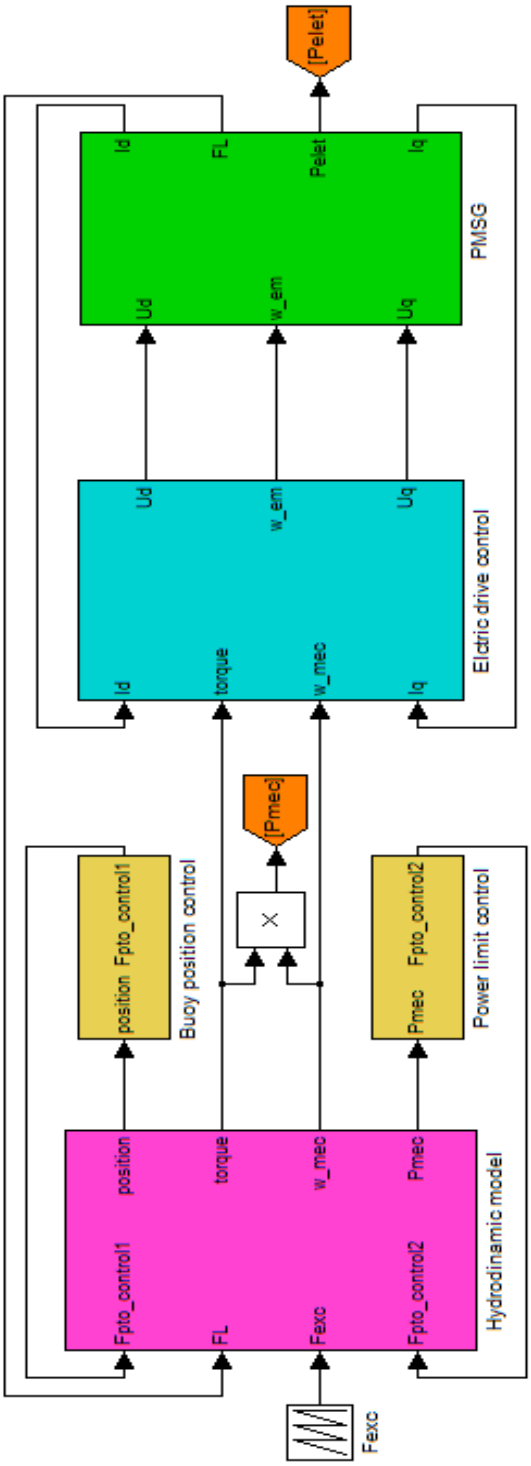

Figure 70 – Simulink wave-to-wire model of the WEC

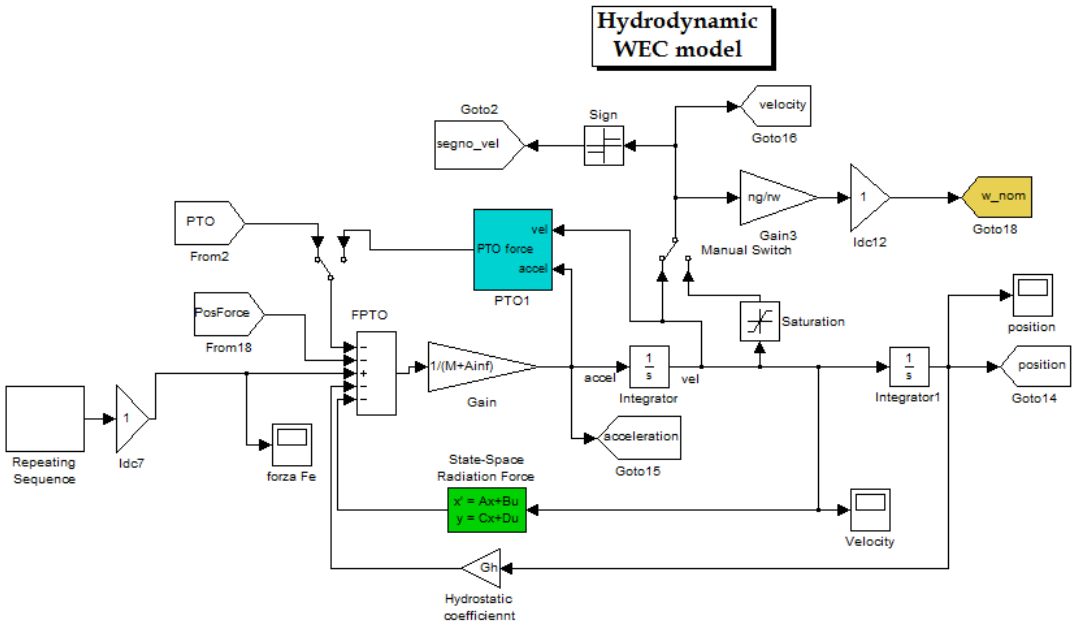

Figure 71 – Simulink model of hydrodynamics

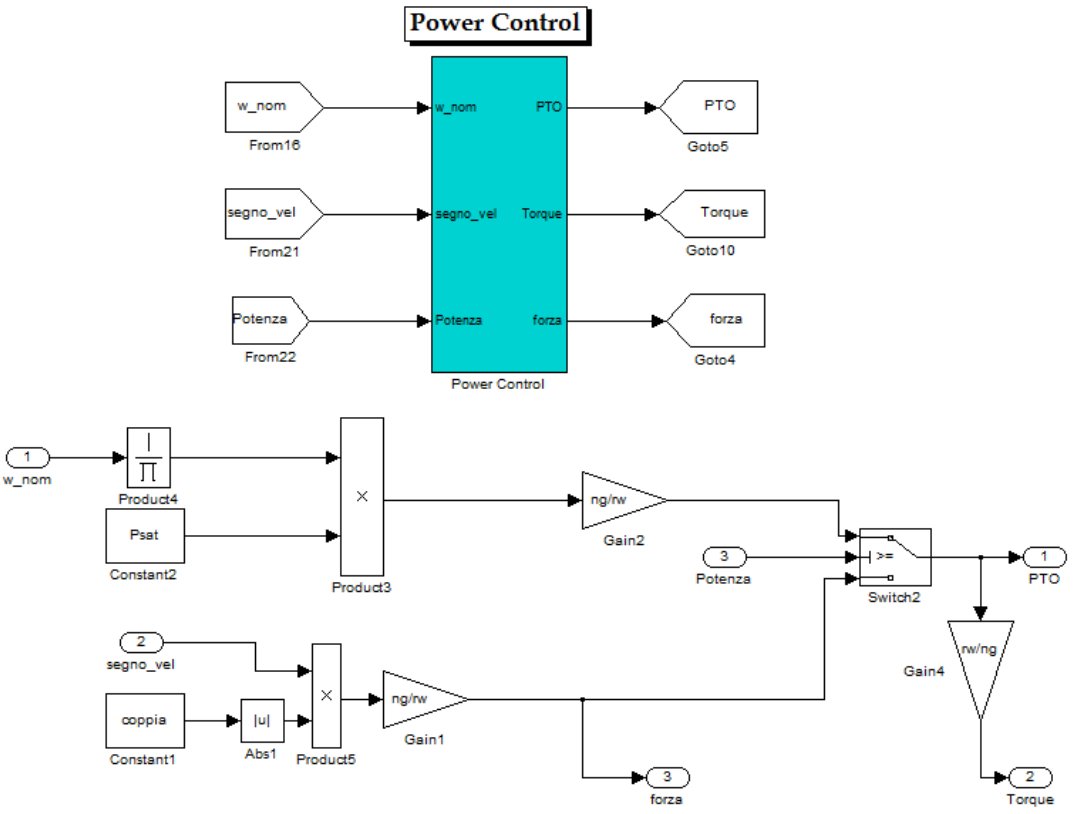

Figure 72 - Simulink model of power control

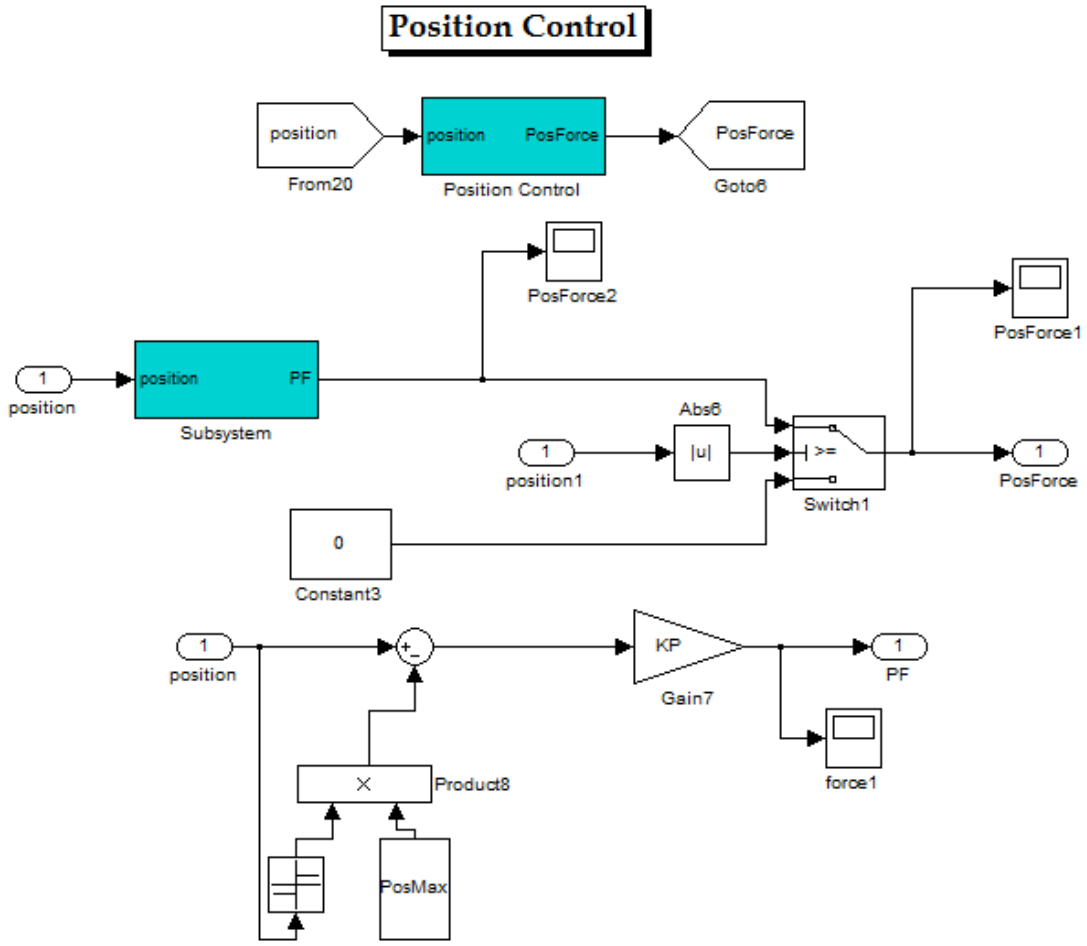

Figure 73 - Simulink model of buoy position control

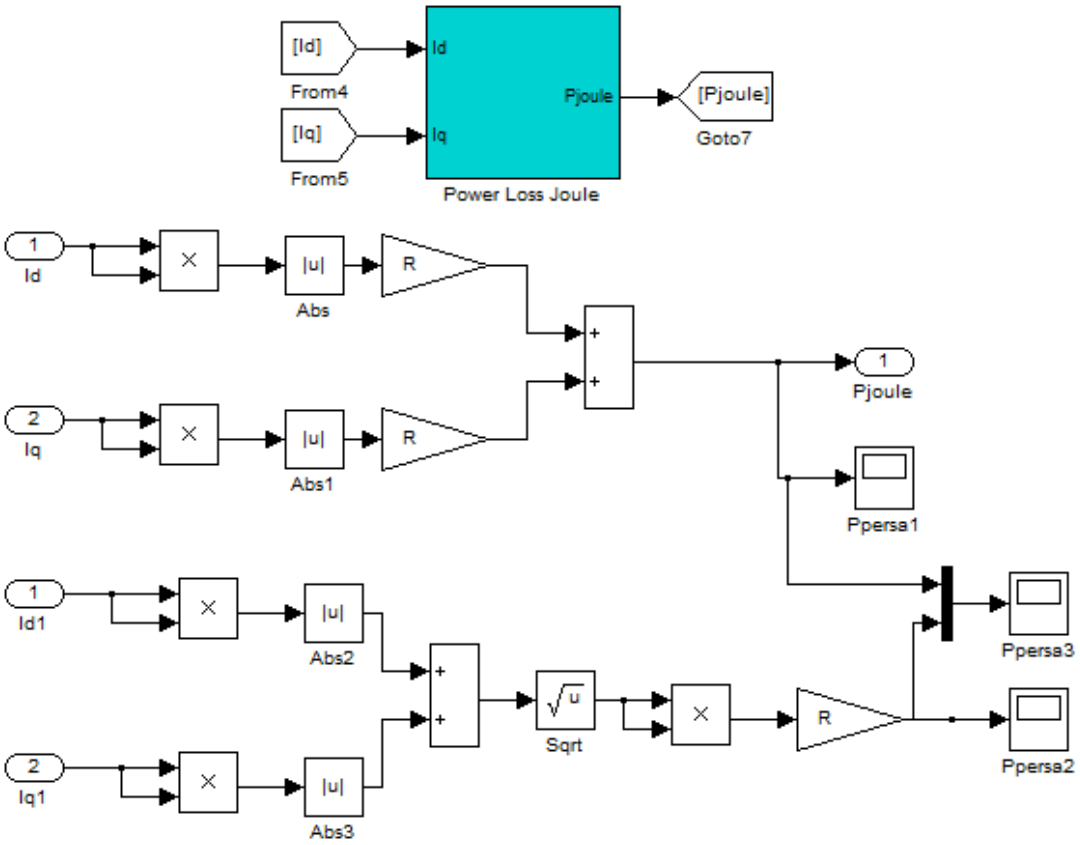

Figure 74 - Simulink block showing the calculation of the Joule losses

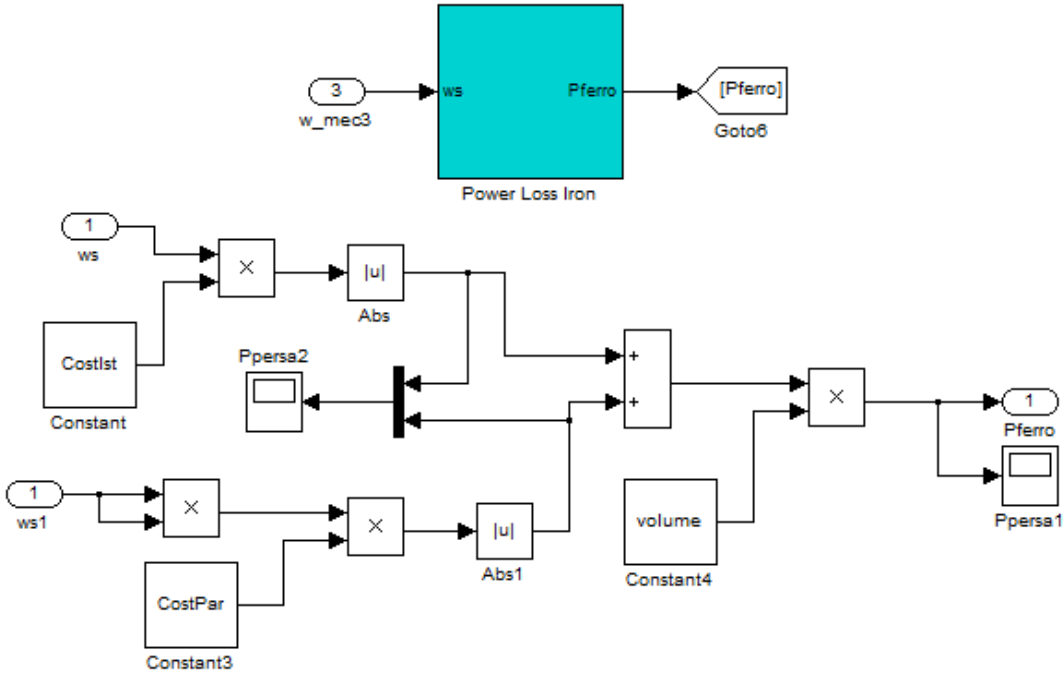

Figure 75 - Simulink block showing the calculation of the iron losses

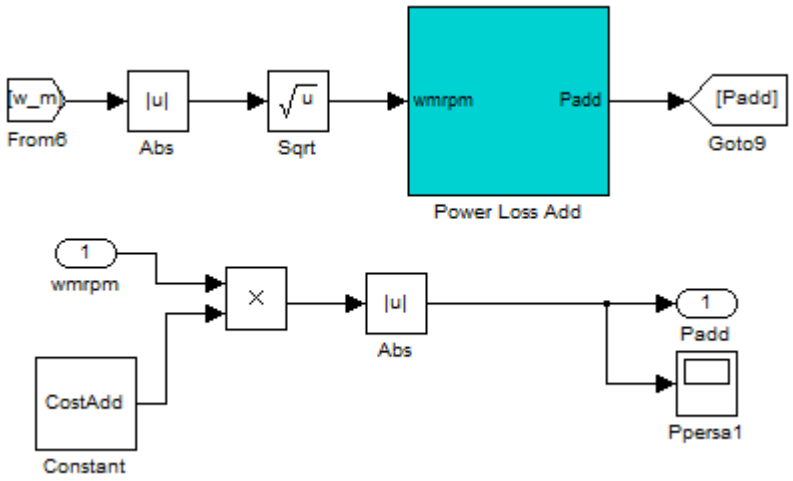

Figure 76 - Simulink block showing the calculation of the additional losses

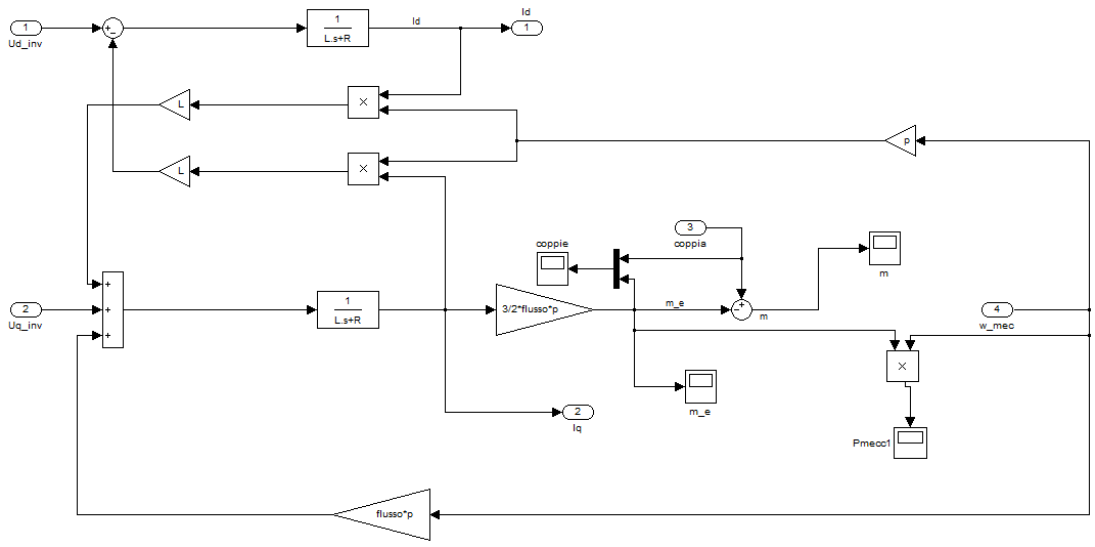

Figure 77 – Simulink model of the PMSG

Appendix B

Sizing of the PMSG

Nominal power: $P_n = 100\ [KW]$

Number of pole pairs: $p = 2$

Nominal frequency: $f_n = 50\ [Hz]$

Nominal voltage: $V_n = 400\ [V]$

Power factor: $cos\varphi = 0.95$

Nominal speed: $\omega_n = \frac{2\pi f}{p} = \frac{2\pi \cdot 50}{2} = 157.08\ \left[\frac{rad}{s}\right]$

$$n_n = \frac{60\omega_n}{2\pi} = \frac{60 \cdot 157.08}{2\pi} = 1500\ [rpm]$$

Nominal torque: $T_n = \frac{P_n}{\omega_n} = \frac{100000}{157.08} = 636\ [Nm]$

Nominal current: $I_n = \frac{P_n}{\sqrt{3}V_n cos\varphi} = \frac{100000}{\sqrt{3} \cdot 400 \cdot 0.95} = 152\ [A]$

Nominal magnetic flux: $\Psi_n = \frac{V_n}{2\pi f} = \frac{400}{2\pi \cdot 50} = 1.27\ [Vs]$

Permanent magnet flux: $\Psi_{pm} = 0.9 * \Psi_n = 1.15\ [Vs]$

Magnetic flux density: $\hat{B} = 0.8\ [T]$

Electric load: $\widehat{K_s} \cong 30000 - 50000\ \left[\frac{A}{m}\right] \rightarrow \widehat{K_s} = 40000\ \left[\frac{A}{m}\right]$

Length/diameter ratio in the gap: $\frac{L_{stk}}{D_i} = \frac{1.2}{\sqrt{2p}} = 0.6$

Air gap diameter: $D_i = \sqrt[3]{\frac{T_n}{\frac{\pi}{4}\left(\frac{L_{stk}}{D_i}\right)\widehat{K_S}\hat{B}}} = \sqrt[3]{\frac{636}{\frac{\pi}{4}\cdot 0.6\cdot 40000\cdot 0.8}} = 0.3482\ [m]$

Air gap length: $L_{stk} = \left(\frac{L_{stk}}{D_i}\right) D_i = 0.6 \cdot 0.3482 = 0.20892\ [m]$

Turns number: $N = \frac{2p\Psi_n}{\hat{B} D_i L_{stk}} = \frac{2\cdot 2\cdot 1.27}{0.8\cdot 0.3482\cdot 0.20892} = 87\ turns$

Total air gap: $g_{tot} = 0.008 - 0.015\ [m] \rightarrow\ g_{tot} = 0.012[m]$

Magnetic constant: $\mu_0 = 4\pi \cdot 10^{-7}\ \left[\frac{Vs}{Am}\right]$

Stator leakage inductance:

$$L_S = \frac{3}{\pi}\mu_0\left(\frac{N}{2p}\right)^2 \frac{D_i L_{stk}}{g_{tot}} = \frac{3}{\pi} 4\pi \cdot 10^{-7}\left(\frac{87}{2\cdot 2}\right)\frac{0.3482 \cdot 0.20892}{0.012} = 0.003441\ [H]$$

Nominal efficiency: $\eta_n = 0.95$

Joule losses: $p_{joule} \cong (1-\eta)P_n = 3R_S I_n^2$

Stator resistance: $R_S = \frac{(1-\eta)P_n}{3I_n^2} = \frac{(1-0.95)\cdot 100000}{3\cdot 152^2} = 0.0722\ [\Omega]$